

D.A.A

THERMODYNAMIC BEHAVIOUR OF OXYGEN IN METALLIC SOLVENTS

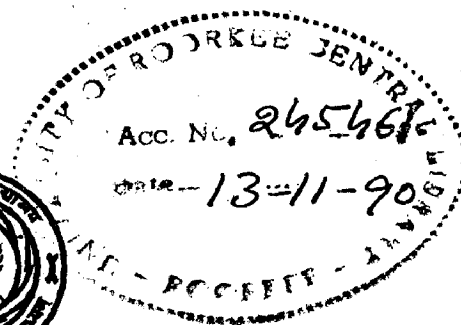
A THESIS

*submitted in fulfilment of the
requirements for the award of the degree.*

of
DOCTOR OF PHILOSOPHY
in
METALLURGICAL ENGINEERING

By

S. R. PRABHAKAR



DEPARTMENT OF METALLURGICAL ENGINEERING
UNIVERSITY OF ROORKEE
ROORKEE-247 667 (INDIA)

JULY, 1989


TO
MY BROTHER
LATE SHRI K.R. PRABHAKAR

CANDIDATE'S DECLARATION

I hereby certify that the work which is being presented in the thesis entitled "Thermodynamic Behaviour of Oxygen in Metallic Solvents" in fulfilment of the requirement for the award of the Degree of Doctor of Philosophy submitted in the Department of Metallurgical Engineering of the University is an authentic record of my own work carried out during a period from 29.5.1985 to 31.3.1989 under the supervision of Dr.M.L.Kapoor, Professor; Dr.V.N.S.Mathur, Professor and Dr.R.D.Aggarwal, Reader; in Metallurgical Engineering Department, University of Roorkee, Roorkee.


The matter embodied in this thesis has not been submitted by me for the award of any other Degree.

Candidate's Signature


(S.R.PRABHAKAR)

This is to certify that the above statement made by the candidate is correct to the best of my knowledge.

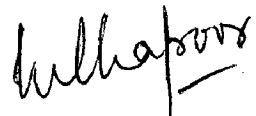
Signature of Supervisor(s)



(R.D.AGGARWAL)



(V.N.S.MATHUR)



(M.L.KAPOOR)

Date: May 30 , 1989

The candidate has passed the Viva-Voce examination on _____ at _____. The thesis is recommended for award of the Ph.D.Degree.

Signature of Guide(s)

Signature of External Examier(s)

ABSTRACT

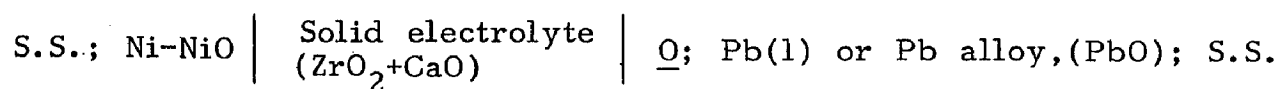
Elements such as arsenic, antimony, tin, bismuth, cadmium, copper, zinc and silver occur commonly in association in the sulphide lead-deposits and therefore constitute the common imperurities in lead bullion obtained in Blast-furnaces melting. These elements are also used as important alloy additions to lead, in desired concentration ranges, to improve its useful mechanical, physical or chemical characteristics for different industrial applications such as bearing metals, soldering alloys, type metal, fusible alloys, electrodes and electrolytes cell-lining material in batteries and similar other applications in engineering, chemical, electrical and electro-chemical industries. Oxidation behaviour of these elements, when present in dilute concentration range in lead, therefore forms an interesting study useful not only for the development and optimisation of different process steps employed in the extraction and refining of lead but also for development of its alloys to meet the stringent service requirements of its various applications.

A critical survey of the available literature on thermodynamic behaviour of oxygen in lead-base alloy solvents revealed only limited studies. It was therefore, felt that there is a need of extensive research input

to generate reliable thermodynamic data for a better understanding of behaviour of oxygen in these metallic solvents, as well as for use in design and development of better production processes.

With this in view, the present investigation was undertaken to study the thermodynamic properties of dissolution of oxygen in lead and its binary alloys with alloy additions in dilute concentration range. The systems studied include lead-oxygen, lead-copper-oxygen, lead-tin-oxygen and lead-bismuth-oxygen with copper, tin and bismuth varying between 0-4 weight percentage in these alloys and the oxygen concentration not exceeding its saturation limit.

A suitable experimental set-up using emf technique and employing solid-electrolyte cell with stainless steel (S.S) leads for study in the temperature range 933-1123K was therefore designed and locally fabricated. The cell employed may be represented schematically as,



Concentration of oxygen in the different lead melts studied was altered by covering these with synthetic slags either $\text{PbO-B}_2\text{O}_3$ or PbO-SiO_2 of desired (PbO) activity made specifically for the purpose. However, in case of studies with lead-tin alloys, the oxygen concentration was varied by the addition of Pb-PbO pellet

to the alloy during the course of experimentation to prevent loss of tin resulting from slag formation.

The cell emf was recorded during the course of experiment and metal samples drawn on attainment of equilibrium, were analysed for their oxygen and alloy addition concentrations. These data were used to calculate the desired thermodynamic properties viz. the free energy of dissolution of oxygen in lead bearing metallic solvents and also the binary and ternary interaction parameters. For comparison and analysis of data of present investigation, values of activity coefficient of oxygen in different Pb-M-O ternary systems have been calculated employing expressions based on classical thermodynamic concepts, to arrive at the model which is most suitable for theoretical calculation and prediction of thermodynamic properties of oxygen in the metallic systems studied.

The entire work presented in this dissertation has been divided into seven chapters. Chapter I, surveys the available literature on thermodynamics of dissolution of oxygen in metallic solvent, different experimental methods of thermodynamic investigation and various theoretical models proposed by different workers. Finally the problem of present investigation has been formulated. Chapter II deals with the experimental set up and materials used, experimental procedure adopted and also

the methods of quantitative analysis employed for estimation of oxygen and alloy additions. Chapters III to Chapter VI present, for the different metallic systems studied, the experimental results, method of calculation used and the computed values of thermodynamic parameters of present investigation as well as their comparison with those obtained by other workers. While Chapter III presents data on lead-oxygen system; Chapter IV to Chapter VI deal respectively with the ternary systems Pb-Cu-O, Pb-Bi-O and Pb-Sn-O. In Chapter VII, the major results obtained in the present investigation are summarised and important conclusions drawn are listed. Finally, suggestions for further work in extension of the present investigations are listed.

ACKNOWLEDGEMENTS

I take this opportunity to express my profound gratitude and indebtedness to Dr. M.L. Kapoor, Professor of Extractive Metallurgy, Department of Metallurgical Engg. University of Roorkee, Roorkee for his invaluable guidance and the illuminating discussions I had with him at all stages of preparation of this dissertation. Without his guidance, it would not have been possible to complete the work. I am also grateful to Dr. V.N.S. Mathur, Professor for his continuous help, guidance and painstaking checking of the manuscript. Heartfelt thanks are also due to Dr. R.D. Aggarwal, Reader for his constant help and useful suggestions.

I am glad to acknowledge with thanks the useful discussions I have had with Dr. G.C. Kaushal and his help in different ways during my entire span of work at Roorkee. I also acknowledge my heartfelt thanks and deep sense of appreciation to Dr. K.K. Sharma and Shri Trilok Singh of D.M.R.L. Hyderabad for their help in getting my numerous alloy samples analysed for their oxygen content at their laboratories and also for providing some of the technical reprints not locally available.

Assistance rendered by laboratory staff Shri S.B. Sharma, Shri S.R. Kaushik, Shri Rajinder Singh Sharma,

Mr. Rajinder kumar and Mr Nautyal during fabrication of experimental set-up, conduct of actual runs and analysis work is thankfully acknowledged. Technical staff of the Metallurgical Engineering Workshop always extended a helping hand; my heartfelt thanks^s are due to them all.

I am also indebted to Principal, Punjab Engineering College, Chandigarh for sponsoring me under the QIP Programme. In particular I feel obliged to my colleagues in the Metallurgical Engineering Department for their encouragement and also sharing my academic load in my absence.

I am also grateful to Mrs. Darshan Kaur for her devoted and expert work in producing the type script. Thanks are also due to S. Babu Singh for his able draftmanship.

My wife Meena deserves special acknowledgement for her continuous encouragement and the perseverance shown by her to bear the extra responsibilities of the family during the period of preparation of this dissertation. My sons Munish and Gautam also felt similar neglect during my involvement in this work. My most affectionate thanks to all of them.

(S.R. PRABHAKAR)

LIST OF FIGURES

Figure No.	Title	Page No
2.1	Schematic diagram of experimental set-up	81
2.2	Cell assembly	83
2.3	Block diagram of experimental set-up	85
3.1	Plot of function $\ln [\text{at pct O}]/p_{\text{O}_2}^{\frac{1}{2}}$ vs [atom pct O] for dissolution of oxygen in pure lead at different temperatures	104
3.2	Plot of function, $\ln KO(\text{Pb})$ vs $1/T$ for equilibria of oxygen in pure lead	106
3.3	Plot of $\Delta GO(\text{Pb})$ vs temperature for equilibria of oxygen in pure lead	107
3.4	Plot of temperature dependence of $\epsilon_{\text{O}}^{\text{O}}$ in liquid lead	108
4.1	Plot of temperature dependence of first order interaction parameter, $\epsilon_{\text{O}}^{\text{Cu}}$, in Pb-Cu-O system	125
4.2	Variation of $\ln KO(\text{Pb}+\text{Cu})$ with concentration of copper in lead-copper alloys	129
4.3	Effect of copper on activity coefficient of oxygen in liquid lead at 967, 1010, 1053 and 1095K	131
4.4	Variation of f_{O}^{Cu} in Pb-Cu alloys with reciprocal of temperature	135
4.5	Activity coefficient of oxygen in Pb-Cu alloys at 1095K	136
5.1	Plot of Temperature dependence of first order interaction coefficient, $\epsilon_{\text{O}}^{\text{Bi}}$	152
5.2	Variation of $\ln KO(\text{Pb}+\text{Bi})$ with concentration of bismuth in lead-bismuth alloys	156
5.3	Effect of Bismuth on activity coefficient of oxygen in liquid lead at 913, 953, 993 and 1034K	159

Figure No.	Title	Page No
5.4	Variation of $\ln f_{\text{O}}^{\text{Bi}}$ in lead-bismuth alloys with reciprocal of temperature	161
5.5	Effect of Bismuth on oxygen in lead-bismuth alloys at 1034K	162
5.6	Activity coefficient of oxygen, $f_{\text{O}}(\text{Pb+Bi})$ in Pb+Bi alloys at $T=1034\text{K}$.	163
6.1	Plot of temperature dependence of first order interaction coefficient, $\epsilon_{\text{O}}^{\text{Sn}}$ in lead-tin alloys	182
6.2	Variation of $\ln K_{\text{O}}(\text{Pb+Sn})$ with atom pct Sn in lead-tin alloys at different temperatures	186
6.3	Effect of Tin on activity coefficient of oxygen in liquid lead at 973, 1014, 1054 & 1095K	189
6.4	Variation of f_{O}^{Sn} in Pb-Sn alloys with reciprocal of temperature	193
6.5	Activity coefficient of oxygen in Pb-Sn alloys at 1014K	194
7.1	Variation of $\ln f_{\text{O}}^{\text{i}}$ and $\ln f_{\text{O}}^{\text{Sn}}$ in the ternary Pb-i-O at 1095K ($i=\text{Cu}, \text{Bi}$)	206

LIST OF TABLES

Table No.	Title	Page
1.1	Electrical properties of solid oxide electrolytes	16
1.2	Problems commonly encountered in solid electrolyte materials and their remedies	18
1.3	Solid electrolyte emf cell details	27
1.4	Typical results on systems with oxygen in pure metals and binary metallic solvents	38
1.5	Multicomponent metallic systems	55
3.1	Emf data on lead-oxygen system	98
3.2	Standard free energy of formation, $\Delta G_{\text{PbO}}^{\circ}$ of yellow PbO	100
3.3	Thermodynamic functions for dissolution of oxygen in molten lead at different temperatures	105
3.4	Free energy change, $\Delta G_{\text{O(Pb)}}^{\circ}$ for dissolution gaseous oxygen into molten lead (1 atom pct standard state)	110
4.1	Emf data at different temperatures and values of copper concentration	116
4.2	Calculated values on oxygen dissolution in Pb-Cu-O system from emf data	120
4.3	Calculated values of ternary interaction parameters at different temperatures	124
4.4	Experimental values of ternary interaction parameter, $\epsilon_{\text{O(Pb)}}^{\text{Cu}}$ at different temperatures	126
4.5	Activity coefficient, $\ln f_{\text{O}}^{\text{Cu}}$ in Pb-Cu-O system at different temperatures and copper concentration	132
4.6	Relative partial molar enthalpy and entropy and entropy of oxygen relative to gaseous oxygen in Pb-Cu-alloys	134

Table No.	Title	Page
4.7	Predicted values of $\ln f_{\text{O}}^{\text{Cu}}$ vs copper concentration at 1095K	136
5.1	Emf data on Pb-Bi-O at different temperatures and values of bismuth concentration	146
5.2	Calculated values on oxygen dissolution in Pb-Bi-O system from emf data	149
5.3	Experimental values of ternary interaction parameter, $\epsilon_{\text{O}}^{\text{Bi}}$ at different temperature	152
5.4	Calculated values of ternary interaction parameter, $\epsilon_{\text{O}}^{\text{Bi}}$ at different temperature	153
5.5	Activity coefficient, $\ln f_{\text{O}}^{\text{Bi}}$ in Pb-Bi-O system at different temperatures and values of bismuth concentration	157
5.6	Predicted values of ternary interaction parameter, $\ln f_{\text{O}}^{\text{Bi}}(\text{Pb})$ at 1034 K	162
5.7	Predicted values of activity coefficient $\ln f_{\text{O}}(\text{Pb+Bi})$ at 1034K	163
6.1	Emf data on Pb-Sn-O system at different temperature and values of tin concentrations	174
6.2	Calculated values on oxygen dissolution in Pb-Sn-O system from emf data	176
6.3	Calculated values of ternary interaction parameter, $\epsilon_{\text{O}}^{\text{Sn}}$ at different temperatures	182
6.4	Comparison of ternary interaction parameter, $\epsilon_{\text{O}}^{\text{Sn}}(\text{Pb})$ at different temperatures	183
6.5	Activity coefficient of oxygen, in Pb-Sn-O system at different temperatures and tin concentrations	186
6.6	$\ln f_{\text{O}}^{\text{Sn}}$ in lead at different atom sn at experimental temperatures	189
6.7	ΔH_{O} & ΔS_{O} at different atom pct tin	189

NOMENCLATURE

A, B	Components of substitutional metallic alloy system
N_A, N_B	Mole fractions of A and B respectively in solution of A+B metallic components
$\Delta G_{X(A)}, \Delta G_{X(B)}$	Gibb's free energy change for dissolution of solute 'X' in metal solvents A & B respectively
$\Delta G_{O(A)}, \Delta G_{O(B)}$	Gibb's free energy change for dissolution of oxygen in metal solvents in A & B respectively.
$\Delta G_{O(A+B)}$	Gibb's-free energy change for dissolution of oxygen in binary metallic system, A+B
$\Delta G^{XS, \text{exchange}}$	Excess free energy change when A-O contact is changed to a B-O contact in a system, A-A-B-O
ΔG_{PbO}°	Standard free energy of formation of yellow lead oxide
ΔG_{SnO}°	Standard free energy of formation of SnO(G)
$\Delta G_{SnO_2}^{\circ}$	Standard free energy change for formation of SnO ₂
$\Delta \bar{H}O(A)$	Partial molar enthalpy of dissolution of oxygen in metal component A
$\Delta \bar{S}O(A)$	Partial molar entropy of dissolution of oxygen in metallic component A
$f_{A(A+B)}, f_{B(A+B)}$	Activity coefficients of components A and B respectively in alloy system A+B
$fO(A), fO(B)$	Activity coefficients of oxygen in pure metals A and B respectively
$f_{O(A)}^B$	Ternary interaction coefficient of solute B on oxygen in metal A.
$\epsilon_{O(Pb)}^O$	Self interaction parameter of oxygen on oxygen in lead
$\epsilon_{O(A)}^B$	Ternary interaction parameter of B on oxygen in metal A

ϵ	Regular solution parameter
Z	Co-ordination number indicating the number of nearest neighbours shared by an atom in solution
α	Regular solution parameter
$\Psi_{O(A)}, \Psi_{O(B)}$	Modified activity coefficients of oxygen in metals A and B respectively
$\Psi_{O(A+B)}$	Modified activity coefficients in binary metallic alloy A+B
ϕ	Ratio of $f_{O(A)}/f_{O(B)}$ in metallic system A-B-O
h	Wagner's single energy parameter
h_1, h_2	Energy parameters suggested by Chiang & Change
$p_{O_2}(Ni, NiO)$	Partial pressure of gaseous oxygen in equilibrium with Ni+NiO
$p_{O_2}(Pb, PbO)$	Partial pressure of gaseous oxygen in Pb+PbO
E	Reversible cell emf of solid electrolyte emf cell
F	Faraday's constant
ΔG°	Free energy change of cell reaction in a concentration cell
V_a, V_b	Valances of metals A & B respectively as given by Pauling

CONTENTS

	Page
CANDIDATE'S DECLARATION	i
ABSTRACT	ii
ACKNOWLEDGEMENTS	vi
LIST OF FIGURES	vii
LIST OF TABLES	x
NOMENCLATURE	xi
CHAPTER I	GENERAL
	1-79
1.1	Introduction
	1
1.2	Literature Survey
	5
1.2.1	Experimental Techniques
	5
1.2.1.1	Calorimetry
	6
1.2.1.2	Vapour Pressure Method
	9
1.2.1.3	Chemical Equilibria
	11
1.2.1.4	Emf Method
	13
1.2.1.4.1	Solid electrolyte cells
	14
1.2.1.4.2	Pre-requisites for cell design
	17
1.2.1.4.3	Sources of error & Precautions required
	19
1.2.1.4.4	Solid electrolyte emf techniques
	21
1.2.1.4.4.1	Coulometric titration technique
	22
1.2.1.4.4.2	Sampling and analysis technique
	24
1.2.2	Experimental Studies
	26
1.2.2.1	Binary systems
	26
1.2.2.1.1	Lead oxygen binary system
	26
1.2.2.1.2	Copper oxygen binary system
	35

	Page
1.2.2.1.3	Tin oxygen binary system 37
1.2.2.1.4	Bismuth oxygen binary system 43
1.2.2.1.5	Other metal oxygen system 43
1.2.2.2	Ternary Systems 44
1.2.2.2.1	Lead-copper-oxygen system 44
1.2.2.2.2	Lead-tin-oxygen 45
1.2.2.2.3	Lead-bismuth oxygen and lead-antimony- oxygen 45
1.2.2.2.4	Other lead base ternary systems 46
1.2.2.2.5	Copper-nickel-oxygen and copper-manganese- oxygen 46
1.2.2.2.6	Copper-bismuth oxygen 47
1.2.2.2.7	Copper-tin-oxygen 48
1.2.2.2.8	Copper-silver-oxygen 49
1.2.2.2.9	Copper-sulphur-oxygen and copper- selenium oxygen 49
1.2.2.2.10	Other copper base ternary systems 50
1.2.2.2.11	Iron based ternary systems 51
1.2.2.2.12	Bismuth based ternary systems 52
1.2.2.2.13	Silver based ternary systems 53
1.2.2.2.14	Other ternary systems 54
1.2.2.3	Multi component systems 54
1.2.3	Theoretical Studies-Thermodynamic Models 56
1.2.3.1	Classical thermodynamic models 57
1.2.3.2	Statistical thermodynamic models 67
1.2.3.3	Quantum mechanical approaches 76
1.3	Formulation of the Problem 77

		Page
CHAPTER II	EXPERIMENTAL	80-94
2.1	Experimental Set-up	80
2.1.1	Cell Assembly & Main Furnace	80
2.1.2	Gas Purification Train	84
2.1.3	Temperature Control Panel & Recording Device	86
2.2	Preparation of Materials	87
2.2.1	Preparatio of Pure Metal & Alloys	87
2.2.2	Preparation of Slags	87
2.3	Experimental Procedure	88
2.4.1	Analysis of oxygen in Metal samples	93
2.4.2	Analysis of Copper, Bismuth & Tin	94
CHAPTER III	LEAD OXYGEN SYSTEM	95-113
3.1	EMF Cell	95
3.2	Testing of <u>Pro</u> per Cell Functioning	96
3.3	Oxygen in Molten Lead	101
3.3.1	Discussion of Results	104
CHAPTER IV	LEAD-COPPER-OXYGEN SYSTEM	114-141
4.1	Results & Calculations	114
4.2	Discussion of Results	119
4.2.1	Wagner's Interaction Parameter Formulation	119
4.2.2	Quasichemical Formulations	127
4.3	Applicability of Solution Model	135
CHAPTER V	LEAD-BISMUTH-OXYGEN SYSTEM	142-169
5.1	Results & Calculations	143
5.2	Discussion of Results	147

	Page
5.2.1	Wagner's Interaction Parameter Formulations 147
5.2.2	Quasichemical Formulation 153
5.3	Discussion of Results 159
5.3.1	Applicability of Solution Models 160
CHAPTER VI	LEAD-TIN-OXYGEN SYSTEM 170-201
6.1	Results and Calculations 171
6.2	Calculation of Interaction Parameters 173
6.2.1	Wagner's Interaction parameter Formulation 176
6.2.2	Quasichemical Formulation 182
6.3	Discussion of Results 188
6.3.1	Applicability of Solution Models 190
CHAPTER VII	SUMMARY AND CONCLUSIONS 201-207
7.1	Lead-Oxygen Binary System 292
7.2	Lead-Copper-Oxygen Ternary System 203
7.3	Lead-Bismuth-Oxygen Ternary Systems 204
7.4	Lead-Tin-Oxygen Ternary System 206
	SUGGESTIONS FOR FUTURE WORK 208
	APPENDIX I 209
	APPENDIX II 211
	REFERENCES 214-225

CHAPTER - I

GENERAL

1.1 INTRODUCTION

Metals are seldom employed in pure state rather invariably as alloys, wherein the presence of alloying elements enhance their useful characteristics. In nature too they occur in ore-values as Oxides, sulphides, halides or oxidised compounds in association with a host of other unwanted constituents called 'gangue' either in elemental form or as compounds. A process metallurgist concerned with the extraction and refining of metals from their primary or secondary sources or a chemist, chemical technologist or a chemical engineer, interested in the recovery of chemicals from these, is involved essentially in devising and operating suitable processes for the controlled removal of unwanted and harmful components present in the feed analysis either as mechanical mixtures, solutions or in a chemical combination. Such processes invariably involve multi-component, single or multiphase reactive systems and undergo either homogeneous or heterogeneous reactions. Metal and slag are the most commonly involved phases in metallurgical reactive systems; wherein the impurities from the former are transferred to the later. However, the behaviour

of any component in a multicomponent system or a solution in any of the phases is governed not merely by its apparent concentration but instead by its effective concentration measured as activity. The thermodynamic properties viz. activity, activity coefficients, interaction parameters, partial molar properties etc. of different components in such multicomponent single or multiphase systems therefore, become basic parameters that determine the feasibility and the extent to which different chemical reactions or phase transformation processes in such systems would take place. An accurate knowledge of these is also important for the optimisation and control of the existing processes and also for the development of new technology.

A material scientist engaged in the development of newer metallic materials is also concerned with metallic solutions as well as multicomponent-multiphase systems. The thermodynamic properties of different components present in such systems play significant role in determining stability limits and the stability characteristics of the different constituents or phases of the alloy being developed. Therefore, extensive thermodynamic data has been experimentally determined on metallic solutions, ionic melts and other compounds by several investigators over the past and presented in tabular and other forms [1-4]. The existing data is also conti-

nuously corrected, modified or substituted by more reliable data as and when acquired by using more accurate and latest research techniques. However, the experimental techniques employed are in general tedious, time consuming and costly, requiring high-purity materials, controlled furnace atmospheres at elevated temperatures over long periods to attain equilibrium in such systems. Attempts have, therefore, been simultaneously made especially in the recent past for the theoretical formulation and prediction of thermodynamic properties of such systems and as a result several theoretical models have been developed to predict their thermodynamic behaviour.

The metal lead has been known since antiquity. As reflected by statistics on world production and consumption of this metal [5] lead and its alloys find extensive applications in engineering, chemical and electrical industries due to an excellent combination of its properties viz. superior formability and workability, higher corrosion resistance towards acids, alkalies and other organic and inorganic chemicals, low melting temperature, good casting characteristics etc. etc. As 'Type-metal' it is extensively used in printing industry for casting letters - both as monotype and lenotype. As die-casting alloys, it is used for parts of measuring instruments such as meters where low strength and high accuracy is desired. Lead alloys,

called babbitts, are used as shell or bushing in journal bearings. With tin it forms a series of solders and with bismuth or cadmium, a series of fusible alloys. On account of excellent extruding characteristics, lead alloys are ideally suited for sheathing of cables used in power installations and communication systems. Lead foils in thicknesses of 0.005 mm upwards are employed for measuring explosion pressures, wrapping cables and in packing industry. Lead powders find application as a constituent of rust-prevention paints for steel, to make lead storage battery plates and in apparatus for radiation protection and also for friction materials in auto-industry. Lead coatings for protection against corrosion are used in case of steel, copper, zinc and aluminium and their alloys. Lead and its alloys are also used for making pipes, bends, wires, strip and also lead-wool or string meant for sealing purpose. As building material, lead sheets are used for lining and bends etc. Its resistance to chemicals makes it an ideal material for chemical storage vessels, evaporating vessels, valves, pumps, stirrers etc.

In all such applications, antimony, tin, copper, bismuth, cadmium etc. constitute the common alloy-additions to improve the mechanical properties or to impart other desirable characteristics for specific applications. These alongwith silver and gold also constitute the

major impurities in the crude lead obtained from lead blast furnace and lead refining is basically concerned with their subsequent elimination. Behaviour of oxygen in lead especially in presence of these elements and also the oxidation behaviour of these elements, when present in dilute concentrations in lead, therefore forms an interesting study. However, a few studies have been reported in literature on these aspects. In view of the versatile nature of lead and its increasing industrial significance as indicated above, the importance of a systematic study of the thermodynamic behaviour of oxygen in lead base metallic solutions, therefore, can't be over emphasized. The different methods employed and important studies made as revealed by a survey of available literature will therefore be reviewed in the following sections.

1.2 LITERATURE SURVEY

1.2.1 Experimental Techniques

Of the several methods employed for the measurement of thermodynamic properties, calorimetry, vapour pressure technique, equilibrium method and emf technique are the commonly employed ones. Extended discussion on the different methods are available in literature [2,6-8]. However, a brief review of these with greater emphasis on emf technique, employed in the present work is presented in the following sub sections:

1.2.1.1 Calorimetry

The term calorimetry refers to the measurement of the change in enthalpy or internal energy associated with any process, chemical reaction or a physical change by measuring the heat exchange, as reflected by a change in temperature in a suitably devised apparatus called 'calorimeter'. Corrected value of change in temperature multiplied by the water equivalent of the calorimeter, invariably gives the desired value of energy or heat exchanged. The data so obtained is employed using appropriate expressions for the calculation of relevant thermodynamic properties viz. the heat of formation, the standard enthalpy change, heat capacity, heat of phase-transformation or the Gibbs free energy change of a reaction etc. The different types of calorimeters employed for such studies may be classified into three categories on the basis of variables i.e. Calorimeter temperature, the temperature of the surroundings and heat produced per unit time into Isotherm, Isothermal, Adiabatic and heat flow calorimeters respectively.

Isotherm calorimeters have their surroundings maintained at constant temperature while the temperature of the inner vessel called 'bomb' is measured before, during and after the reaction is over. The 'bomb' consists of a strong steel shell lined with an inert material and fitted with a gas tight screw cap. It is provided

with arrangement for filling inside it oxygen at high pressures ~ 25 atmospheres and later igniting a fuse wire to initiate a reaction under study. For temperature measurement either a beckmann thermometer or a platinum resistance thermometer is employed. To determine the heat change in a process, the 'bomb' is charged with a known amount of the reactant, the calorimeter assembled and reaction is initiated. The corresponding change in temperature as well as its rate of change till it attains the temperature of the surroundings is noted to arrive at the desired heat effect. The water equivalent of the calorimeter is determined by carrying out the said process with a standard substance of known heat content.

In the isothermal calorimeters, the temperature of the surroundings and the inner vessel of the calorimeter is maintained equal as well as constant during the time an experiment is conducted. The accompanied heat change is measured through a phase transformation. Commonly a mixture of ice and water are employed for this purpose and any change in their proportion due to an exchange of heat is reflected through a change in the volume of the system.

In the adiabatic calorimeters, the changes in temperature of the calorimeter and the surroundings are so adjusted that they remain numerically equal. This advantageously eliminates any correction needed for heat exchanged with the surroundings. In construction,

these resemble isoperibol calorimeters except that a heating coil is provided in the former either at the outerwall of the inner vessel or on the innerwall of the outer vessel; the procedures followed in the two being also similar. The energy input is measured by the current and the voltage drop. Adiabatic calorimeters are used for the determination of heat capacity of a substance as well as heat of a slow or an endothermic reaction. The 'constant heat flow type calorimeters' designed to keep the temperature difference between the surroundings and the inner calorimeter constant are employed for determination of heat capacities of substances. These enable a constant amount of heat to flow from the calorimeter to the surroundings. However, these need standardization.

Several sources of error are encountered during a calorimetric measurement and unless adequate precautions are taken, the heat changes determined are not reliable. The random, physical or statistical errors include errors involved in measurement of temperature, inaccurate determination of water equivalent of calorimeter or on account of an inadequate compensation of heat losses. With proper control these can be easily controlled or minimised. The systematic errors on the other hand are chemical in nature and are far more serious. These may be owing to the presence of impurities in

the test sample or in the reaction vessel of the calorimeter employed leading to simultaneous side reactions or on account of reaction under investigation not attaining completion. This can be taken care of, if the test sample is properly analysed so that the amount of impurities is known and suitable correction applied. X-ray and micrographic analysis may also be undertaken to ascertain the completeness of the reaction under examination.

1.2.1.2 Vapour pressure method

Vapour pressure studies are undertaken to determine the activity of a component in an alloy as also the free energy change, enthalpy and entropy of formation of gaseous as well as condensed species. Depending upon the magnitude of the pressure to be measured, the vapour pressure methods are grouped as 'Direct' and 'Indirect' methods. For vapour pressures greater than 10^{-3} atm., direct pressure measurements are employed using mechanical devices such as manometers, sickel gauges or diaphragm gauges etc. These have been discussed at length by Clopper et al. [9].

At vapour pressures below 10^{-3} atmosphere, the mean free path of molecules becomes progressively large and methods for vapour pressure measurement are based on the principle of kinetic theory of gases. The two techniques used viz. the Knudsen Technique [10]

and the Langmuir Technique [11] involve 'effusion principles'. In the Knudsen method, the effusion rate of molecules is measured through a knife edged orifice of diameter less than one tenth of the mean free path of the molecules in the vapour, drilled into the lid of a gas tight container holding the vapour species. Knowing the weight loss accompanying the effusion process, the orifice area, temperature and time of effusion, the desired partial pressure can be calculated. The loss in weight accompanying the effusion process being determined by employing any of the techniques viz. weighing the cell before and after the experiment; suspending the cell from a vacuum balance to directly read the change in weight accompanying the process or else by collecting the effusion vapours on one or more targets for a known interval of time etc.

For still lower vapour pressure, the free evaporation method of Langmuir offers advantage, in that it allows measurement of pressure as low as 10^{-7} mm Hg. Here the rate of vapourization of molecules from the surface of a sample heated in vacuum is measured. For accurate measurements it is ensured that all vapours must condense and the temperature of the sample must be higher than the surrounding walls. The effusion methods are applicable provided the effusing vapour species are simple and chemically well defined (i.e. the molecular

weight of the species is known). However, if the vapour species is complex, use of mass-spectrometer is advantageous for the identification of the vapour species as well as for the determination of vapour pressure. It also permits the measurement of vapour pressure of a vapour species without interference by impurities.

1.2.1.3 Chemical equilibria

Chemical equilibria techniques have been more commonly employed for determination of chemical potential and activity of components especially in the high temperature studies involving reactions between a gaseous phase and a condensed phase or between two condensed phases. In the former case a suitably selected gaseous mixture is equilibrated with a condensed phase at a preselected temperature. From the data so obtained, the thermodynamic behaviour of the species in the condensed phase is predicted. The choice of gaseous mixture depends upon the specific chemical potential desired, the ease of developing a gas mixture and the capability of transporting the species at a reasonable rate. The commonly used gaseous mixtures include $H_2 - CH_4$ (for C and H Chemical potentials), $O_2 - H_2O$ or $O_2 - CO_2$ mixtures (for O-potential) $SO_2 - O_2$ mixtures (for S and O potentials), $H_2 - NH_3$ mixtures (for N-potential) $H_2 - HCl$ mixture (for H and Cl potentials) and $CO - CO_2$ mixture (for C potential) etc.

Three types of experimental set-up viz. the 'open circuit', 'closed circuit' and 'static atmosphere' experiments have been used of which the former two are more common. In open-circuit experiments, a gas is passed over a particular condensed phase to saturate it with the desired vapour species and then allowed to react with another condensed phase contained in the same reaction vessel. In closed circuit experiments, the reacting species are transferred from one condensed phase at any temperature to the other condensed phase at a different temperature via a suitable gas circulating device. The reacting specie in the gas phase is thus transferred to the condensed phase under study. In static atmosphere technique on the other hand, either a pure gas or a gas mixture of definite composition is encapsulated with the condensed phase under isothermal conditions. Twin quartz capsules have been used for such studies.

Major problems and sources of error in this technique [12] include:

- i) Evolution of occluded gases from materials of construction of apparatus. This may be taken care of by conducting few blank determinations to compensate for error and making use of specially prepared materials.
- ii) Thermal diffusion due to difference in densities of constituents of the gaseous mixture leading to segregation of lighter ones in high temperature

zones and vice-versa. This may be compensated by having faster flow rates.

- iii) Non-availability or limited availability of material of construction for high temperature work including gas tight and leak proof joints. Equilibria between condensed phases such as slag-metal systems involve extensive sampling and chemical analysis for study of equilibrated components, indicating obvious preference for 'labelled compounds' for study, whenever possible.

1.2.1.4 Emf method

Of the various techniques used for experimental determination of thermodynamic properties of metallic solutions, the emf method is most convenient and yields very reliable results, provided of course the cell has been properly set up and operated with well defined and reversible cell reactions. The necessary condition for its usage, however, is that the process under study be such that, its energy is capable of generating a reversible emf either in a 'galvanic cell' for estimation of free energy of chemical reactions or in a concentration cell for determination of activity of a component in binary or higher component systems. The emf method permits direct measurement of thermodynamic properties, is quicker and more reliable.

Different types of cells employed for emf studies

are generally classified as aqueous-electrolyte cells, fused-salt electrolyte cells and solid-electrolyte cells, of which the last group has become very significant recently and has been used in the present study. It has therefore, been discussed in greater detail in the following sub-sections.

1.2.1.4.1 Solid electrolyte cells

The usefulness of the solid halide and oxide-electrolytes for determination of thermodynamic properties of metallic compounds has been known since the beginning of this century, but the real impetus to renewed interest in the possible applications of solid-electrolytes was initiated by Kiukkola and Wagner [13], who, in the year 1957, demonstrated their immense potentialities in the determination of thermodynamic properties of metals and alloys. Recently these have been extensively employed for equilibrium applications to study the thermodynamics and solubility of oxygen in pure metals, binary alloys, multicomponent alloy systems and also in studies on oxide-slugs, determination of phase boundaries as well as for the studies concerning evaporation and condensation, diffusion in metals, and also, Kinetic studies. The solid electrolytes have also been advantageously used in fuel cells, in which their applications offer solution to various problems encountered with aqueous electrolytes in solid state batteries. However, to build-

up and keep a stable potential difference of the order of one volt in a galvanic cell, a certain minimum conductivity of the electrolyte must be exceeded and Schmalzried [14] puts this value of $10^{-6} \Omega^{-1} \text{ cm}^{-1}$. In view of the extensive studies made using solid electrolytes, excellent reviews have been written to cover the different aspects of their usage by Etsell and Flengas [15] on electrical properties of solid electrolytes; by Schmalzried [14] on emf measurements in different metallurgical and chemical systems by Fitterer [16] and also by Ramarao and Tare [17] on their applications to metallurgical systems by Iwase and More [18], on some of the problems encountered in their use as oxygen probes as well as on general aspects, by Rapp et al. [7], and Kubaschewski and Evans [2].

Several species of specially formulated chemicals serve as solid electrolytes. The commonly used ones being, $\text{ThO}_2\text{-Y}_2\text{O}_3$ (1-25 mole percent Y_2O_3), $\text{ZrO}_2\text{-CaO}$ (5-20 mole percent CaO), $\text{ThO}_2\text{-CaO}$ (5 mole percent CaO), $\text{ThO}_2\text{-LaO}_{1.5}$ (10-15 percent $\text{LaO}_{1.5}$). Of these $\text{ZrO}_2\text{-CaO}$ solid electrolytes have been most commonly employed. Table 1.1 presents the important characteristics of commonly used solid electrolytes and does not need any further explanation.

Several problems are encountered in the use

Table 1.1 : Electrical properties of solid oxide electrolytes [15]

(a) Electrical Conductivities

Electrolyte	% anion vacancies	Ionic conductivity at 1000° cm ⁻¹ x 10 ² ohm ⁻¹	Activation energy KJ /mol
ZrO ₂ + 12% CaO	6.0	5.5	105.43
ZrO ₂ + 9% Y ₂ O ₃	4.1	12.0	76.98
ZrO ₂ + 10% Sm ₂ O ₃	4.5	5.8	92.05
ZrO ₂ + 8% Y ₂ O ₃	0.7	8.8	72.4
ZrO ₂ + 10% Sc ₂ O ₃	4.5	25.0	62.34
ThO ₂ + 8% Y ₂ O ₃	3.7	0.48	106.27
ThO ₂ + 5% CaO	2.5	0.047	106.69
CeO ₂ + 11% La ₂ O ₃	5.0	8.0	87.86
CeO ₂ + 15% CaO	7.5	2.5	72.38
HfO ₂ + 8% Y ₂ O ₃	3.7	2.9	107.95
HfO ₂ + 12% CaO	6.0	0.40	138.07
La ₂ O ₃ + 15% CaO	2.7	2.4	84.93

(b) Transport Numbers

Electrolyte	Temperature °C	Oxygen pressure range for t _i >0.99
ZrO ₂ - CaO	1000	1 to 10 ⁻²⁰
	1600	1 to 10 ⁻¹²
ThO ₂ - Y ₂ O ₃	1000	10 ⁻⁷ to 10 ⁻²⁴
	1600	10 ⁻⁷ to 10 ⁻¹⁶
La ₂ O ₃ - CaO	1000	10 ⁻⁸ to < 10 ⁻²¹

of solid electrolyte materials for emf studies. Unless proper care is taken, the results obtained do not confirm to equilibrium and lead to serious errors. Table 1.2 lists the problems commonly encountered, factors influencing, their probable causes and remedies needed to do away with them.

1.2.1.4.2 Pre-requisites for cell design

Zirconia and Thoria electrolytes have the advantage that these can be shaped into crucibles and tubes and very safely provide electrode separation in the solid electrolyte cells for emf measurement. In the selection of an electrolyte, the experimental technique and oxygen pressure of the melt form important criterion. Zirconia based electrolytes are preferred for oxygen pressures greater than 10^{-2} atms. at 1000°C while thoria based electrolytes are generally employed when working in the lower pressure range up to 10^{-30} atm. of oxygen at 1000°C . For emf measurements in liquid melts, the electrode lead wire is also chosen carefully so that it is insoluble in the melt and avoids any side reaction that may add or remove oxygen from the melt. Table 1.3 presents different contact materials employed for emf studies. However, the most important consideration in the cell design is the development of a reversible emf due only to the cell reaction under study. It is therefore, ensured that only the reaction under investi-

Table 1.2 : Problems commonly encountered in solid electrolyte materials and their causes and remedies [18,19]

Sr.No.	Problems	Probable causes	Suggested remedies
1.	Lower t_{O_2} - due to electron conduction	<ol style="list-style-type: none"> 1. Presence of impurities 2. Inhomogeneous distribution of phases (especially partially stabilized) 	<ol style="list-style-type: none"> 1. Use of high purity and fully stabilized material 2. Doping with a material possessing minimum electron conduction
2.	Oxygen permeability (at open circuit condition) from one electrode to another through electrolyte wall.	<ol style="list-style-type: none"> 1. Ionic conductivity 2. Electron conduction parameters 3. Wall thickness 	<ol style="list-style-type: none"> 1. Increasing wall thickness 2. Use of high purity and fully stabilized material
3.	Poor thermal shock resistance	Initiation of phase inversion of pure ZrO_2 (creates large crack density)	Use of partially stabilized solid electrolyte material

gation occurs in the cell and no other process: chemical reaction, physical or physico-chemical phenomenon nor any other external source should directly or indirectly contribute to the emf so produced or measured. The cell feasibility should therefore be adequately studied before hands.

The reference electrode should be chosen which most nearly matches the oxygen potential of the unknown system under investigation. Minimising this difference or in other words lowering the emf of the cell reduces considerably the effect of any electronic short circuiting within the cell.

1.2.1.4.3 Sources of error and precautions required

Properly designed and set up galvanic cells incorporating solid electrolyte often yield very accurate thermodynamic data. However, there are several sources of error [14,69] which must be avoided by taking adequate precautions, viz.

- i) The external emf due to thermoelectric or 'eddy currents' should be avoided. This is achieved by suitably locating the cell in the constant temperature zone of the furnace, preferably surrounded by an earthed metallic tube of high thermal conductivity to extend the constant temperature zone and also to neutralise any interfering eddy current emf. Absence of any

- stray emf is reflected by momentarily switching off the furnace when the cell remains unaltered.
- ii) Preferably same lead wires should be used for the melt and the reference electrode. If however, different wires are employed, the observed voltage must be corrected for the thermoelectric voltage.
- iii) The lead wire to the melt should be held above the melt and immersed for short duration during which the cell voltage is measured. This would avoid any dissolution of the lead material into the melt.
- iv) The low melting solute viz. Sn etc. when present in the liquid electrode undergoes vapourization during the course of an experiment. Adequate compensation for the loss needs to be given in the measurements.
- v) Attainment of equilibrium in the melt must be ensured for development of reversible emf in all thermodynamic measurements. This can be judged:
- a) from the constancy of cell emf vs. time,
 - b) by disturbing the equilibrium momentarily by either raising or lowering its temperature by small amounts. The emf returns to the same constant value at the experimental

temperature,

- c) By passing a small current approx. 50 mA through the cell for 5 mins. in either direction to see that emf returns to its initial value in a few minutes and thereafter remains constant with time [22, 23],
 - d) the emf should be independent of the flow rate of inert gas (say Argon) in the cell [7].
- vi) Electrodes should consist of fresh and high purity materials. The impurities lead to the formation of localized concentration cells and give rise to errors in the cell emf. The solid electrolyte containing the reference Metal-Metal oxide mixture should be properly packed and sintered under an inert atmosphere and sealed.
- vii) Other sources of error viz. permeability or electron conduction in the electrolyte; short-short circuiting by gaseous environment should be avoided as far as possible

1.2.1.4.4 Solid electrolyte emf techniques

The following solid electrolyte emf techniques have been extensively employed by different investigators to study the thermodynamic behaviour of oxygen in pure metals and alloy systems.

1.2.1.4.4.1 Coulometric titration technique

Although first introduced by Wagner [24], the technique was extensively employed by Alcock and Belford in their studies on Lead-oxygen [25] and tin-oxygen [26] systems. In this method a weighed amount of metal under study is taken in a solid electrolyte crucible and constitutes one electrode. Two identical Ni-NiO electrodes are used, one for oxygen variation in the metal and the other as reference electrode for measurement of oxygen activity in the liquid alloy system under study. This arrangement is necessary, otherwise coulometric transfer of oxygen from Ni-NiO electrode will lead to polarisation rendering it unsuitable as reference electrode. During the experimental run, a known amount of oxygen is either added to or removed from the metal system by passing a known quantity of electricity across the cell. The attainment of steady emf during the titration is a linear function of the magnitude of current and inverse function of the cell temperature and oxygen concentration in the metal/alloy. Kayahara et al. [27] Tyler [28] also employed similar coulometric techniques in their studies.

Pastorek and Rapp [29], and Szwarc, Oberg and Rapp [30] studied properties of oxygen in the lower concentration range. In metallic systems, at which the electron conduction is not negligible by making use

of the potentiostatic coulometric titration. For such studies, the cell consisted of liquid metal contained inside a solid electrolyte tube, whose outer surface up to the level of liquid metal had three or four coatings of porous-platinum (with each layer fired at 800°C , before the coating of next layer) to achieve low contact resistance. An inside platinum lead and an outer chromel lead were connected to a working potentiostat. For an experimental run, the cell was initially brought at a steady state at a voltage say E_1 applied by the potentiostat which was slowly changed to E_2 and the resulting diffusion controlled current was recorded till a constant residual current was indicated. To have reproducible and consistent results, oxygen concentration was restricted to a low concentration range corresponding to an applied voltage in the range $700\text{ mv} < E_{\text{app}} < 900\text{ mv}$. At higher oxygen concentrations corresponding to $E > 500\text{ mv}$, sustained transient ionic current caused the experiment to deviate from a truly potentiostatic one. To approximate truly potentiostatic conditions, the voltage drop, $I_{\text{ion}} \cdot \Omega_{\text{ion}}$ was maintained relative to ΔE applied by selecting an 'advantageous oxygen concentration range'.

Otsuka and Kozuka employed a modified coulometric titration technique for an extension work on diffusivity and solubility of oxygen in several liquid metallic

systems viz. Cu-Pb[31], Pb,Sb[32], Te[33], Th & In[34], Pb & Sb[35], Bi,Sn & Ge[36], In-Sb[37], Cu & Ag[38], Bi-Ti[39], Elements of group I(b) and VI(b)[40], Cu-Bi[41], Cu-Ti[42], Cu-Sb[43], Oxygen in copper melt with Selenium & Tellurium [44], Ti-Te[45], Cu-In and Cu-Sn[46], Ag-Bi & Ag-Ti[47], Ag-Pb[49] and Bi-Pb as well as Bi-Sb[50]. They also studied the diffusivity of oxygen in Indium and Tin [48] using modified coulometric titration technique.

Their cell assembly was identical to that used by Rapp et al.[51,152] except that in their experimental set-up, two lead wires were connected to each electrode. The potentiostatic experiments became possible by applying a voltage between one pair of leads (connected to each electrode) so that emf developed between the other pair (connected to the same electrode) of leads had a pre-selected value. Such an arrangement eliminated the IR drop in the lead wires and thus enabled equally successful and reliable studies conducted both in low as well as high oxygen concentration range in metals and alloys.

1.2.1.4.4.2 Sampling and analysis technique

This method has been extensively employed to study the thermodynamic behaviour of oxygen in metals and alloys by a large number of investigators. Kemori et al. studied solubility of oxygen in liquid copper [53] and nickel (liquid and solid) equilibrated with both NiO(S) and $NiX_2O_4(S)$ [X=Al,Ga] [54], Iwase, Takeshita

& Mori studied oxygen in liquid iron-nickel alloys [55] and in liquid nickel [56]. Seetharaman et al. used this technique in their study on Zinc-oxygen interaction on liquid Cu [57] and Mn-O interaction in dilute liquid copper alloys [58] and Anja Taskinen on study of oxygen in Lead [59] and Pb-Ag alloys [63], Pb-Ni [64], Pb-Bi [65]. Anja et al. employed such an arrangement to study oxygen in Pb-Cu [60, 61, 62], Jacob to study Pb-O system [66] & Jacob & Jeffes studied Pb, Cu & Pb-Cu alloys [22] Pb-Sn [23] Cu-Sn [67], Ag-Pb [68], while Jacob et al. employed analysis and sampling technique in the study of Cu-Ag [69] Cu-Fe [70], liquid Sb [72] & liquid Mn [73]. In this, the cell assembly consists of a reference electrode constituted by a solid electrolyte tube containing inside it a mixture of Metal & Metal oxide of known oxygen potential with a lead embedded inside it. The solid electrolyte tube is immersed in a refractory crucible containing the molten metal or the alloy under study. The latter with a contact lead serves the other half cell. The alloy may be taken in a solid electrolyte tube and the other half in the outer crucible. The oxygen content in the metal/alloy is varied either by adding into it a calculated amount of an oxide of the metal constituting the alloys [68-75] or by equilibrating the melt with a suitable slag [54,74,84]. After a reversible emf has been reached at a preselected temperature, a

sample of molten metal is withdrawn from the cell system to give on analysis, the oxygen as well as alloy concentration.

Table 1.3 presents details of different S.E. cell systems used by different workers and needs no further explanation.

1.2.2 Experimental Studies

As pointed out earlier several studies on metal-oxygen systems have been conducted due to their technological importance. The reported studies, relevant to the present investigation and generally making use of solid electrolyte emf cells are briefly reported in the following sub-sections. The binary metal-oxygen systems involving lead, copper, tin and bismuth will be first reviewed. This will be followed by behaviour of oxygen in binary, ternary and quaternary metallic solvent systems.

1.2.2.1 Binary systems

1.2.2.1.1 Lead-oxygen binary systems

Alcock and Belford [25] studied the solubility and free-energy of dissolution of oxygen in liquid lead, $\Delta G_O(\text{Pb})$ in the temperature range 773-973K employing solid electrolyte emf cell. The oxygen concentration in the metal was changed using solid state coulometry from saturation down to 0.002, 0.0003 and 0.0002 atomic percent respectively at 973, 868 and 773K. On further lowering

Table 1.3 Solid electrolyte emf cell details

System	Temp. range	Reference electrode	S.E. used	Contact electrode	Emf Technique	Oxygen concentration variation	Oxygen analysis Technique	Authors	Reference
1	2	3	4	5	6	7	8	9	10
In-O	973-1073	Air, Pt	ZrO ₂ +CaO	Rhenium	Modified Coulometry	Current variation	Coulometric Titration	Otsuka & Kozuka	34, 48
Sb-O	973-1173	-do-	-do- 5%CaO	-do-	-do-	-do-	-do-	Otsuka, Kaku & Kozuka	35
Sn-O	973-1173	-do-	-do-	-do-	-do-	-do-	-do-	Otsuka, Sano & Kozuka	36, 48
Thall-O	973-1173	-do-	-do-	-do-	-do-	-do-	-do-	Otsuka & Kozuka	34
Pb-O	1073-1323	-do-	-do-	Iridium	-do-	-do-	-do-	-do-	32
Cu-O	1373	-do-	-do-	Rhenium	-do-	-do-	-do-	-do-	38
Pb-O	723-873	O ₂ , Pt	ZrO ₂ +Y ₂ O ₃	Platinum	Open top bubble method	Oxygen injection in open top bubble	S.E. oxygen monitor	Conochie, Ebiogwn & Robertson	75
Ag-O	1373	Air, Pt	ZrO ₂ +5% CaO	Iridium	Mod. Coulometry	Current variation	Coulometric Titration	Otsuka & Kozuka	38
Bi-O	973-1173	-do-	-do-	-do-	-do-	-do-	-do-	Otsuka, Sano & Kozuka	36

Contd...

Table 1.3 Contd...

1	2	3	4	5	6	7	8	9	10
Pb-O	783-973	Ni-Nio; Pt	ThO ₂ +15% Y ₂ O ₃	Iridium	Mod. Coulometry	Current variation	Solid State coulometry	Alcock & Bedford	25
Pb-PbO	713-1073	Cu-Cu ₂ O;Pt	ZrO ₂ +14% MgO	-do-	-do-	-do-	-do-	-do-	25
Sb-O	997-1175	-	ZrO ₂ +CaO		Isopeptic technique	Oxide addition	Sampling & Analysis	Jacob & Mathew	72
Pb-O	1073-1203	O ₂ (1 bar), Pt	ZrO ₂ +7%CaO	Pt/Cr- Cermet or LaCrO ₃	Conventional emf tech.	PbO addition	-do-	A.Taskinen	59
Cu-O	1430-1600	N _i -N _i O; Pt	ZrO ₂ +CaO	LaCrO ₃	-do-	Oxide addition	-do-	Kayahara et.al.	27
Cu-O	-	N _i -N _i O	-do-	LaCrO ₃ ; Pt	-do-	-do-	-do-	Yoshihiro Kayahara et.al.	78
Pb-O	1003-1353	Air,Pt.	ZrO ₂ +5%CaO	Chromel wire	Coulometry	Current variation	Coulometric titration	Szwarc, Oberg & Rapp	30
Ge-O	1233-1373	-do-	-do-	Tungsten	Mod.Coulo.	-do-	-do-	Otsuka, et.al	36
Cu-O	1373-1673	N _i -N _i O ;Pt	ZrO ₂ +CaO	Cr-Cermet	Conven. emf.tech.	Oxide addition	Sampling & Analysis	Zacob & Jeffes	22
Pb-O	1023-1173	-do-	-do-	Iridium	-do-	-do-	-do-	-do-	-do-
Cu-Pb-O	1373	-do-	-do-	Cr-Cermet	-do-	-do-	-do-	-do-	-do-

Table 1.3 Contd..

1	2	3	4	5	6	7	8	9	10
N ₂ O	1560		ZrO ₂ +CaO	Lanthanum-chromite	Mod.Coulo. (diffusivity study)	-	-	Otsuka & Kozuka	77
Fe-O	-do-		-do-	-do-				-do-	
Oxygen in Cp Ib-4b	773	Air, Pt	-do-	Rhenium	Mod.Coulo.	Current variation	Coulometric titration	Otsuka, Kurose & Kozuka	40
In-O	1000-1130	-do-	-do-	Tungsten	-do-	-do-	-do-	K.F.Tyar	28
In-Sb-O	-do-	-do-	(Fully Stab.)	-do-	-do-	-do-	-do-	-do-	
Ag-Pb-O	1273-1473	-do-	ZrO ₂ +5%CaO	Rhenium	-do-	-do-	-do-	Otsuka, Kaku & Kozuka	49
Bi-Sb-O	1073	-do-	-do-	-do-	-do-	-do-	-do-	Otsuka & Kozuka	50
Bi-PbO	-do-	-do-	-do-	Iridium	-do-	-do-	-do-	-do-	
In-Sb-O	1073	-do-	-do-	Rhenium	-do-	-do-	-do-	Otsuka et.al.	37
Bi-Ti-O	1073	-do-	-do-	Iridium	-do-	-do-	-do-	-do-	39
Bi-Pb-O	1073	-do-	-do-	-do-	-do-	-do-	-do-	-do-	50
Cu-Pb-O	1403	-do-	-do-	-do-	-do-	-do-	-do-	Otsuka & Kozuka	31

Contd.....

Table 1.3 Contd....

1	2	3	4	5	6	7	8	9	10
Pb-Sn-O	823-1373	N_i - N_iO , Pt, Fe-FeO,Pt	ZrO ₂ +CaO	Cr-Cermet	Conventional emf Tech.	PbO or SnO addition	Sampling and analysis	Jacob & Jeffes	23
Cu-Bi-O	1373-1473	Air, Pt.	ZrO ₂ +7%CaO	Cr, Cr ₂ O ₃ (preoxidised)	-do-	Cu ₂ O addin.	Mass balance	Pekka Taskinen et al.	79
Pb-Bi-O	1103-1173	-do-	-do-	-do-	-do-	Oxide addin.	-do-	Hikka Hiltunen	65
Pb-Sb-O	-do-	-do-	-do-	-do-	-do-	-do-	-do-	A.Taskinen	
Cu-Pb-O	1373-1473	-do-	-do-	-do-	-do-	-do-	-do-	A.Taskinen et al.	61
Pb-Cu-O	1101-1173	O ₂ , Pt.	-do-	-do-	-do-	-do-	-do-	Taskinen & Holopainen	62
Cu-Zn-O	-	N_i - N_iO , Pt.	ZrO ₂ +3.5% CaO	Tungsten	-do-	-do-	Sampling & Analysis	Seetharaman & Staffonson	57
Cu-Mn-O	1473-1573	-do-	-do-	-do-	-do-	-do-	-do-	Seetharaman et al.	58
Te-O ₂ Te-O ₂	753-823	Air, Pt	ZrO ₂ +Y ₂ O ₃	Platinum	Modified Coulo.	Current variation	Coulo. Titration	Otsuka & Kozuka	33
Ag-Bi-O	1273	-do-	ZrO ₂ +CaO	Iridium Spot welded to Kanthal	-do-	-do-	-do-	-do-	47
Ag-Ti-O	1273	-do-	-do-	-do-	-do-	-do-	-do-	-do-	47

Contd.

Table 1.3 Contd..

1	2	3	4	5	6	7	8	9	10
Cu-In-O	1373	Air, Pt	ZrO ₂ +CaO	Rhenium spot welded to Kanthal/Pt.	Modified coulo.	Current variation	Coulometry titration	Otsuka, Kurose & Kozuka	46
Cu-Sn-O	-do-	-do-	-do-	-do-	-do-	-do-	-do-	-do-	45
Ti-Te-O	1073, 1223	-do-	-do-	Rhenium	-do-	-do-	-do-	do-	44
Cu-Se-O	1373	-do-	-do-	-do-	-do-	-do-	-do-	-do-	44
Cu-Te-O	1373	-do-	-do-	-do-	-do-	-do-	-do-	Otsuka, Harnoka & Kozuka	42
Cu-Ti-O	1373	-do-	-do-	Rhenium + Kanthal	-do-	-do-	-do-	Sampling & Katayama & Kojuka Analysis	110
Ni-Cu-O	1733	Ni-NiO	-do-	Pt, LaCrO ₃	Conventional emf Tech.	Oxide addn.			

the emf, the oxygen concentration became non reproducible probably due to slow uptake of oxygen from lead. Their results on oxygen solubility in lead and $\Delta G^{\circ}(\text{Pb})$ are reported in Table 1.4. The values for partial enthalpy and excess entropy of solution of oxygen in lead have been deduced by these authors and are -26540 ± 630 cal/g.atom and $-(12.55 \pm 0.75)$ cal/g.atom per degree respectively. They also obtained the free energy of formation of PbO , $\Delta G^{\circ}\text{PbO}$ using conventional sampling technique and the result is reported in Table 1.4.

Szwarc, Oberg and Rapp [30] studied diffusivity and solubility of oxygen in liquid lead employing potentiostatic technique in the temperature range 1000-1353K. Their results on oxygen solubility and free energy of oxygen dissolution are presented in Table 1.4.

Fischer and Ackerman (91) employed conventional sampling and analysis emf method to study the thermodynamic behaviour of oxygen in molten lead in the temperature range 1003-1353K. Their result on oxygen solubility and free energy of oxygen dissolution are presented in Table 1.4.

Jacob and Jeffes [22] also employed the conventional sampling and analysis technique to study the activity coefficient of oxygen in liquid lead, Copper and copper lead alloys, using Ni and NiO as reference electrode. Their results on $\Delta G^{\circ}(\text{Pb})$ and its temperature depen-

dence are presented in Table 1.4. However, due to uncertainty in the analysis of oxygen and restricted number of experiments performed on Lead-oxygen, deviation from Sievert's law could not be drawn. Calculated values of saturation solubility based on Sievert's law were found to be 3.08 atom percent in equilibrium with lead and lead oxide as compound to 2.9 atom percent reported by Richardson and Web [74]. Their result on $\Delta G^{\circ}(\text{PbO})$ is also reported in Table 1.4.

Shinya Otsuka and Z-Kozuka [35] using modified coulometric titration measured the activity of oxygen in liquid lead in the temperature range 1073-1323K and in low oxygen concentration range. Their values on $\Delta G^{\circ}(\text{Pb})$ with reference state for oxygen as infinitely dilute solution (1 atom %) are also presented in Table 1.4. Deviation of activity from Henry's law reported by Charle et al. [92,93] was, however, not observed by these workers.

A Taskinen [59] also studied the thermodynamic behaviour of oxygen using the conventional emf technique with O_2 (1 bar) as the reference electrode in the temperature range 1103-1173K. Their values on $\Delta G^{\circ}(\text{Pb})$ and self interaction parameter of oxygen, $\epsilon_{\text{O}}^{\circ}(\text{Pb})$ and activity coefficient and their temperature dependence are presented in Table 1.4.

Recently Conochie, Ebiogwn and Robertson [75]

measured the solubility and free energy change for solubility of oxygen in molten lead in the temperature range 723-882K. They employed an open bubble top apparatus for their measurements. Their results on $\Delta G_O(\text{Pb})$ are presented in Table 1.4.

Charle [92,93] studied lead-oxygen system to study the free energy of dissolution of oxygen in lead and its self-interaction parameter. He made his measurements by adding PbO pills one by one to the melt and gradually lowering the temperature of the melt.

Isecke [94] also studied the lead oxygen system by devising the runs isothermally and reducing the dissolved oxygen by means of a gas mixture containing hydrogen and making the succeeding runs immediately without removing the dissolved hydrogen from the melt.

1.2.2.1.2 Copper-oxygen binary system

Keomori, Katayama and Kozuka [53] determined activity coefficient of oxygen at infinite dilution in liquid copper employing the conventional sampling and analysis method. Their results on $\Delta G_O(\text{Cu})$ and $\varepsilon_{\text{O}}^{\text{O}}(\text{Cu})$ as a function of temperature are presented in Table 1.4. The results are in good agreement with those obtained in other studies conducted with Ni-NiO as reference electrode and in the temperature range of 1373-1473K. There is also good agreement with results obtained using

H_2/H_2O [95] and CO/CO_2 [96] gas equilibration method.

S. Otsuka and Z.Kozuka [38] employing their modified coulometric titration technique determined oxygen activities in liquid copper in the low concentration range. The result on $\Delta GO(Cu)$ are presented in Table 1.4 and are in good agreement with those obtained by Osterwald et al. [97], Fischer and Ackerman [98] and Sano and Sakao [99].

Kulkarni [100] measured oxygen activities in Cu-O and Cu-Fe-O alloys in the temperature range 1373-1573K using solid electrolyte galvanic cell with mixture of Ni-NiO and Co+CoO as reference electrodes. His results on $\Delta GO(Cu)$ are presented in Table 1.4. He also studied the activity coefficient of oxygen at infinite dilution and was found to be 0.115, 0.195 and 0.286 respectively at temperatures 1373, 1473 and 1573K. He also studied the liquid Cu-Fe-O system at 1473K using the same technique and determined value of interaction coefficient, $\epsilon_{O(Cu)}^{Fe}$ to be - 565 at this temperature.

Jacob and Jeffes [22] as already discussed studied copper-oxygen system and measured the activity coefficient of oxygen at 1373K and 1573K. The variation of activity coefficient of oxygen $f_O(Cu)$ with temperature and $\log K'$ (where $K' = \text{atom pct } \underline{O}/pO_2$) are given in Table 1.4. They observed that Sievert's law is not strictly

obeyed by oxygen in liquid copper. They also obtained the standard free energy of formation of Cu_2O in the temperature range 1338-1473K, this is also presented in the Table 1.4.

Taskinen and Hiltunen [70] studied the oxygen activity in copper and Cu-Bi alloys in the temperature range 1373-1473K by solid electrolyte emf method. The activity coefficient of oxygen at infinite dilution, f_{O}^0 , the self-interaction parameter ϵ_{O}^0 and the free energy of dissolution of oxygen in copper were calculated and the results so obtained are presented in Table 1.4.

1.2.2.1.3 Tin-Oxygen binary system

Only a few studies have been reported on this system. Bedford and Alcock [26] studied the tin-oxygen system using coulometric technique in the temperature range 773-1023K. Their results on dissolution of oxygen, $\Delta G_{\text{O}}(\text{Sn})$ and its temperature dependence, the free energy of formation of $\text{SnO}_2(\text{S})$ in the temperature range 505-1273K are presented in Table 1.4.

Ramanarayanan and Rapp [101] studied the solubility of oxygen in liquid tin in the range 1021-1237K using coulometric technique with the implicit assumption of Henry's law. Their results are reported in Table 1.4. Fischer & Ackermann [98] also estimated the free energy for the dissolution reaction, $\Delta G_{\text{O}}(\text{Sn})$. Their values are

Table 1.4 Typical results on systems with oxygen in pure metals and binary metallic solvents

System	Temperature range (K)	Typical results	Standard state for oxygen	Authors	References
Pb-O	1373	$\Delta G_{\text{O}}(\text{Pb}) = -118336.1 + 50.428T \text{ Jmol}^{-1}$	atom pct.	Jacob & Jeffes	22
Pb-PbO	748-1130	$\Delta G_{\text{PbO}}^{\circ}(\text{s}) = -218099.4 + 98.889T \text{ Jmol}^{-1}$		-do-	
	1130-1423	$\Delta G_{\text{PbO}}^{\circ}(\text{l}) = -191007.9 + 74.906T \text{ Jmol}^{-1}$			
Pb-O	783-973	$\log N_{\text{O}}^{\text{S}}(\text{at } \%) = -5220/T + 4.53$		Alcock & Belford	25
		$\Delta G_{\text{O}}(\text{Pb}) = -119411.4 + 52.509T \text{ Jmol}^{-1}$	atom pct.	-do-	
Pb-PbO	720-1070	$\Delta G_{\text{PbO}}^{\circ}(\text{s}) = -219367.1 + 100.918T \text{ Jmol}^{-1}$			
Pb-O	1003-1353	$\log N_{\text{O}}(\text{at } \%) = 3.87 - 5600/T$		Szwarc Oberg & Rapp.	30
		$\Delta G_{\text{O}}(\text{Pb}) = -105855.2 + 56.928T \text{ Jmol}^{-1}$	atom pct.		
Pb-PbO	1023-1170	$\Delta G_{\text{PbO}}^{\circ}(\text{s}) = -215057.6 + 96.232T \text{ Jmol}^{-1}$		-do-	
		$\Delta G_{\text{PbO}}^{\circ}(\text{l}) = -190623 + 74.894T \text{ Jmol}^{-1}$			
		$\Delta G_{\text{PbO}}^{\circ}(\text{l}) = -190623 + 74.894T \text{ Jmol}^{-1}$			

Contd....

Table 1.4 contd...

1	2	3	4	5	6
Pb-PbO	1073-1323	$\Delta G_{\text{O}}(\text{Pb})$ = -118407.2+		Otsuka & Kozuka	35
Pb-O	1103-1173	$\Delta G_{\text{O}}(\text{Pb})$ $\epsilon_{\text{O}}^{\text{O}}(\text{Pb})$ $\ln f_{\text{O}}^{\text{O}}(\text{Pb})$	atom pct. atom pct. atom pct.	A. Taskinen -do- -do-	59
Pb-PbO	1073-1145	$\Delta G_{\text{PbO}}^{\text{O}}(s)$ $\Delta G_{\text{PbO}}^{\text{O}}(l)$		-do- -do-	
Pb-O	723-883	$\Delta G_{\text{O}}(\text{Pb})$	wt pct.	Chonochie, Obiogwer Robertson	75
Pb-O	1003-1353	$\Delta G_{\text{O}}(\text{Pb})$	atom pct.	Fisher & Ackerman	91
Pb-O		$\Delta G_{\text{O}}(\text{Pb})$	atom pct.	Charle	92, 93
Pb-PbO	1143-1343	$\Delta G_{\text{PbO}}^{\text{O}}(s)$		Charle & Osterwald	103
	1143-1343	$\Delta G_{\text{PbO}}^{\text{O}}(l)$		-do-	
Pb-O		$\Delta G_{\text{O}}^{\text{O}}(\text{Pb})$	atom pct.	Iscke	94

Contd...

Table 1.4 contd....

1	2	3	4	5	6
Cu-O	1373-1573	$\Delta G_{\text{O}}(\text{Cu})$ = -66467.02+13.292T, (± 628) Jmol ⁻¹	atom pct.	Jacob & Jeffes	22
		$\epsilon_{\text{O}}^{\text{O}}$ = 3.42-7767/T	-do-	-do-	
		$\log f_{\text{O}}(\text{Cu})$ = -104/T+0.034 (at % O)	-do-	-do-	
Cu-Cu ₂ O	1338-1473	$\Delta G_{\text{O}}^{\text{O}}(\text{PbO})$ = -196258.9+89.538T Jmol ⁻¹	-do-	-do-	
Cu-O		$\Delta G_{\text{O}}^{\text{O}}(\text{Cu})$ = -75479.3-0.1255T, (± 502) Jmol ⁻¹		Otsuka & Kozuka	49
Cu-O	1373-1573	$\Delta G_{\text{O}}(\text{Cu})$ = -(82399.7 \pm 2900)+(3.999 \pm 1.967)T Jmol ⁻¹		Kemori Katayama & Kozuka	53
		$\epsilon_{\text{O}}^{\text{O}}(\text{Cu})$ = -4.47-3440/T, (± 0.8)		-do-	
Cu-O	1373-1473	$\Delta G_{\frac{1}{2}\text{O}_2}^{\text{E}}$ = -86650.6+45.48T Jmol ⁻¹	1 atom pct.	Seetharaman & Staffanson	57
Cu-O	1373-1473	$\Delta G_{\text{O}}(\text{Cu})$ = -70320.5+34.31T, (± 251) Jmol ⁻¹	-do-	P.Taskinen H.Taskinen	79
		$\ln f_{\text{O}}^{\text{O}}(\text{Cu})$ = 4.133-8457/T, (± 0.2)		-do-	
		$\epsilon_{\text{O}}^{\text{O}}(\text{Cu})$ = 35.94-63.4x10 ³ /T, (± 0.5)		-do-	
Cu-O	1373-1573	$\Delta G_{\text{O}}(\text{Cu})$ = -84265.8+5.104T Jmol ⁻¹	1 atom pct.	Kulkarni	99(a)

Table 1.3 contd....

1	2	3	4	5	6
Cu-O	1373-1773	$\Delta G_{\text{O}}(\text{Cu})$ = -85947, 7+7.209T Jmol ⁻¹	1 atom pct.	Kulkarni	99(a)
Bi-O	973-1173	$\log f_{\text{O}}(\text{Cu})$ = -60.4/T. (at % O)		Young DR	135
Bi-O	997	$\Delta G_{\text{O}}(\text{Bi})$ = -102294+14.309T (± 837) Jmol ⁻¹	1 atom pct.	Otsuka and Kozuka	36
Bi-O	997	$\log[\text{at \% O}]$ = 4.96-5543/T		Fitzner	102
Bi-O	997	$\log[\text{at \% O}]$ = 4.19-4778/T		-do-	
Sn-O	773-1023	$\Delta G_{\text{O}}(\text{Bi})$ = -55502.8+9.677T Jmol ⁻¹	1 atom pct.	-do-	
Sn-O	773-1023	$\Delta G_{\text{O}}(\text{Sn})$ = -182464.2+25.648T Jmol ⁻¹	1 atom pct.	Alcock & Belford	26
Sn-O	1021-1237	$\Delta G_{\text{O}}(\text{Sn})$ = -192715+33.514T Jmol ⁻¹	1 atom pct.	Fischer & Ackerman	91
Sn-O	1021-1237	$\Delta G_{\text{O}}(\text{Sn})$ = -167360+6.862T Jmol ⁻¹	Wt.pct.	Ramanarayanan & Rapp	135(a)
Fe-O	1823-1973	$\Delta G_{\text{O}}(\text{Fe})$ = -7211916.8-14.414T (± 1000) Jmol ⁻¹	1 atom pct.		162
N ₁ -O	1373-1973	$\Delta G_{\text{O}}(\text{Ni})$ = -79470.9-4.393T Jmol ⁻¹	1 atom pct.		
Ag-O	1246-1433	$\Delta G_{\text{O}}(\text{Ag})$ = -14121+5.247T (± 1255) Jmol ⁻¹	1 atom pct.		
Bi-O	973-1173	$\Delta G_{\text{O}}(\text{Bi})$ = -24450+3.42T (± 200)		Otsuka & Kozuka	36

Table 1.4 contd..

Pb-Cu-O	1373	$\epsilon_{O(Cu)}^{Pb}$	= -7.4	Atom pct.	Jacob & Jeffes	22
	1023-1373	$\epsilon_{O(Pb)}^{Cu}$	= -7.767/T+3.42	-do-	Taskinen & Holopainen	62
Pb-Cu-O	1103-1173	$\epsilon_{O(Pb)}^{Cu}$	= 5.93-11600/T		Taskinen & Holopainen	62
Pb-Bi-O	1103-1173	$\epsilon_{O(Pb)}^{Bi}$	= -9.84+11780/T		A. Taskinen	65
Pb-Sb-O	-do-	$\epsilon_{O(Pb)}^{Sb}$	= 15.30 - 22160/T		-do-	
Pb-Bi-O	1073	$\epsilon_{O(Sn)}^{Pb}$	= 0.1 (at $N_{Bi}=0.1$)		Otsuka, Kurose and Kozuka	50
Pb-Sn-O	823-1173	$\epsilon_{O(Sn)}^{Pb}$	= 2.16, 1.84, 1.63 at 823, 1023 & 1223 K respect.		Jacob & Jeffes	23
Pb-Ag-O	1130-1203	$\epsilon_{O(Pb)}^{Ag}$	= -14.71+20420/T		Anja Taskinen	63
Pb-Au-O	-do-	$\epsilon_{O(Pb)}^{Au}$	= -8.0+13570/T		-do-	
Pb-Ni-O	1035-1273	$\epsilon_{O(Pb)}^{Ni}$	= 8.55-31410/T		-do-	64
Cu-Ni-O	-	$\epsilon_{O(Cu)}^{Ni}$	= 17.0-36000/T		Kulkarni & Johnson	100
Cu-Mn-O	1473, 1573	$\epsilon_{O(Cu)}^{Mn}$	= -1802 at 1473 K = -1078 at 1573 K		Seetharaman & Abraham & Staffanson	58
Ni-Cu-O	1733	$\ln f_{O(Ni)} - \ln f_{O(Ni)} = 1.0$	= -0.792 N_{Cu} , $N_{Cu} = 0.03$ at T = 1733K		N. Kemori, I. Yatayama & Z. Kozuka	116

Table 1.4 Contd..

Cu-Ag-O	1173-1273	$\epsilon_{\text{O}}^{\text{Ag}}$	= -0.76 at T = 1373	K. Fitzner	121
Cu-Thall-O	1373	$\epsilon_{\text{O}(\text{Cu})}^{\text{Thal}}$	= -7.5	Otsuka, Kazu & Kozuka	34
Cu-Bi-O	1373	$\epsilon_{\text{O}(\text{Cu})}^{\text{Bi}}$	= -12	Otsuka, Oka & Kozuka	41
Cu-Bi-O	1373-1543	$\ln f_{\text{O}(\text{Cu}+\text{Bi})}$	= 4.133-8457/T (± 0.2)	Pekka Taskinen and Hikka Taskinen	60
		$\epsilon_{\text{O}(\text{Cu})}^{\text{Bi}}$	= 31.3-58.2x10 ³ /T		
Cu-Se-O	1373	$\epsilon_{\text{O}(\text{Cu})}^{\text{Se}}$	= -13.8	Otsuka, Oka & Kozuka	44
Cu-Te-O	1373	$\epsilon_{\text{O}(\text{Cu})}^{\text{Te}}$	= -16.6	-do-	
Cu-In-O	1373	$\epsilon_{\text{O}(\text{Cu})}^{\text{In}}$	= -8.9	Otsuka, Yoshihiro and Kozuka	46
Cu-Sn-O	1373	$\epsilon_{\text{O}(\text{Cu})}^{\text{Sn}}$	= -2.8	-do-	
Cu-Zn-O	1373-1473	$\epsilon_{\text{O}}^{\text{Zn}}$	= -203(1423K) = -203(1423K) = -160(1473K)	Seetharaman & Staffanson	
		$\epsilon_{\text{O}(\text{Cu})}^{\text{Zn}}$	= -15899.2 Jmol ⁻¹		
		$\epsilon_{\text{O}(\text{cu})}^{\text{Zn}}$	= -9468.4KJ mol ⁻¹ K ⁻¹		
Fe-O-S	1651-2013	log[O]	= -2.76-6358/T	M. Naduaguba & J.F. Elliott	133

reported in Table 1.4.

1.2.2.1.4 Bismuth-oxygen binary system

Fitzner [102] studied diffusivity, activity and solubility of oxygen in liquid bismuth. The results are reported in Table 1.4. Otsuka et al [36] employed modified coulometric titration technique to determine the oxygen activities and gibb's energy of dissolution of oxygen in bismuth at 973, 1073 and 1173K and the results are presented in Table 1.4.

Charle & Osterwald [103,104] estimated the deviation of oxygen dissolution in liquid bismuth and also $\Delta G_O(\text{Bi})$ at infinite dilute solution while Griffith and Mallett [105] studied the saturation solubility of oxygen in liquid bismuth.

1.2.2.1.5 Other metal-oxygen systems

Scattered studies have also been reported in literature on other metal-oxygen systems using emf technique, besides those reported above. These include studies on dissolution of oxygen in liquid nickel by Iwase et al. [18], in liquid Indium by Tyler [28] Otsuka et al. [39,48] and Alcock et al. [109]. Otsuka et al. have studied the behaviour of oxygen in liquid Titanium, tellurium [33], liquid Bi, Sn & Ge [36] and also in elements of group I(b) and IV(b) [40]. Thermodynamic behaviour of oxygen has been studied in liquid antimony by Jacob & Mathew [72] and Otsuka et al. [110], in liquid silver by Diaz

et al. [106], in liquid iron by Iwase et al. [107] and in liquid germanium by Fitzner, Jacob & Alcock [108]. The diffusivity and solubility of oxygen have been studied in solid copper by Narula, Tare & Worrell [111] using potentiostatic and potentiometric technique; while Srivastava and Siegel [113] studied the thermodynamics of oxygen in solid molybdenum. The experimental details of these investigations have been presented in Table 1.3, while Table 1.4 summarises the important results.

1.2.2.2 Ternary systems

1.2.2.2.1 Lead-copper-oxygen system

Two studies have been reported on this system in the literature. Jacob and Jeffes [22] using solid electrolyte cell studied the thermodynamic behaviour of oxygen over the entire composition range in Pb-Cu alloy system, by adding either copper to Pb-O melt at 1023, 1173 and 1373K or lead to Cu-O melt at 1373K. Their values on $\epsilon_{O(Cu)}^{Pb}$ and $\epsilon_{O(Pb)}^{Cu}$ are presented in Table 1.4.

Taskinen and Holopainen [62] studied the Pb-Cu-O system with reference electrode constituted by gaseous oxygen at 1 bar. The concentration of copper at the temperatures of study was raised to its saturation value and estimated from emf vs. molefraction plot of copper in the melt. The value of $\epsilon_{O(Pb)}^{Cu}$ in dilute Pb-Cu alloy range is presented in Table 1.4. They also observed

the plot of $\ln f_{\text{O}}^{\text{Cu}}$ vs atom pct. Cu in lead to be linear up to 3.5 atom pct. copper in lead. Their results on $\ln f_{\text{O}}^{\text{Cu}}$ at 1173 and 1023K were found to be too negative when compared with the corresponding values of Jacob & Jeffes [22]. On the other hand results on $\epsilon_{\text{O}(\text{Pb})}^{\text{Cu}}$ in the two studies showed a reasonable agreement.

1.2.2.2.2 Lead-tin-oxygen system

Jacob and Jeffes [23] studied the activity coefficient of oxygen in Pb-Sn system over the entire composition range of the metallic solvents in the temperature range of 823-1373K employing solid electrolyte technique already reported. On the lead rich side, non linear variation of $\log f_{\text{O}}^{\text{Sn}}$ in lead was observed; $\epsilon_{\text{O}(\text{Pb})}^{\text{Sn}}$ was therefore not calculated. On the other hand, $\epsilon_{\text{O}(\text{Sn})}^{\text{Pb}}$ was estimated and found to decrease with rise in temperature; its values being 2.16, 1.84 and 1.63 at temperatures respectively, 823, 1023 and 1223K.

1.2.2.2.3 Lead-bismuth-oxygen and lead-antimony-oxygen

Taskinen [65] studied the effect of bismuth and antimony on the activity coefficient of oxygen in lead by solid electrolyte technique in the temperature range 1103-1173K. The behaviour of $\ln f_{\text{O}}^{\text{Bi}}$ vs N_{Bi} was found to be linear up to 4 atom % of bismuth in lead. The first order interaction parameter was obtained and is presented in Table 1.4.

Otsuka, Kemori and Kozuka [50] using modified coulometric technique measured the activity coefficient of oxygen in liquid Bi-Pb alloys at 1073K over the entire composition range of metallic solvents. Their results are presented in Table 1.4 and are found to be in agreement with those of Taskinen [65].

1.2.2.2.4 Other lead base ternary systems

Taskinen [63] studied silver-oxygen and gold-oxygen interactions in dilute molten lead alloys employing solid electrolyte emf technique. He calculated the oxygen activities in these alloy systems in the range of 1130-1203K. The results on $\epsilon_{O(Pb)}^{Ag}$ and $\epsilon_{O(Pb)}^{Au}$ and their inverse temperature dependence are given in Table 1.4.

Taskinen [64] also studied the oxygen activity in lead containing nickel up to the saturation point in the range 1035-1273K using S.E. emf technique. The result on $\epsilon_{O(Pb)}^{Ni}$ are presented in Table 1.4.

1.2.2.2.5. Copper-nickel-oxygen and copper-manganese-oxygen

Kulkarni and Johnson [100] studied the thermodynamics of oxygen in copper nickel metallic solvents using S.E. emf technique and observed that the addition of nickel lowered the activity coefficient of oxygen liquid copper. Their result on $\epsilon_{O(Cu)}^{Ni}$ is presented in Table 1.4. The effect of nickel on the upper-oxygen

interaction was also studied by Abraham [114] and Fischer & Janke [115]. Kemori et al. [116] studied the behaviour of oxygen in nickel-copper alloys at 1733K employing S.E. galvanic cell. Based on the results, the dependence of activity coefficient of oxygen at infinite dilution on copper concentration in liquid nickel was determined and has been presented in Table 1.4.

Seetharaman, Abraham and Staffansson [58] employed emf technique using sampling and analysis method and studied the influence of manganese on the activity coefficient of oxygen in liquid copper. The interaction parameter $\epsilon_{O(Cu)}^{Mn}$ was obtained in the range 1473-1573K and presented in Table 1.4. The enthalpy interaction parameter, ϵ_O^{Mn} was obtained using the relation, $d(\epsilon_O^{Mn})/d(1/T) = \eta_O^{Mn}/R$. The value so obtained was -0.022×10^5 KJ. They also obtained the entropy interaction parameter, τ_O^{Mn} using the relation, $\epsilon RT \eta_O^{Mn} = \eta_O^{Mn} - T \cdot \tau_O^{Mn}$. The value of τ_O^{Mn} was obtained as $-68 \text{ KJ deg}^{-1} \text{ mole}^{-1}$.

1.2.2.2.6. Copper-bismuth-oxygen

Otsuka, Oka & Kozuka [41] studied oxygen activity coefficient of oxygen in liquid Cu-Bi system at 1373K using modified coulometric technique as a function of alloy composition. The value of ϵ_O^{Bi} at 1373K was determined as -12.

P.Taskinen & H. Hiltunen [79] studied oxygen activity in Cu-Bi alloys at 1373-1473K using S.E. emf technique. They observed that the addition of bismuth

lowers the activity coefficient of oxygen in liquid copper. The temperature dependence of ϵ_O^{Bi} is presented in Table 1.4.

Wypartowicz and Fitzner [81] using emf technique measured the change in activity coefficient of oxygen at temperatures 1373, 1423 and 1473K in the dilute concentration range with bismuth concentration varied from 0-4 atomic pct. in copper. The oxygen concentration was maintained at about one atom percent. The data was used to arrive at Wagner's first interaction parameter, and was found to be in fair agreement with the results obtained by Belton and Tankins [81a].

The system Cu-Bi-O has also been studied by Puchi & Froberg [87] by bubbling air-oxygen mixture containing oxygen at a partial pressure of 10^{-5} to 10^{-8} bar in the temperature range 1400-1479K. The partial pressure of oxygen in the escaping gas was measured by means of an oxygen electrode placed above the surface of melt.

1.2.2.2.7 Copper-tin-oxygen

U. Block and H. Stüwa [117, 118] and Fruehan et al. [119] studied the behaviour of oxygen in copper-tin alloys. Jacob Seshadri & Richardson [67] studied activity coefficient of oxygen in copper-tin alloys at 1373K using two different equilibrium methods. In one, a solid electrolyte cell wherein the oxygen of

the metal was varied by adding spec pure cupric oxide while in the other an equilibrium between Cu+Sn alloys and Sn+SnO₂ slags was established via SnO vapour. The results both measurements confirmed the work of Block et al. [117,118]. The deoxidation equilibria for tin in liquid copper with solid SnO₂ as dioxidation product were also evaluated at temperatures of interest in copper smelting.

1.2.2.2.8 Coper-silver-oxygen

Schmalzried [14], Jakob and Jeffes [69], Tankins and Gocken [120] have studied the behaviour of oxygen in copper-silver alloys. Fitzner [121] also studied the solubility of oxygen in liquid Cu-Ag alloys in the temperature range of 1173-1273K by a phase equilibrium technique. The oxygen solubility at 1373K was determined by linear extrapolation and $\log \epsilon_O^{Ag}$ was calculated as a function of alloy composition. The interaction parameter was measured by emf technique and is presented in Table 1.4.

1.2.2.2.9 Copper-sulphur-oxygen and copper-selenium oxygen

Otsuka and Chang [122,123] studied the activity coefficient of oxygen in sulphiderich and metal rich melts in the copper-sulphur system at 1423 and 1523K using a modified coulometric titration technique. The activity coefficient values increase rapidly with sulphur

concentration in the vicinity of $N_s=0.333$. The data obtained for the metal rich are in good agreement with the results of Sano and Sakao [99].

The influence of Selenium on the oxygen activity in liquid copper has been studied by Staffansson et al. [124] at 1473K using solid electrolyte emf technique having one electrode of molten copper to which selenium was added as Cu_2Se . The interaction parameter, ϵ_0^{Se} at 1473K was determined as -745 i.e. the effect of selenium on the activity of oxygen in molten copper has a strong negative effect. Otsuka et al. [44] studied the effect of selenium on the activity of oxygen in liquid copper at 1373K.

1.2.2.2.10 Other copper base ternary systems

Otsuka, Hara Oka & Kojuka [34] studied the activity coefficient of oxygen in copper-Thallium system at 1373K using their modified emf technique. The data is presented in Table 1.4. The same authors [42] also studied the behaviour of oxygen in Cu-Ti system.

Otsuka, Hara Oka & Kojuka [43] studied the activity coefficient of oxygen in copper-antimony and copper-germanium [47] alloys at 1373K as a function of alloy composition.

Otsuka and Kojuka [46] studied the activity of oxygen in Copper-Indian System at 1373K using their

245461

modified coulometric method. The value of ϵ_O^{In} is presented in Table 1.4.

1.2.2.2.11 Iron based ternary systems

Iwase, Takeshita and Mori [55] used solid electrolyte emf technique to study the thermodynamic properties of oxygen in Fe-Ni alloys at 1873K. The activity of oxygen estimated represents a good agreement with the results obtained earlier using $\text{H}_2/\text{H}_2\text{O}$ equilibrium method, but showed a fairly large discrepancy with results obtained using CO/CO_2 gas equilibrium method in case of high nickel alloys.

Kiyoshi Terayama et al. [126] established phase equilibria in Fe-Ni-O system at temperatures 1153 and 1213K by varying oxygen partial pressure. Besides thermogravimetric and quenching methods, emf measurements using calcia-stabilized zirconia were adopted in order to determine the oxygen partial pressure in an atmosphere of $\text{CO}_2\text{-H}_2$ mixture. A nonstoichiometric spinels and metallic phases were observed in the oxygen partial pressures between $10^{-11.46}$ and $10^{-12.45}$ p a at 1153 K. The spinel type solution was converted into FeO phase at much lower oxygen pressures.

The Fe-Ni-O system has also been studied by Hanriet and Olette [127] and Fisher, Janke and Ackermann [128]. The later authors also studied Fe-Co-O system.

Oeters et al. [129] studied iron and oxygen

contents under FeO-MnO slags upto 38 wt.% at 1370, 1520 and 1600°C. The study was conducted to determine the liquidus and solidus lines of binary FeO-MnO system in presence of iron.

G. Gustafsson [130] performed experiments on calcium-oxygen in liquid iron at 1600°C. Strong negative and composition sensible interaction has been revealed. The authors have discussed the significance of strong negative interactions.

Nduaguba & Elliott [133] employed a novel method viz. Levitation melting in the temperature range 1378-1740K to study the solubility of liquid oxide phase in liquid Fe-O system. The solubility of liquid oxysulphide phase in Fe-O-S alloys has been estimated for the composition range of 0.08-0.3 wt.% oxygen and 0-0.5 wt.% sulphur. The oxygen content of the liquid iron saturated with liquid oxy-phase was estimated as; $\log O = -6358/T + 2.76$.

Other iron based systems studied include Fe-Na-O by Dai, Seetharaman & Staffanson [131], Fe-Nb-O, Fe-Al-O, Fe-Ti-, Fe-Na-O discussed by Sigworth & Elliott [132].

1.2.2.2.12 Bismuth based ternary systems

Kamel, Osterwalt & Toishi [134] studied activity of tin and bismuth in Sn-Bi-O system in the temperature range, 1073-1373K. They employed solid oxide galvanic

cell. The activities revealed a small positive deviation from Rault's law at 1273K & that of oxygen in liquid tin obeyed Henry's law upto the oxygen concentration at which solid SnO_2 precipitates.

Otsuka, Oka & Kojuka [39] employed modified coulometric titration technique and estimated activity coefficient of oxygen in liquid Bi-Ti alloys at 1073K as a function of alloy composition. The experimental values of $\ln f_{\text{O}}$ exhibited positive deviation over entire composition range of alloys. The experimental results were predicted on the basis of solution models with Wagner's equation fitting closely.

Otsuka et al. [50] also studied Bi-Sb-O system at 1073K while, Otsuka & Chang [48 b] studied Bi-In-O system.

1.2.2.2.13 Silver based ternary systems

Otsuka & Kojuka [47] studied the thermodynamic behaviour of oxygen in Ag-Ti alloys using modified coulometric titration at 1273K. Otsuka, Kaku & Kojuka [49] studied the activity coefficient of oxygen in Ag-Pb alloys at 1273 and 1473K using modified coulometric titration Technique. The measured results on $\ln f_{\text{O}}$ at these temperatures are presented in Table 1.4. The results obtained have been analysed on the basis of solution models and were found in close agreement with those predicted on the basis of quasichemical equation of Jacob & Alcock.

However, the enthalpy and entropy values for oxygen dissolution, evaluated from the present data were significantly different from those predicted on the basis of above model. Jacob & Jeffes [68] also calculated the activity coefficient of oxygen in liquid Ag-Pb alloys at 1273K using emf technique. The measurements were made by adding oxygen free silver/lead to lead-oxygen or silver-oxygen melts. Their results agreed with those predicted on the basis of Jacob & Jeffes quasichemical equation. However, their study was confined only to 1273K and did not measure other thermodynamic functions.

1.2.2.2.14 Other ternary systems

The system In-Sb-O has been studied by Tyler [28] and by Otsuka and Kozuka [37]. Both employed coulometric titration technique. Tyler estimated the activity coefficient of oxygen in liquid indium and In-Sb alloys in the range 1000-1130K. The free energy change in the liquid Indium for the dissolution reaction is presented in Table 1.4. In the In-Sb alloys, the activity coefficient of oxygen at 1083K was measured. The experimental results have been discussed on the basis of solution models.

1.2.3 Multi component systems

On account of their difficult theoretical interpretation, not much work has been undertaken to study the multi-component metallic systems with oxygen as the non-metallic solutes. However, some of the studies reported in literature are presented in Table 1.5.

Table 1.5 Multi component metallic systems studied

System	Author	Study	Reference
Cu-Se-Te-O	S.Otsuka, H. Haraoka and Z. Huzuka	Oxygen activity in Cu-Se-Te-O systems	44
Fe-V-Mn-O	S.M. Averbukh et al	Equilibrium of V and Mn with oxygen in liquid iron	137
Sn-Cu-Ag-O	D.C. HU , A.Z. Vanzeland W.W. Liang and Y.A. Chang	Activity coefficient of oxygen in ternary liquid Sn-Cu-Ag and similar alloys	138
Ni-Al-Cr-O	V.B. Tare, Dieter Janke and W.A. Fischer	Activity of oxygen in Ni base melts at 1100°C	139
K-Ni-Mn-O	V.E. Shevtrov V.L. LeKhtmet	Oxygen dissolution in Fe-Ni-Mn melts	140
Cu-Fe-S-O	Carl Wagner	Application of Gibb's Duhem Equation to Cu-Fe-S-O mattes	141

1.2.3. Theoretical Studies-Thermodynamic Models

Employing experimental techniques reviewed briefly under Section 1.2.2, extensive experimental data has been obtained on thermodynamic properties of metallic systems, such as properties of mixing, interaction parameters, phase stability criteria and a host of other properties. These are compiled as reference material by Hultgren et al. [1], Kubaschewski & Evans [2], Smithal [4] Sryvalin et al. [142] Scheneck and Steinmetz [143]. Subsequently in an effort to minimise on experimentation especially at the elevated temperatures in different concentration ranges, effort has been made on quantitative formulation for interpretation and possible prediction of properties of binary and multicomponent systems. For this purpose several thermodynamic models have been proposed based on different approaches and basic assumptions. Wilson [142] comprehensively reviewed the properties of liquid metals and alloys dealing mainly with qualitative and empirical relationships between fundamental properties of metals, namely their electro-negativity, valancy, Crystal structure, atomic radii as well as thermodynamic properties, and structure and phase equilibria in the metallic alloy systems. Kubaschewski (145,146) has reviewed the calculation of phase boundaries in the metallic systems, while Insara [147] and Insara and Bonnier [148] the application of various theoretical

and empirical equations to predict the thermodynamics of ternary systems from a knowledge of corresponding binaries. Lupis [149] has discussed interaction parameters and the stability of phases in multicomponent systems. Kapoor [150, 151] has reviewed the derivation and application of different expressions arrived at in such theoretical models as well as classical thermodynamic models. The various theoretical approaches or models can be classified into three categories, namely

- i) those based on the concepts of classical thermodynamics called classical thermodynamic models,
- ii) those based on the concepts of statistical thermodynamic principles are known as statistical thermodynamic models, and,
- iii) those based on quantum mechanics principles are referred to as quantum mechanical models.

The important approaches especially relevant to the computations of properties of oxygen and relevant to the present study in each of the above categories are very briefly reviewed in the following subsections.

1.2.3.1 Classical thermodynamic models

These approaches are based on the assumption of certain configurations in the solutions that can be expressed by means of suitable chemical equations and to which laws of chemical equilibrium are assumed to hold good for calculation of properties of the assumed species.

In one of the earliest approaches in this group, Alcock and Richardson [153] showed that a regular solution model presents a reasonable description of the activity coefficient of a dilute solute in binary molten metallic solvents. By assuming that

- i) the distribution of atoms in the solution is random,
- ii) the co-ordination number of all the three types of atoms are equal, and
- iii) the energy of interaction between the different atom-pairs is independent of the concentration.

Following expressions were derived for calculation of activity coefficient, $f_X(A+B)$, of the solute, x , at infinite dilution i.e. at $N_X \rightarrow 0$, in binary solvent of composition N_A (or N_B), from a knowledge of properties of corresponding binaries.

$$\ln X(A+B) = N_A \ln f_{X(A)} + N_B \ln f_{X(B)} - N_A \ln f_{A(A+B)} - N_B \ln f_{B(A+B)} \quad (1.1)$$

and for interaction coefficient, $\epsilon_{X(A)}^B$

$$\begin{aligned} \epsilon_{X(A)}^B &= (\partial \ln f_{X(A+B)} / \partial \ln N_B)_{N_B \rightarrow 0} \\ &= \ln f_{X(B)} - \ln f_{X(A)} - \ln B(A) \end{aligned} \quad (1.2)$$

However, when applied by Gockeen and Chipman [153] to Fe-Al-O system the value of interaction parameter,

$\epsilon_{O(Fe)}^{Al}$ obtained at 1760°C was -10 as compared to the measured value of -780. This large deviation was attributed by the same authors [154] to the preferred or preferential disdistribution of the solvent atoms around the solute atom, i.e. clustering around non-metallic solute by the metallic solvent components that interacted more strongly. They, therefore, modified their random distribution approach employing quasi-chemical approximation to predict the effect of a metallic component on the activity coefficient of an electronegative solute (oxygen or sulphur) assuming that each atom interacts with the same number of nearest neighbours (same Co-ordination number) of different types of atoms present in the solution. With this, they arrived at the following expression for the Raoultian activity coefficient, $f_{X(A+B)}$ of a solute, X, at infinite dilution in the binary solvent (A+B),

$$\begin{aligned} [1/f_{X(A+B)}]^{1/z} &= N_A [f_{A(A+B)}/f_{X(A)}]^{1/z} + \\ &N_B [f_{B(A+B)}/f_{X(B)}]^{1/z} \end{aligned} \quad (1.3)$$

Where, N_A , N_B are the mole fractions of components A+B of the solution; $f_{A(A+B)}$, $f_{B(A+B)}$ are respectively the activity coefficients of A and B in (A+B) solvent, and $f_{X(A)}$ and $f_{X(B)}$, the activity coefficients of the nonmetallic solute, X, in the binaries A-X and B-X respectively;

Z being the co-ordination number. However, the model in its modified form too could at best qualitatively explain the experimental data on the thermodynamic properties of oxygen and sulphur in binary metallic solvents. The authors concluded that the major source of error in the model was the assumption that pairwise interaction energies were independent of composition.

Belton and Tankin [155] proposed a simple solution model based on the formation of metallic species AX and BX in solution. It was thus developed for dilute & strongly electronegative solute viz sulphur and oxygen in liquid binary metallic solvents. They further assumed that the average energy of interaction of these molecular species AX and BX or the dipoles with the surrounding metal atoms is small and also that, to a first approximation, the partial molar properties of the species may be considered ideal. Thus, the internal bond energies and the thermal entropies of the species would be independent of composition of the solvent and these will have random configurational distribution of the species. With these simplifying assumptions and following elementary treatment analogous to that of Alcock and Richardson [154] they developed following expressions for the free energy, of mixing of the solute viz. oxygen,

$$\begin{aligned} \Delta \bar{G}_{X(A+B)} = & N_{AX}/N_X [\Delta \bar{G}_{X(A)} - H_A^M + RT \ln(N_{AX}/N_X)] \\ & + N_{BX}/N_B [\Delta \bar{G}_{X(B)} - H_B^M + RT \ln(N_{BX}/N_X)] \end{aligned} \quad (1.4)$$

where symbols H_A^M and H_B^M are the partial molar heats of mixing of the metal in the binary metal mixture at a given composition. However, on application of the expression so arrived at, the experimental data on properties of oxygen in ternary systems Cu-Ni-O and Cu-Co-O, a positive excess entropy of solution of oxygen in the above liquid alloys above that expected from a regular solution model or existing thermochemical theory was observed, which was attributed by the authors to configuration effects in view of similar values of the entropy of solution in these different metals.

Jacob and Jeffes (68) proposed a model based on the formation of species of the type A_2X and B_2X in the ternary solution (A+B+X) which lead to the following expression for the partial molar free energy of the solute,

$$\Delta \bar{G}_{X(A+B)} = N_A \Delta \bar{G}_{X(A)} + N_B \Delta \bar{G}_{X(B)} - 2\Delta H_{(A+B)}^M \quad (1.5)$$

As compared to Eq.1.4 this expression was found to give a better fit to experimental data on oxygen and sulphur in binary metallic solvents.

In order to explain the experimental results to a better degree of accuracy, Jacob and Alcock [156] suggested a further modification for predicting the activity coefficient of oxygen and sulphur in dilute

solutions in binary alloy solvents based on quasi-chemical approach, when metal atoms and solute atoms were assigned different bond numbers. This was an improvement on the earlier treatment of Alcock and Richardson [154] where all the three types of atoms were assigned the same coordination number. However, the activity coefficient predicted by the new set of expressions appeared to be similar to those obtained from Eq. 1.1 for a number of alloy systems, when co-ordination number of oxygen in this model was the same as the average co-ordination number used in Eq. 1.1. The following set of equations, based on the formation of molecular species of the type A_nX and B_nX in solution, was derived, where A and B atoms attached to oxygen were assumed not to make any other bond,

$$1/f_{X(A+B)}^{1/n} = N_A [f_{A(A+B)}^\alpha / f_{X(A)}^{1/n}] + N_B [f_{B(A+B)}^\alpha / f_{X(B)}^{1/n}] \quad (1.6)$$

and for the interaction parameter,

$$\epsilon_X^B = -n [(f_{X(A)} / f_{X(B)})^{1/n} (f_B) - 1] \quad (1.7)$$

Values of n and α in above expressions assigned by the authors are 4 and 1/2 respectively for a co-ordination number $Z=8$. The 'two-bond' model could predict activity coefficients, in a manner similar to that based on Alcock and Richardson's model in most of the systems considered

but disagreement was considerable when applied to Cu-Sn-O, Ag-Pb-O and Fe-Cu-O systems. The molecular model with $n=4$ predicts activity coefficients of oxygen that are considerably higher than the measured values in Cu-Sn-O, Ag-Pb-O systems and considerably lower than the measured values in Ag-Pb-O and Pb-Sn-O. The three bond number treatment however could predict all the alloy systems considered.

To explain the behaviour of solute atoms, wagner [157] proposed a new approach with one adjustable energy parameter. Knowing this parameter and the thermodynamic properties of the solute, one can compute the variation of the activity coefficient of the solute with alloy composition.

With the following basic assumptions:

- i) The concentration of the solute in the solution is so low that it follows Sievert's law,
- ii) On account of the high diffusivities in molten metals, the dissolved solute atoms occupy quasi-interstitial sites with a co-ordination number of $Z=6$ (for oxygen), and
- iii) Binomial distribution of complexes, which consist of a non-metallic solute (say Oxygen) surrounded by solvent metals in varying proportions.

Wagner arrived at the following expression for the activity coefficient of oxygen at infinite dilution in a binary metallic solvent having in its first co-ordination shell iA atoms and $(Z-i)B$ atoms:

$$f_{X(A+B)} = \left\{ \sum_{i=0}^{i=Z} \binom{Z}{i} \left[\frac{1-N_B}{f_{X(A)}} \right]^{Z-i} \left[\frac{N_B}{f_{X(B)}} \right]^i \cdot \exp[(Z-i)ih/ZRT] \right\}^{-1} \quad (1.8)$$

where, h in the above expression is a system-dependent constant, given by the following expression,

$$\begin{aligned} \Delta H(i+1 \rightarrow i+2) - \Delta H(i \rightarrow i+1) &= \Delta H(i-2 \rightarrow i+3) \\ -\Delta H(i+1 \rightarrow i+2) &= h \end{aligned} \quad (1.9)$$

where, $H(i \rightarrow i+1)$ is the enthalpy change for the exchange of a solute atom X from a complex $A_{Z-i-1}B_{i+1}$. The model has been verified for its applicability and predictability using experimental data available in literature on the solubility of oxygen in different binary alloy solvents such as in systems Ag-Cu-O [118,120,158] Ag-Sn-O [118,120] Ag-Pb-O [68], Au-Ni-O [159], Pb-Sn-O [23] Cu-Sn-O [67,118,158], Cu-Ni-O [160], Cu-Co-O [161] Ni-Co-O [128] and Ni-Fe-O [128]. For analysis on solubility of nitrogen and carbon in binary metal alloys also, this model was highly successful.

Chiang and Chang [162] pointed out that in alloy systems with oxygen as the solute, such as Cu-Sn-O,

picture of the melt. The problem of evaluation of thermodynamic properties of the system reduce to the evaluation of the partition function. Some of the basic assumptions made regarding the structure of a metallic melt are,

1. The molecules or atoms present in a solution form a quasi-crystalline lattice with atoms of each of the species being assigned a particular type of site. In case the atoms of different constituent species are similar in size, they can be considered to form only one lattice as in substitutional solutions. However, if the solute atoms are much smaller in size than solvent atoms, they will occupy the interstitial sites.
2. The atoms of a solution vibrate around their mean positions in a small space called cell. The volume of such a cell is determined by the interaction of the atom occupying it with those in its first coordination shell. On account of vacancies existing in liquids, no long range order exists and an average co-ordination number is assumed.
3. The energy of an atom (in the earlier approaches) taken to be a linear function of the atoms in its first co-ordination shell and the total

Sn-Pb-O, Cu-Fe-O, and Cu-Ni-O and Cu-Co-O, the Wagner's model was inadequate. These authors therefore, altered the Wagner's model by assumption of two energy parameters h_1 & h_2 instead of Wagner's assumption of the enthalpy difference between the consecutive exchange reaction to be constant, and equal to h . For this extension of Wagner's approach, Chiang and Chang assumed this difference to vary linearly with i , i.e.

$$\Delta H(i+1 \rightarrow i+2) - \Delta H(i \rightarrow i+1) = h_1 + h_2 i \quad (1.10)$$

The corresponding expression for the activity coefficient of solute X took the following form,

$$\ln f_{X(A+B)} = \frac{1}{2} \ln [f_{X(A)} f_{X(B)}] - \ln \left\{ \prod_{i=0}^{i=Z} \binom{Z}{i} [1 - X/\phi]^{1/2Z} \right\}^{z-i} \cdot [X\phi^{1/2Z}]^i \cdot \exp\{(Z-i)i(h_1-h_2)/2RT + (z^2-i^2)ih_2/6RT\} \quad (1.11)$$

The only difference in Eqs. 1.8 and 1.11 is because of the expression containing the energy parameters in exponential terms. At $h_2 = 0$, Eq. 1.11 reduces to Eq. 1.8. Validity of Eq. 1.11 was tested by the same authors using data available in the literature for twelve ternary systems containing oxygen in binary metallic solvents. It was found that the two parameter equation was capable of quantitatively accounting for the compositional dependence of the activity coefficient of oxygen even with systems where Wagner's model was found inadequate.

Chiang and Chang however, did not propose any correlation in their model [162] to predict the value of energy parameters h_1 and h_2 . Kuo and Chang [163] based on the properties of relevant binaries reported two such relations to evaluate the energy parameters. Chang and Hu [164] tested by validity of these relations using large number of experimental data available in literature by calculating the Gibb's energy interaction parameter values of oxygen and nitrogen.

Kapoor [165] has extended the Wagner's approach and developed an expression for calculation of solubility and activity coefficient of an interstitial solute, such as oxygen, sulphur etc. in molten ternary substitutional metallic solvents using thermodynamic data of the solute in corresponding pure and binary solvents. D.C. HU and Y.A. Chang [166] also extended the Wagner's approach to systems comprised of ternary and multicomponent metallic systems.

1.2.3.2 Statistical thermodynamic models

The application of concepts of statistical thermodynamics to metallic solutions forms a more general and rigorous method as it simultaneously takes into consideration various atomic interactions. This approach consists in general in the construction of a partition function of the system on the assumption of certain

energy of a state of an ensemble is equal to some of the energies of all atoms in the system.

If one counts together all the states of an ensemble possessing the same total energy $g(E_i)$, the partition function, Ω can be written as,

$$\Omega = \sum_{E_i} g(E_i) \cdot \exp(-E_i/KT) \quad (1.12)$$

where the summation extends over all the accessible states of the total energy of the system. Such an approach was first made by Ising [167] in the theoretical treatment of ferromagnetism and was later adopted for the quantitative interpretation of the physico-chemical properties of condensed phases and even for gaseous phases.

Since metallic solution are in general non-ideal, so various approximate methods with further simplifying assumptions to solve Ising's model for the evaluation of their thermodynamic properties have been put forth. These approaches, reviewed critically by Kapoor [150] are grouped as 'regular solution model', 'quasi-chemical theory', 'Kirkwood method', the 'Matrix method', the 'Central' or 'Surrounded' atom model and those based on free volume theory.

The term 'regular solution' was first introduced by Hildibrandt [168] in connection with binary substitutional solutions and were defined as those having random distribution of atoms on lattice sites for which

the excess entropy of mixing is zero and the enthalpy of mixing being given by $WN_A N_B$, where W is a system dependent constant independent of temperature and composition. Mathematical formulation of regular solution is based on additional assumptions of :

- i) random distribution of atoms at their allowed substitutional or interstitial sites,
- ii) total energy of a state is equal to the sum of the energy of all the bonds, with each bond having the same fixed energy between like and unlike atoms, and
- iii) the internal partition function of atoms remains unchanged on mixing because of no change in the configurational partition function as also in the vibrational and rotational characteristics of atoms and their mean positions on mixing.

Expressions arrived at for the α -function indicated its system dependence on bond energies and temperature of the system but independent of composition - a result found contrary to the experimental evidence. Expressions for dilute solutions of a solute in binary solvents, similar to those arrived at by Alcock and Richardson [152,154] were derived, but as shown by Gluck and Pehlke [169], these have only qualitative applicability

in explaining the behaviour of binary or dilute ternary solutions and failed to explain their quantitative interpretation. The main reason for its failure was found to lie in its basic assumption that although the interaction energies amongst different atomic species were considered different yet no preferential distribution of atomic species had been taken into account.

Quasichemical theory was developed jointly by Fowler [170-171] Bethe [172] Rushbrooke [173] and Guggenheim [174]. Its complete and rigorous development was due to Guggenheim, who has written on the development and application of this theory to the physico-chemical properties of simple and polymer solutions. This approach differs from regular solutions as it takes into account the preferential distribution of various components of the solution. This preferential distribution arises from the difference in the interaction energies of like and unlike atoms in the system. It is assumed that the possibility of occupation of a particular site by a particular atomic species surrounded by a particular arrangement of nearest neighbours is proportional, apart from the fractional sites of the species, to $\exp(E_i/KT)$, where E_i is the energy of an atom of component i at this site and is taken to be equal to the sum of energies of the bonds which it makes with its nearest neighbours.

The nearest neighbours of an atom are assumed not to be present in the first co-ordination shell of each other. All other assumptions of regular solutions, namely, of no change in the internal partition function and specific volumes on mixing, are considered to be valid. The present treatment is however more general and the expression derived are applicable to dilute ternary solutions of all those systems whose binaries show quasi-chemical behaviour. The relation is not expected to hold good for dilute solution of strongly electro-negative elements such as sulphur in binary metallic solvents. Kapoor has extended the treatment for dilute solutions of an interstitial component X in a binary substitutional solvent of components A and B to yield the relation,

$$\frac{1}{[\Psi_{X(A+B)}^\circ]^{1/ZXS^{\rho X}}} = Y_A / [\Psi_{X(A)}^\circ]^{1/ZXS^{\rho X}} + Y_B / [\Psi_{X(B)}^\circ]^{1/ZXS^{\rho X}} \quad (1.13)$$

where ZXS is the coordination number of interstitial to substitutional and Y_A and Y_B represent lattice ratios of solute X in the binary solvents and $\Psi_{X(A)}^\circ$, $\Psi_{X(B)}^\circ$ and $\Psi_{X(A+B)}^\circ$ being the modified coefficients of solute X in metallic solvents, A, B and A+B.

To explain the behaviour of symmetric systems sharkley et al. [179b] have suggested a modified quasi-chemical approach. They considered, together with the

preferential distribution of atoms due to the difference in their interaction energies, the perturbation effect and the effects of crystal structure transformation as well as the dilation transformation, but the derivation of the expression is not sufficiently rigorous.

In the Kirkwoods method [176] the energy of an atom being equal to the sum of energies of the bonds which it makes with the surroundings; the atoms in the first co-ordination shell of an atom are not the nearest neighbours of each other and that no change in the internal partition function of the atoms takes place on mixing are common to regular and quasi-chemical approaches. Kirkwood instead of replacing the series summation by the maximum term, formulated the free energy of the system in terms of a power series. He, as a result concluded that the regular model was crude and quasi-chemical a better approximation to the exact solution of lattice problem.

In matrix method, reviewed by Nawall and Montroll [176A], Domb [177] and applicable essentially to the analysis of order-disorder reactions and phase transformations in binary substitutional solid solutions; the general partition function was calculated based on the constant absolute activities of its components. However, it involved complicated mathematical treatment and has rarely been used by the metallurgists.

Central - (Surrounded-) atom model were separately but simultaneously developed by Lupis and Elliot [178, 179] as the Central atom model and by Mathieu et al. [180-181] as the surrounded atom model. It differs from the previous models in the sense that it considers as the basic units, the atoms instead of their bonds. This it could evaluate energy of each atom as affected by its nearest neighbours and also the internal partition function due to changes in vibrational degrees of freedom on mixing. Calculation of thermodynamic properties requires an assumption of replacement of the summation series by the maximum term in randomly distributed systems with atoms in their allowed substitutional or interstitial sites. Assumptions of linear forms of energy and no change in vibrational partition function led to expressions similar to those obtained in earlier models but asymmetric behaviour of solutions was explained on assumption of parabolic form (i.e. nonlinear form) by Mathieu et al. [182] of energy and internal partition functions on mixing. Expressions for different thermodynamic properties reflected clearly to two terms, one corresponding to random distribution and the other temperature dependent and corresponding to preferential distribution of atoms in such solutions. Brion et al. [183,184] extended this approach to ternary substitutional systems and concluded that precise determination of properties

of ternary system was not possible without knowing certain system-dependent parameters in corresponding binaries. This approach therefore, successfully explained asymmetric behaviour and infinite dilution parameters of such systems and also the different interaction energies among the same interstitial components occupying neighbouring allowed sites in different components but had several objections to adoption of techniques for its mathematical treatment, such as use of combinative formulae and parabolic forms of energy and partition function, without adequate proof and thus further required improvement.

For a binary interstitial solution using the parabolic form of function for the energy and vibrational partition functions, one obtains an expression similar to the one in quasichemical theory, but in this case the constants contain a temperature - dependent and a temperature independent component [185]. For extension to higher components it required further mathematical treatment. Kapoor [186] extended this approach for application to dilute solutions.

Anik, Kapoor and Froberg [187] proposed a statistical thermodynamic model based on free volume theory and presented a unified approach for the quantitative description of dilute solution of strongly interacting solute (i.e. oxygen) and is probably the first approach capable of evaluation of self interaction parameter,

$\epsilon_{O(A+B)}^O$ of oxygen in binary metallic solvents. The following simplified assumptions formed the basis in this approach;

- i) The solvent atoms form a three dimensional lattice in which the interstitial sites are occupied by oxygen atoms and there exists no vacancy at substitutional sites.
- ii) The number of oxygen atoms in the system is so small that no two neighbouring interstitial sites are simultaneously occupied by it and no substitutional atom has more than one interstitial atom at interstitial sites surrounding it.
- iii) The energy of an oxygen atom is a quadratic function of the type of atoms in its co-ordination shells as has been first proposed by wagner [157] in his one parameter approach.
- iv) Summation of equation for partition function can be replaced by the maximum term in the series when it is expanded in such a way that the terms for the same energy are written together.
- v) Exchange of oxygen atoms in the solution with gas phase does not cause a rearrangement of the solvent atoms.

With these basic assumptions, the authors arrived at an expression to calculate the modified activity

coefficient of oxygen in an infinitely dilute solution of oxygen in binary substitutional metallic solvents (A+B). This however, necessitated the use of activity coefficients, $f_{O(A)}$ and $f_{O(B)}$ for the dissolution of oxygen in each metallic solvent respectively and also the co-ordination number of first substitutional or first interstitial coordination shell. The self interaction parameter, $\epsilon_{O(A+B)}$, could next be calculated employing the modified activity coefficients and functions g_A and g_B , defined as the free enthalpy for an exchange reaction viz. $O_A^{1B} + O_A^{1B} = O_A^{2B} + O_A^{0B}$. The latter correspond to constants h_A and h_B in Chiang & Chang's two energy parameter approach. The present authors however, derived suitable expressions to calculate g_A and g_B unlike Chiang and Chang who used empirical relations to calculate h_A and h_B .

The applicability of the model has been quite successfully illustrated by the authors [188] covering both congruent and inverse binary metallic solvents.

1.2.3.3 Quantum mechanical approaches

These approaches are based on the solution of Schrodinger equation under the conditions assumed in a model. These assumed conditions in general pertain to the form of potential function prevalent in the system under consideration at 0K. The solution of the Schrodinger

equation yields the heat of formation of the solution at this temperature. One of the earliest approaches was due to christman and Huntington [189] who applied Hartree-Fock approximation to the system sodium - Potassium at $N_{Na} = 0.5$ and determined the enthalpy of mixing as well as the extent of electron transfer from one component to the other. Bolsaitis [190] made use of single electron approximation and calculated the heat of mixing of Pb-Au-Ag alloys, while Bansil et al. [191] calculated the heat of mixing of disordered alloys. The essential feature of this approach is that the individual atoms are viewed as being embedded in a periodic effective media whose choice is open and can be made either self consistently or non-self consistently. In each case, exact analysis of the problem based on quantum mechanics is highly complicated and thus approximations are putforth which lead the results to be of no practical use. Use of this approach is still to be made to study the effect of a non-metallic solute in metallic solvents.

1.3 FORMULATION OF THE PROBLEM

From the discussion in the earlier sections, necessity of systematic experimental and theoretical studies of thermodynamic properties of metallic solutions in general and those containing oxygen in metallic solvents in particular has been amply demonstrated. In section

1.2.1.4 the preferred applicability of solid electrolyte emf technique over other experimental methods used for such studies especially in the dilute solution range of the solute has been described. The thermodynamic behaviour of oxygen in metals and alloys is undoubtedly a topic of increasing theoretical and technological interest. A critical survey of the studies of properties of oxygen, in section 1.2.2 has revealed that studies so far undertaken in either pure metal solvents, bi-metallic or in multi-component solvents are far from complete. The empirical data obtained is inadequate as well as incomplete, since most of the studies pertain, either to a single temperature or conducted in a narrow temperature range. The composition range selected also shows considerable variation in systems selected for study.

Although some efforts have been made with different degrees of success, to predict theoretically, the behaviour of oxygen in such metallic systems on the basis of quasichemical models including Wagner's single parameter and Chiang and Chiang's two parameter approaches; yet little effort has been put in; to interpret the empirical data based on statistical thermodynamic concepts. Further only a few studies have been undertaken on the properties of oxygen in lead base alloys, in spite of the immense commercial importance of this metal; either

as pure metal, obtained generally by oxidative refining or as alloys containing copper, tin, bismuth, antimony etc. as alloying elements.

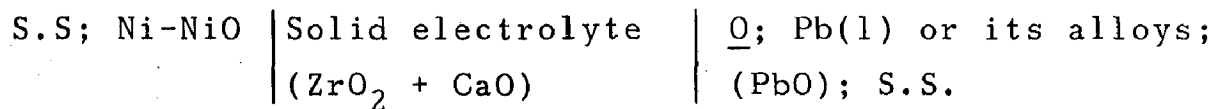
In the present investigation, therefore it is planned to study the behaviour of oxygen in pure lead and lead base binary metallic alloys containing copper, bismuth and tin in dilute concentrations as other solutes. For the experimental runs, a suitable set-up for adopting the 'conventional solid electrolyte emf technique' would be designed and fabricated. Actual experimental studies will be conducted in the temperature range 900-1100K, with concentration of other metallic solute varying in the broad range of 1-5 weight percent depending upon their solubility in solvent lead, in the selected temperature range. The oxygen concentration in lead and its alloys will be regulated by employing a suitable slag cover constituted by $\text{PbO} - \text{B}_2\text{O}_3$ melts of varying B_2O_3 concentration and $\text{PbO} - \text{SiO}_2$ with $N_{\text{PbO}} = 0.4$, under chemical equilibrium with the metallic melt.

An effort would also be made to interpret the experimental data on activity coefficients or interaction parameters so obtained, on the basis of thermodynamic models.

CHAPTER - II

EXPERIMENTAL

For the study of thermodynamic properties of oxygen in dilute solution range in pure molten lead and lead-base dilute solutions with copper, bismuth and tin as solutes, the following solid electrolyte galvanic cell was designed in the present investigation,



A brief account of the experimental set-up, materials used and procedure employed is presented in this chapter.

2.1 EXPERIMENTAL SET UP

The experimental set up used in the present investigation is schematically shown in Fig. 2.1 and essentially consists of,

- i) Cell assembly and main furnace
- ii) Gas purification train, and
- iii) Temperature control panels and recording unit.

These are briefly described as follows:

2.1.1 Cell Assembly and Main Furnace

A detailed view of the cell assembly is shown in Fig. 2.2. It essentially consists of a vertical Kanthal

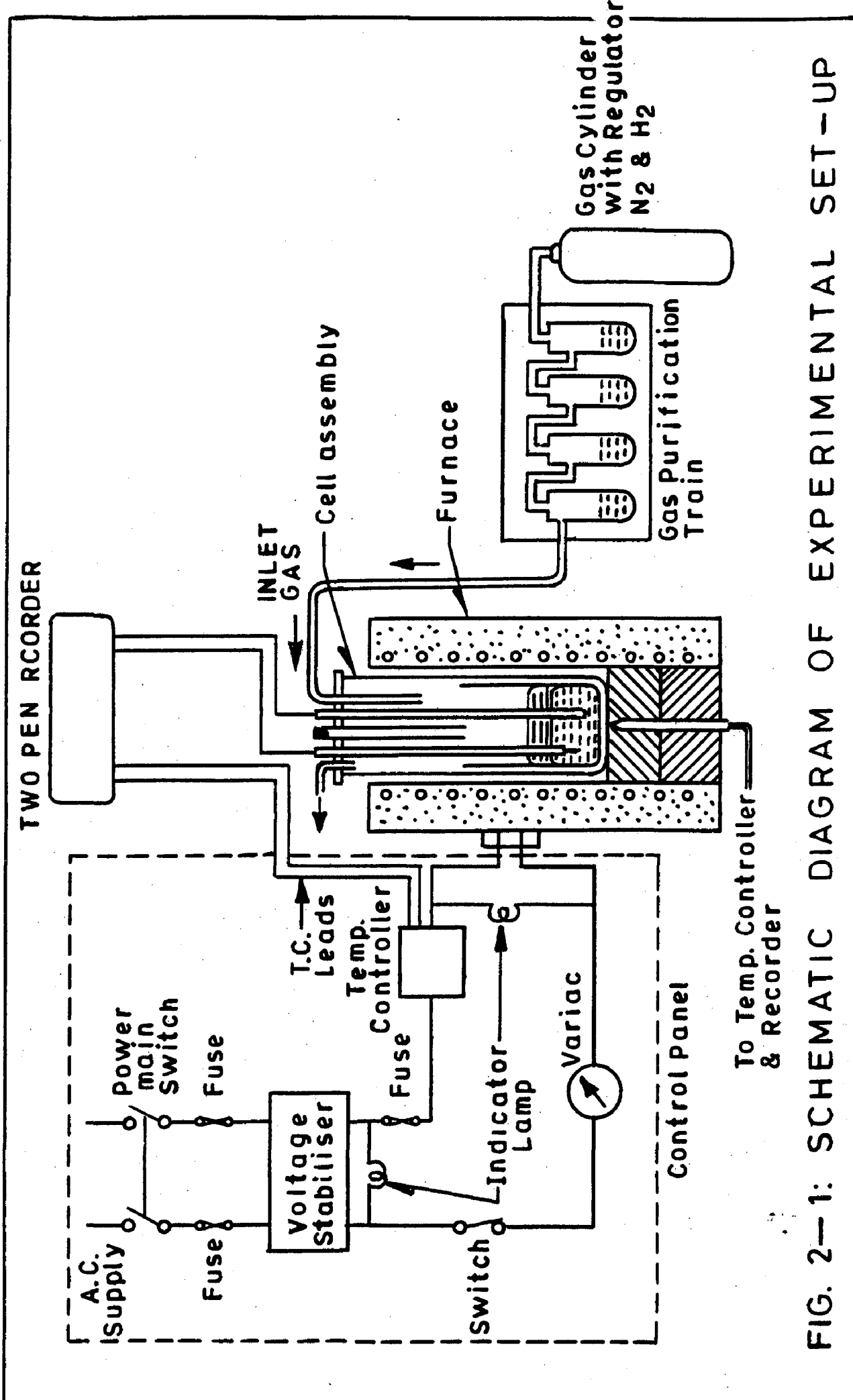


FIG. 2-1: SCHEMATIC DIAGRAM OF EXPERIMENTAL SET-UP

wound tubular electrical resistance furnace of 3.0 KW rating, using a mullite tube of 72 mm dia, 80 cms length and closed at lower end, was locally fabricated to operate in a temperature range of 600-900°C. The furnace was suitably wound to yield a non-inductive uniform temperature zone of approximately ten centimeters length in the central portion of the mullite tube. The cell assembly consisted of an outer recrystallised high alumina tube of 42 mm internal diameter and 4 mm thickness with one end closed and fitted with a gas - tight water cooled brass head at its upper end. The latter consisted of a lower annular brass flange permanently fixed to the alumina tube using araldite as sealant. This provides a platform to tighten on to it, an upper brass flange, 12 mm thick with a rubber annular gasket placed in between for gas tight seal. The upper brass flange was specially designed to have gas tight arrangement for lowering through it a solid electrolyte tube, 8 mm diameter and an alumina sheath, 3 mm diameter, containing the second stainless steel lead. 'O' ring and pusher type arrangements were used to not only have the gas tight system but also allow the lowering or raising of these accessories as and when required during the course of an experiment. A detailed view of the arrangement is separately shown in Fig. 2.2. Provision was also made to insert through separate holes drilled in the upper brass-flange,

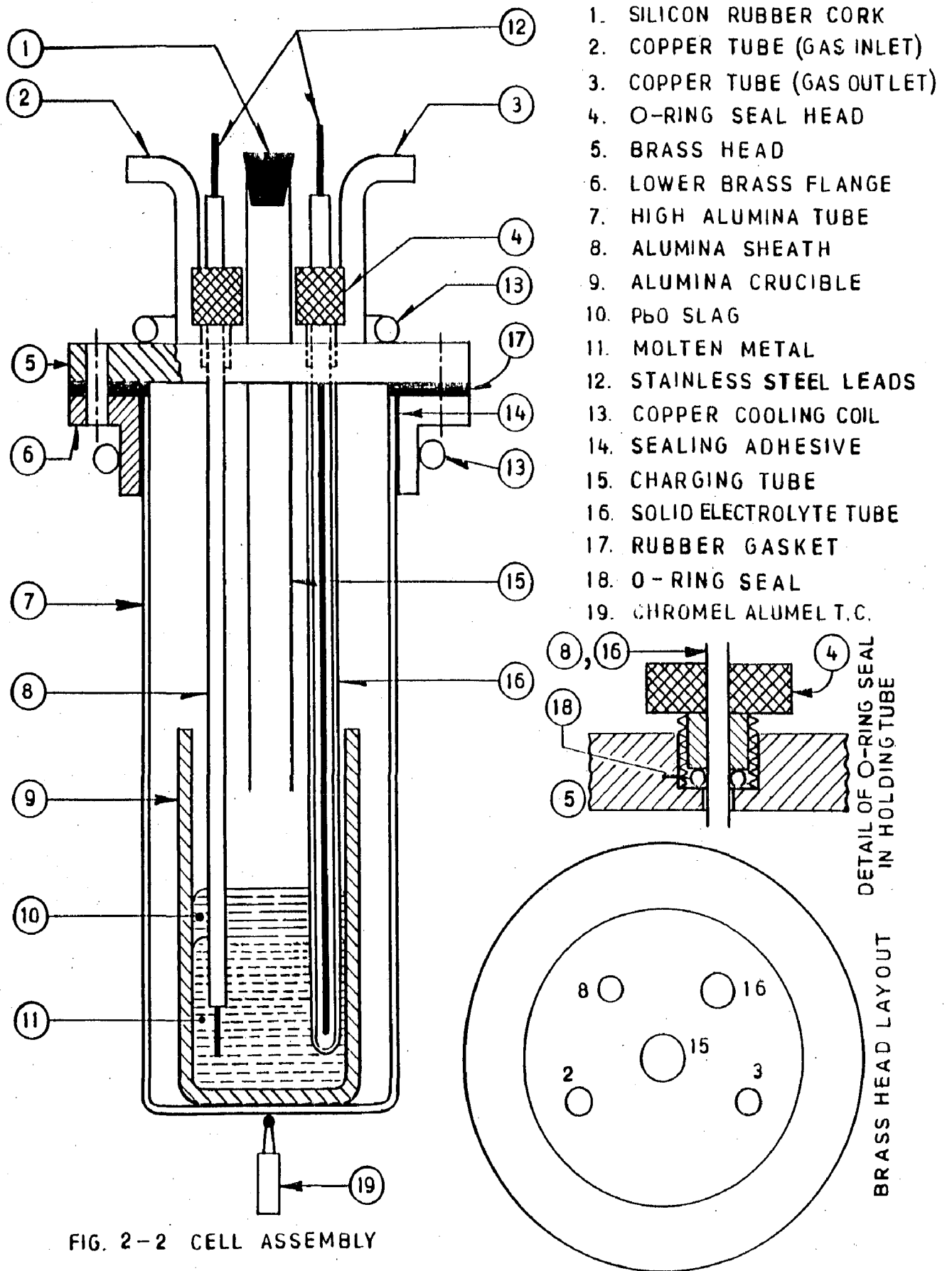


FIG. 2-2 CELL ASSEMBLY

an inert-gas inlet tube; an outlet tube as well as a 12 mm diameter high alumina recrystallised sampling-cum-charging tube. All these tubes were fixed permanently using araldite as sealant. A flexible Copper-tubing coil was soldered to both upper and lower flanges for water cooling. An earthed mild-steel tube was placed around the high alumina reaction tube in the furnace to enlarge the constant temperature zone and eliminate any opposing emf due to furnace winding.

2.1.2 Gas Purification Train

High purity nitrogen gas (99.99%) supplied by M/s Indian oxygen Ltd. Delhi, was used to maintain an inert atmosphere inside the cell assembly. The gas was further purified to eliminate any traces of its oxygen and moisture contents before entry into the cell-assembly by passing it through a gas purification train, a block diagram of which is given in Fig. 2.3. It consisted of a battery of bubblers containing dibutyl-phthalate; sulphuric acid to absorb moisture, followed by bubblers filled with freshly prepared alkaline pyrogallol solution for oxygen-absorption. This partially purified gas was next passed through two high alumina tubes inserted in tubular furnaces and fitted at their ends with standard glass joints and water cooling copper jackets, the first containing copper turnings and maintained at 600 °C and the other titanium chips and

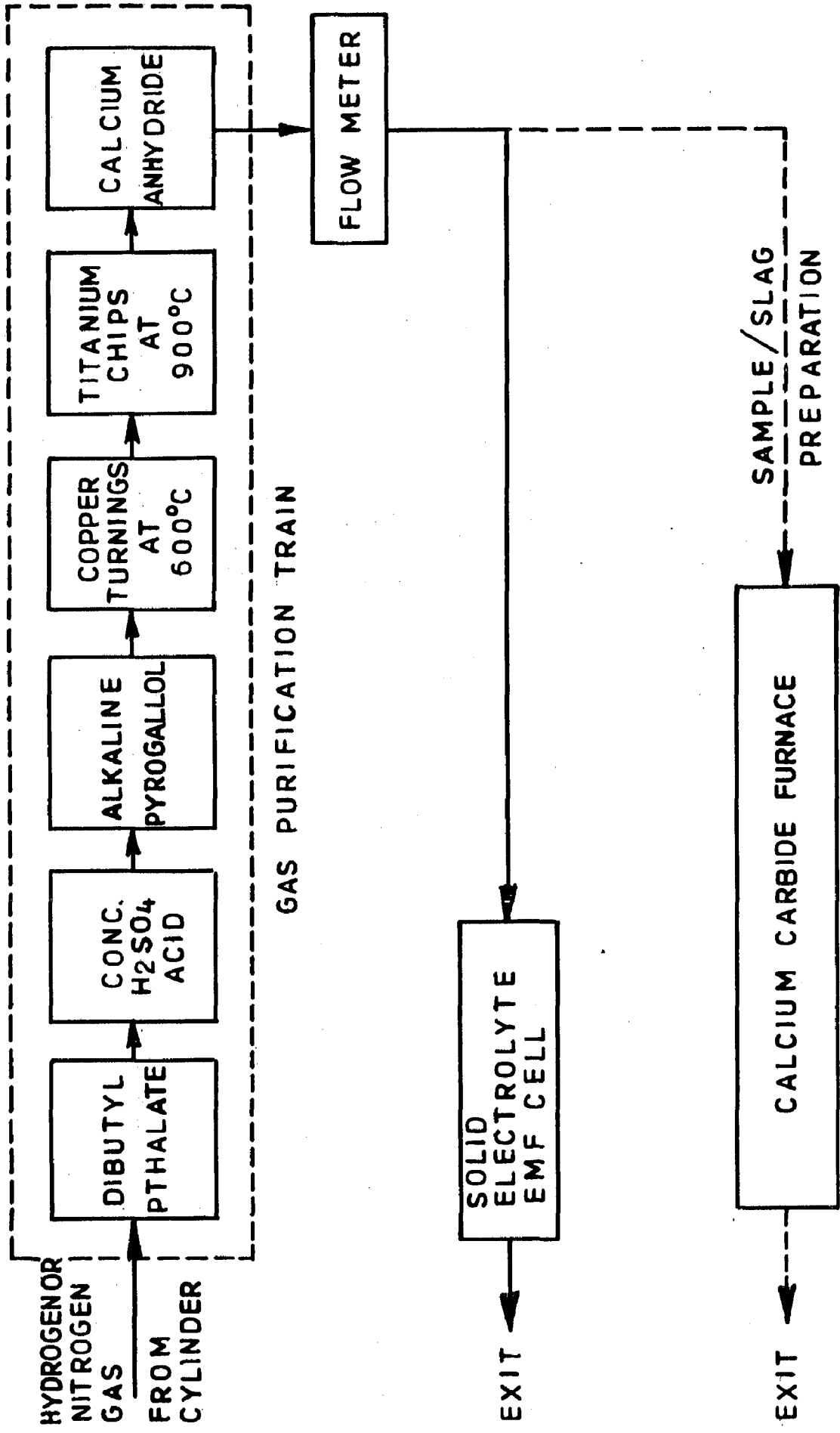


FIG. 2-3: BLOCK DIAGRAM OF EXPERIMENTAL SETUP

maintained at 900°C respectively. Two electric resistance tubular furnaces of 1.5 KW and 2.0 KW rating respectively were used for this purpose. Before entry into the cell-assembly, the gas so purified was passed through two columns filled with silica-gel to absorb traces of moisture, if any.

2.1.3 Temperature Control Panels and Recording Device

For measurement and control of temperature in the purification train furnaces, chromel-alumel thermocouples were used, whereas for the main furnace cell assembly, a Pt/Pt-13% Rh thermocouple was employed. Temperature of each furnace was independently controlled to an accuracy of $\pm 2^\circ\text{C}$ with an 'on' and 'off' type temperature controller of APLAB-Make supplied by M/s Applied Electronics, Thana, India. Power was supplied to the furnace through an automatic solid-state voltage stabilizer (NELCO-Indian make, 7.5 KVA capacity, 230 V output and 175/260 V input) and auto transformers (15 A, 260 V capacity). The thermo emf of the main furnace and cell emf were continuously recorded with a two pen strip chart recorder (Houston Instruments inc., U.S.A.). This enabled not only an accurate measurement of temperature but also proper attainment and control of thermal electrochemical equilibria in the cell assembly.

2.2 PREPARATION OF MATERIALS

2.2.1 Preparation of Pure-metals and Alloys

Analytical grade, +99.9% purity metals, lead, copper, bismuth and tin supplied by M/s P.D. Gupta Pvt. Ltd., New Delhi were used for the present investigation. These metals were further purified for removal of traces of their oxygen, by melting them in graphite crucibles for about six hours and subsequent solidification and cooling to room temperature under an atmosphere of hydrogen purified by passing through the gas-purification train already described in Section 2.1.2. Later these were cut to small pieces and preserved in a gas tight dessicator for use. Binary alloys, Lead copper, lead-bismuth and lead-tin of specific compositions were made by melting together purified metals similarly in small graphite crucibles under hydrogen atmosphere. These were also stored for use as master alloys in the experimental runs.

2.2.2 Preparation of Slags

PbO-SiO_2 ($N_{\text{PbO}}=0.4$) and $\text{PbO-B}_2\text{O}_3$ ($N_{\text{PbO}}=0.5$ and 0.7) slags were prepared for use in the experimental run to vary the oxygen concentration in the underneath metallic phase constituted by lead or lead base alloys except lead-tin, which was studied without any slag cover. For this purpose Analar reagent grades lead oxide and

diborontrioxide for $\text{PbO-B}_2\text{O}_3$ slags and lead oxide and silica for PbO-SiO_2 slag in powder form, were intimately mixed in the correct proportions. The powder mixtures were next heated in an alumina crucible first at 600°C for about 5 hours followed by melting the fused mass at 800°C for another 5 hours in a silicon carbide furnace. The temperature was next raised to 900°C , accompanied with constant stirring of the molten mass with an alumina rod to make it homogeneous. The contents were finally poured into an earthen vessel to solidify. The solid mass so obtained was crushed and stored in a dessicator over phosphorous penta-oxide to avoid any moisture pick-up, especially in case of $\text{PbO-B}_2\text{O}_3$ slag owing to its hydroscopic nature.

2.3 EXPERIMENTAL PROCEDURE

Equimolar mixture of spec.pure nickel and nickel oxide was gently packed inside the round-bottomed calcia stabilised zirconia electrolyte tube, obtained from M/s Friedrichsfeld, Mamheim 71, West Germany. A stainless steel wire of 16 gauge, was embedded in the mixture to serve as the contact lead. The solid electrolyte tube was sealed with araldite at its upper end under an atmosphere of purified nitrogen. Another piece of stainless steel wire to serve as contact lead was inserted in an alumina sheath with a small length of it projecting

out to dip into the metal when inserted in position; was sealed at the upper end using araldite as sealant. The alumina sheath not only avoids the lead wire to come in contact with (PbO) slag but also helps in attainment of air tight system. About 140 grams of pure lead and 25 grams of synthetic slag were charged into a recrystallised alumina crucible, 38 mm diameter. The charged crucible was lowered into the reaction tube and upper brass flange fitted in position. The solid-electrolyte tube, prepared as above, and alumina sheath with stainless steel contact lead were next inserted through their respective inlets in the upper brass-flange and lowered to a height of 15-20 cms above the solid charge in the crucible and the knurled-caps tightened with 'O' rings in position as shown in Fig. 2.2. The Pt/Pt-Rh thermocouple was inserted with its head at the preselected level as shown. After closing the charging tube with a tight fitting silicon-rubber stopper, the cell-assembly was flushed with purified nitrogen gas to expell air present in it as well as to ascertain that all connections were gas tight. A steady flow of nitrogen at approximately 50 mls/min was maintained throughout the entire duration of the experimental run.

After the furnaces in the gas purification train attained their respective temperatures, the main-furnace was 'switched on' and the temperature of the

cell assembly slowly raised to the desired value. A weighed amount of master alloy cut to proper size was charged into the molten metal through the charging tube and the stopper replaced in position. The molten metal/alloy in the crucible was homogenised by stirring with an alumina rod. During operations viz., making alloy additions or withdrawing alloy samples, wherein the rubber stopper was temporarily removed, the rate of flow of nitrogen gas was slightly increased. The solid-electrolyte tube, being thermally unstable, was slowly lowered in steps, not more than a centimeter each time, until its lower end dipped well into the pool of molten metal in the crucible. The other lead was also lowered to proper position and electrical connections made to the two-pen recorder. The system was allowed to attain thermal as well as electrochemical equilibrium. This was indicated by the constant values of thermal and cell emf recorded independent of time. The cell reversibility was checked by momentarily disturbing the equilibrium, first by raising and then lowering the temperature of the furnace by a small interval of say 5°C. Attainment of the same constant value of emf within ± 1 mv ensured the cell reversibility. After a constant emf had been recorded for about 30 minutes, recording was dispensed with. A metal sample was drawn with the help of a special 'Metal Sampling Gun' supplied by M/s Visheshika Electronics,

Ambala cantt, India. It could easily draw a sample of up to 6 cms length and 5 mm diameter into a borrocil glass tube, with its one end fitted to the gun and the other end dipping into the molten metal/alloy in the crucible, through the Charging/sampling tube. After a sample had been taken, it was held under the brass flange for a few seconds, withdrawn and quenched in water. Sampling with the gun was quite fast and invariably took less than 30 seconds. The cell emf was again checked after sampling to ensure its constant value.

The temperature of the cell assembly was changed to another pre-selected value and the experimental procedure repeated to record the new equilibrium value of cell-emf. Normally it took around 1.5-2 hours for the equilibrium to be attained and observations for cell emf were taken atleast at four different temperatures in each experimental run either with pure lead or binary alloys viz. Pb-Cu or Pb-Bi. In each experimental run with a binary alloy melt, the composition of the solute Cu or Bi was preselected and kept fixed during the course of the experimentation for that particular run.

Experiments on pure lead oxygen system were performed using different slags viz. PbO-SiO_2 ($N_{\text{PbO}}=0.4$) and $\text{PbO-B}_2\text{O}_3$ ($N_{\text{PbO}}=.5$ and 0.7) and pure PbO. While experiments on the turnary systems Pb-Cu-O, Pb-Bi-O were conducted

under PbO-SiO_2 ($N_{\text{PbO}} = 0.4$) and $\text{PbO-B}_2\text{O}_3$ ($N_{\text{PbO}} = 0.5$) slags only.

Studies on Pb-Sn alloys were conducted following the procedure as has been described above with the only difference that slag cover was not used in this study. The oxygen concentration in the alloy was rather changed by adding Pb-PbO pellet into the alloys through the charging tube after the master alloy had been added to the molten lead in the crucible. With Pb-Sn alloys the time taken for attainment of equilibrium was less than an hour and therefore the time for an experimental run was shorter in comparison with studies on Pb-Cu and Pb-Bi systems. Some loss of tin was observed in the trial runs. Adequate precautions were therefore taken to compensate for the loss of metal during experimental runs while studying alloys of this system.

It was observed that solid electrolyte tube could be used at the most for about 8-10 hours, after which irreverssible emf values were recorded, necessitating their change for subsequent experimental runs. No polarization of the reference electrode was experienced during any experimental run.

2.4 CHEMICAL ANALYSIS

The metal samples were gently ground on fine emery papers to remove any surface contamination. The end portions were cut with a sharp knife and the central

portions were used for analysis of the following elements.

2.4.1 Analysis of Oxygen in Metal Samples

The metal/alloy samples were tested for their oxygen content at DMRL Hyderabad using TC-136 micro processor based oxygen analyser supplied by LECO Corporation, USA. The analyser consisted mainly of three units viz. a measurement unit (Model 782-400), an electrode furnace (model 777-200) and control console (Model 781-300). Built into the measurement unit is a pan balance with the measurement range for oxygen from 0.00001 to 0.2% at one gram. Helium is used as the carrier gas. A weighed amount of the sample is subjected to induction fusion under the flow of carrier gas here helium. The decrease in weight is due to the oxygen in the metal carried away and is indicated in ppm.

To check for segregation of oxygen samples, as has been reported by Jacob and Jeffes [22] two large samples of 10-12 gms were obtained. One centimeter from each end was removed and the rest was divided into four equal sections and analysed for oxygen with the Leco analyser reported above. The analysed oxygen content in all four samples agreed closely, indicating that no significant segregation of oxygen had occurred during solidification of the drawn samples.

2.4.2 Analysis of Copper, Bismuth and Tin

The alloy sample of lead-copper, lead-bismuth and lead-tin drawn during the course of experiments were cut into two portions. One portion was subjected to wet analysis for the element copper, bismuth or tin using standard method of wet analysis prescribed [193] for lead base alloys.

The second portion of each of the samples was used for analysis of its respective element Cu, Bi or Sn using Atomic absorption spectrometry at the University Scientific Instruments Centre (USIC), University of Roorkee, Roorkee. An agreement of the two results confirmed the percentage of the solute element present in each sample.

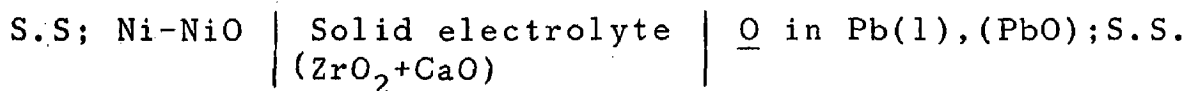
CHAPTER - III

LEAD-OXYGEN SYSTEM

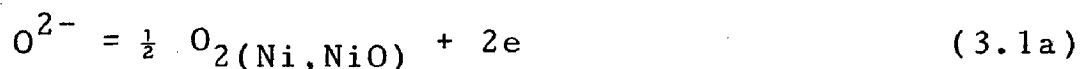
The present chapter deals with the experimental results and thermodynamic properties derived from emf data of the lead-oxygen system in the temperature range, 933-1095K. For oxygen variation, the metal was equilibrated with synthetic slags viz. pure PbO, PbO-B₂O₃ (N_{PbO} = 0.7 and 0.5), PbO-SiO₂ (N_{PbO} = 0.4) specially prepared for the purpose. The experimental method employed, the preparation of materials and the analysis techniques have been discussed earlier in Chapter II.

3.1 E.M.F CELL

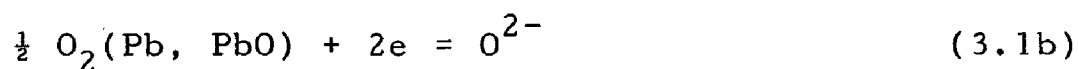
The solid-electrolyte galvanic cell used in the present investigation may be schematically represented as,



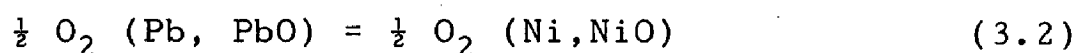
The left hand side in the above cell scheme, represents the reference electrode consisting of an equimolar mixture of pure nickel and nickel oxide powders; embedded inside a solid electrolyte tube. While, the R.H.S. represents the oxygen dissolved in the molten metal lead when equilibrate with a slag represented by (PbO). The reference electrode, Ni-NiO acts as anode and undergoes oxidation,



The electrode, lead - lead oxide constitutes the cathode,



The half cell reactions (3.1a) and (3.1b) together constitute the cell reaction,



and the free energy change, ΔG for the cell reaction being,

$$\Delta G = -nFE \quad (3.3)$$

where, E is the cell emf in volts.

F the faraday's constant ($96484.56 \text{ Cmol}^{-1}$)

n =the number of electrons exchanged for the transfer of one oxygen anion between two electrodes; being 2 in the present case.

The emf of the cell may therefore, be written as,

$$E = - RT/4F \ln [P_{O_2}(Ni, NiO) / P_{O_2}(Pb, PbO)] \quad (3.4)$$

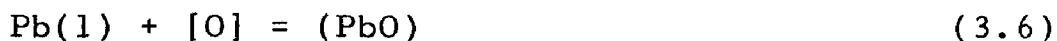
$P_{O_2}(Ni, NiO)$ may be calculated using the free energy of formation of nickel oxide, $NiO(s)$ viz. $Ni(s) + \frac{1}{2} O_2 = NiO(s)$, given [2] as,

$$\Delta G^\circ_{NiO(s)} = -234346 + 85.228T, \text{ Jmol}^{-1} \quad (3.5)$$

3.2 TESTING OF PROPER CELL FUNCTIONING

In the present study, the metal phase was covered by a slag phase of pre-determined activity. The amount

of oxygen dissolved in the metal will therefore be governed by the following slag-metal reaction,



As our aim is to determine the thermodynamics of dissolution of oxygen, so we are primarily interested in the study of the reaction in pure lead Oxide equation below, as well as, in studying the thermodynamic properties of oxygen in lead base alloys.



Thus one requires splitting Eq. 3.6 into Eq. 3.7 and the following reaction, viz.,

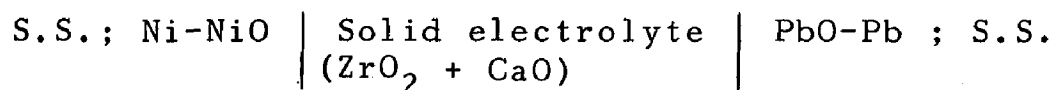


Eq. 3.8 represents the partial pressure of oxygen in equilibrium with (PbO) slag and the metal underneath. This is also the oxygen partial pressure that governs the oxygen dissolution in the metal, as per Eq. 3.7 and is reflected in the emf readings concerning the solution of oxygen in lead (Table 3.1). This may be easily determined when lead is equilibrated with a slag of known activity viz. pure lead oxide. This would also allow determination of standard free energy of formation of lead oxide already available in the literature. Comparison of our results with the standard data will serve as an indication of the satisfactory performance of the cell.

Tabel 3.) : EMF data on Lead-oxygen system (In each set the first value corresponds to pure PbO slag, the second to PbO-BO₃ (N_{PbO} = 0.7) third to PbO-B₂O₃ (N_{PbO} = 0.5) and the fourth to PbO-SiO₂ N_{PbO} = 0.4 respectively)

Temperature (K)	Oxygen conc. atom pct x10 ²	Emf (mv)	$\ln \left[\frac{\text{atom pct O}}{pO_2^{\frac{1}{2}}} \right]$
923	0.1031	163.23	13.6269
	0.01129	75.23	13.6049
	0.002477	14.37	13.6029
	0.002075	07.30	13.6014
967	0.1695	167.30	13.0939
	0.0192	77.77	13.0652
	0.004523	17.61	13.0623
	0.004006	12.56	13.0621
1010	0.3008	172.30	12.4836
	0.03553	81.04	12.4443
	0.009042	21.65	12.4404
	0.008394	18.42	12.4402
1057	0.5047	177.28	11.9248
	0.06237	84.29	11.8803
	0.01693	25.65	11.8736
	0.01624	23.67	11.8754
1095	0.8021	182.19	11.4075
	0.1046	88.09	11.3656
	0.0301	29.59	11.3603
	0.02941	28.49	11.3605

For this, an emf cell with lead and pure lead oxide in the crucible represented by the following cell scheme was constituted,



The emf data thus obtained in the temperature range, 933-1095K is presented in Table 3.1. Using the method of linear regression analysis (computer programme appended in Appendix-I), the emf can be represented as a linear function of temperature,

$$E = 0.0541146 + 11.6965 \times 10^{-5}T, \text{ volts} \quad (3.9)$$

This when multiplied by $-nF$ as per expression 3.3, gives the standard free energy change for the overall cell reaction; $\text{PbO(s)} + \text{Ni(s)} = \text{NiO(s)} + \text{Pb(l)}$ and is given as,

$$\Delta G^\circ = -10445 - 22.57T, \text{ joules} \quad (3.10)$$

Combining Eq. 3.10 with the standard free energy change for formation of nickel oxide vide Eq. 3.5, the standard free energy change for the formation of solid, (yellow) lead oxide, $\Delta G^\circ_{\text{PbO(s)}}$ is obtained as,

$$\Delta G^\circ_{\text{PbO(s)}}(933-1095\text{K}) = -223901 + 107.8T, (\pm 400) \text{ Jmol}^{-1} \quad (3.11)$$

The value of $\Delta G^\circ_{\text{PbO(s)}}$, thus obtained is compared with the corresponding values obtained by other workers reported in Table 3.2.

Table 3.2 Standard free energy of formation, $\Delta G_{\text{PbO}}^\circ$ of solid yellow PbO.

Temperature range (K)	$\Delta G_{\text{PbO}}^\circ$ (J.mol ⁻¹)	$\Delta G_{\text{PbO}}^\circ$ (J.mol ⁻¹) (at 1000K)	Crucible material	Author	Reference
760-1150	-223,007 + 107.53T	-115,477.0	-	Kubaschewski et al.	2
748-1130	-218,099.4 + 98.889T	-119,210.4	Al ₂ O ₃	Jacob & Jeffes	22
720-1070	-219,367.1 + 100.918T	-118,449.1	ZrO ₂ (MgO)	Alcock & Belford	25
1023-1170	-215,057.6 + 96.232T	-118,825.6	ZrO ₂ (CaO)	Szwarc, Oberg & Rapp	51
1145-1203	-215,231.4 + 96.537T	-118,694.4	ZrO ₂ (CaO)	A.Taskinen	59
865-1159	-214,660.1 + 95.646T	-119,014.1	ZrO ₂ (CaO)	Caby & Masson	103
772-1160	-215,057.6 + 96.387T	-118,670.6	ThO ₂	Charette & Flengas	103a
993-1159	-214,095.3 + 94.140T	-119,955.3	Al ₂ O ₃	Mehrotra et al.	103b
1008-1159	-218,279.3 + 97.487T	-120,792.3	Al ₂ O ₃	Mehrotra	103c
933-1095	-222,901 + 107.8T	-116,101	Al ₂ O ₃	This study	-

When compared at 1000K, the value of $\Delta G_{\text{PbO}}^{\circ}$ obtained in this study is quite comparable with that reported in the compilation of Kubaschewski and Evans [2] but is somewhat lower than that obtained by other authors. This difference may be due to the different values of the free energy of formation of nickel oxide employed by these authors in their calculations. The variation in results with other studies may also be attributed to the different crucible materials employed in various investigations reported in the Table 3.2.

The results on the free energy of formation of lead oxide and its comparison with the literature establish the proper working of the cell. This has been employed to study the thermodynamics of dissolution reaction, Eq. 3.7 in lead and its alloys in the subsequent sections.

3.3 OXYGEN IN MOLTEN LEAD

When lead is equilibrated with a slag of given oxygen potential, the equilibrium reaction for the transfer of oxygen between slag and metal can be rewritten as:



where [O] represents the oxygen dissolved in solvent lead and the left hand side represents the gaseous oxygen in equilibrium with (PbO) phase. Since the solubility

of oxygen in the metal is observed to be low, one can consider the resulting solution to be a dilute solution of oxygen in lead. One can, therefore, work with henrian activity with any standard state viz. 1 wt.% standard state or 1 atom % standard state because of the ease of conversion from one standard state to another.

Assuming 1 atom % as the standard state, the equilibrium constant, $K_{O(Pb)}$ for the dissolution reaction 3.7 can be written as,

$$\begin{aligned} K_{O(Pb)} &= \frac{h_{O(Pb)}}{(P_{O_2})^{\frac{1}{2}}} \\ &= \frac{[\text{at \% O}] \cdot f_{O(Pb)}}{(P_{O_2})^{\frac{1}{2}}} \end{aligned} \quad (3.12)$$

where, $h_{O(Pb)}$, $f_{O(Pb)}$ and $[\text{at \% O}]$ are respectively, the henrian activity, henrian activity coefficient and atom per cent oxygen dissolved in pure lead. In the above expressions the fugacity of oxygen has been represented by its partial pressure. In the logarithm form, Eq. 3.12 may be rewritten as,

$$\ln K_{O(Pb)} = \ln \{ [\text{at.\%O}] / (P_{O_2})^{\frac{1}{2}} \} + \epsilon_O^O \cdot [\text{at.\% O}]$$

or,

$$\ln \{ [\text{at.\% O}] / (P_{O_2})^{\frac{1}{2}} \} = -\epsilon_O^O \cdot [\text{at.\%O}] + \ln K_{O(Pb)} \quad (3.13)$$

where ϵ_0^O , is the self interaction parameter of oxygen in lead defined by wagner [104a] as,

$$\epsilon_0^O = \left\{ \ln f_{O(Pb)} / [\text{at.}\% O] \right\}_{\text{at.}\% O \rightarrow 0} \quad (3.14)$$

If $\Delta G_{O(Pb)}$ is the free energy change of dissolution of oxygen in pure lead, referred to 1 at.% O as standard state, Eq. 3.13 can be rewritten as,

$$\ln \left\{ \frac{[\text{at.}\% O]}{(p_{O_2})^{\frac{1}{2}}} \right\} = -\epsilon_0^O \cdot [\text{at.}\% O] - \Delta G_{O(Pb)} / RT \quad (3.15)$$

As seen from Eqs. 3.13 and 3.15 if ϵ_0^O , is independent of oxygen content of solution, the plot of function (Fig.3.1) $\ln \left\{ \frac{[\text{at.}\% O]}{(p_{O_2})^{\frac{1}{2}}} \right\}$ vs $[\text{at.}\% O]$ should be a straight line.

One can therefore calculate the values of $K_{O(Pb)}$, $\Delta G_{O(Pb)}$ and $\epsilon_0^O(Pb)$ from the linear plot. Using experimental data given in Table 3.1, the above functions have been plotted in Fig. 3.2 - 3.4 at different temperatures viz. 933, 967, 1010, 1053 and 1095K. The linear regression analysis of the data plotted at these temperatures yields the following expressions,

$$T = 933 \text{ K}$$

$$\ln \left\{ \frac{[\text{at.}\% O]}{(p_{O_2})^{\frac{1}{2}}} \right\} = 0.244 \cdot [\text{at.}\% O] + 13.602 \quad (3.16)$$

$$T = 967 \text{ K}$$

$$\ln \left\{ \frac{[\text{at.}\% O]}{(p_{O_2})^{\frac{1}{2}}} \right\} = 0.1917 \cdot [\text{at.}\% O] + 13.061 \quad (3.17)$$

$$T = 1010 \text{ K}$$

$$\ln\{[\text{at.}\% \text{ O}]/(\text{P}_{\text{O}_2})^{\frac{1}{2}}\} = 0.1484[\text{at.}\% \text{ O}] + 12.439 \quad (3.18)$$

$$T = 1053 \text{ K}$$

$$\ln\{[\text{at.}\% \text{ O}]/(\text{P}_{\text{O}_2})^{\frac{1}{2}}\} = 0.1025[\text{at.}\% \text{ O}] + 11.873 \quad (3.19)$$

$$T = 1095 \text{ K}$$

$$\ln\{[\text{at.}\% \text{ O}]/(\text{P}_{\text{O}_2})^{\frac{1}{2}}\} = 0.0607[\text{at.}\% \text{ O}] + 11.359 \quad (3.20)$$

Comparison of expressions 3.13 and 3.15 with Eqs. 3.16 to 3.20 yields values of $\ln K_{\text{O}(\text{Pb})}$, $\Delta G_{\text{O}(\text{Pb})}$ and $\epsilon_{\text{O}(\text{Pb})}^{\text{O}}$ at different temperatures of study. These are summarised in Table 3.3.

Figs. 3.2, 3.3 and 3.4 plot respectively the functions $\ln K_{\text{O}(\text{Pb})}$ vs $(1/T)$; $\Delta G_{\text{O}(\text{Pb})}$ vs T and $\epsilon_{\text{O}(\text{Pb})}^{\text{O}}$ vs $(1/T)$. The linear regression analysis of the data plotted yield the following temperature dependence of these functions,

$$\ln K_{\text{O}(\text{Pb})} = -1.56 + 14146/T \quad (3.21)$$

$$\Delta G_{\text{O}(\text{Pb})} = -117,616 + 12.983 T, (\pm 400) \text{ J gm.atom}^{-1} \quad (3.22)$$

$$\epsilon_{\text{O}(\text{Pb})}^{\text{O}} \text{ (mole basis)} = 97.335 - 113,270/T, (\pm 0.8) \quad (3.23)$$

3.3.1 Discussion of Results

The free energy of dissolution of oxygen at infinite dilution in molten lead, $\Delta G_{\text{O}(\text{Pb})}$ as per reaction

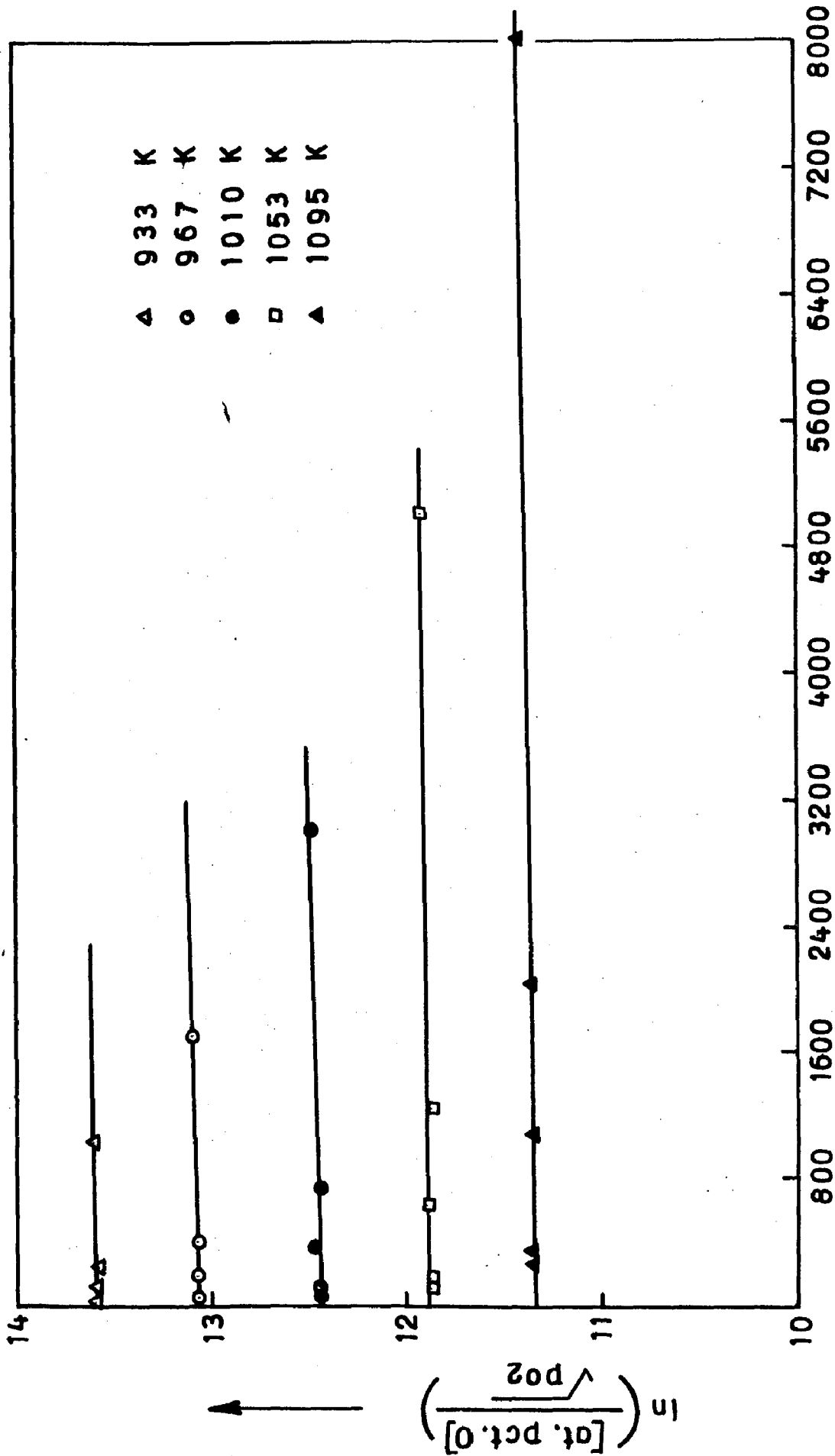


FIG. 3-1: PLOT OF FUNCTION $\ln\left(\frac{[\text{at. pct. O}]}{p_{\text{O}_2}^{1/2}}\right)$ vs [atom pct. O] FOR DISSOLUTION OF OXYGEN IN PURE LEAD AT DIFFERENT TEMPERATURES

Table 3.3 Thermodynamic functions for dissolution of oxygen in molten lead at different temperatures

Temperature (K)	$\ln K_{\text{O}}(\text{Pb})$	$\Delta G_{\text{O}}^{\circ}(\text{Pb})$ (J gm atom ⁻¹)	$\epsilon_{\text{O}}^{\circ}(\text{Pb})$ (at.% basis)	$\epsilon_{\text{O}}^{\circ}$ (mole % basis)
933	13.602	-105,515.4	0.244	24.40
967	13.061	-105,010.9	0.1917	19.17
1010	12.439	-104,457.2	0.1484	14.84
1053	11.873	-103,949.0	0.1025	10.25
1095	11.359	-103,415.5	0.0607	6.07

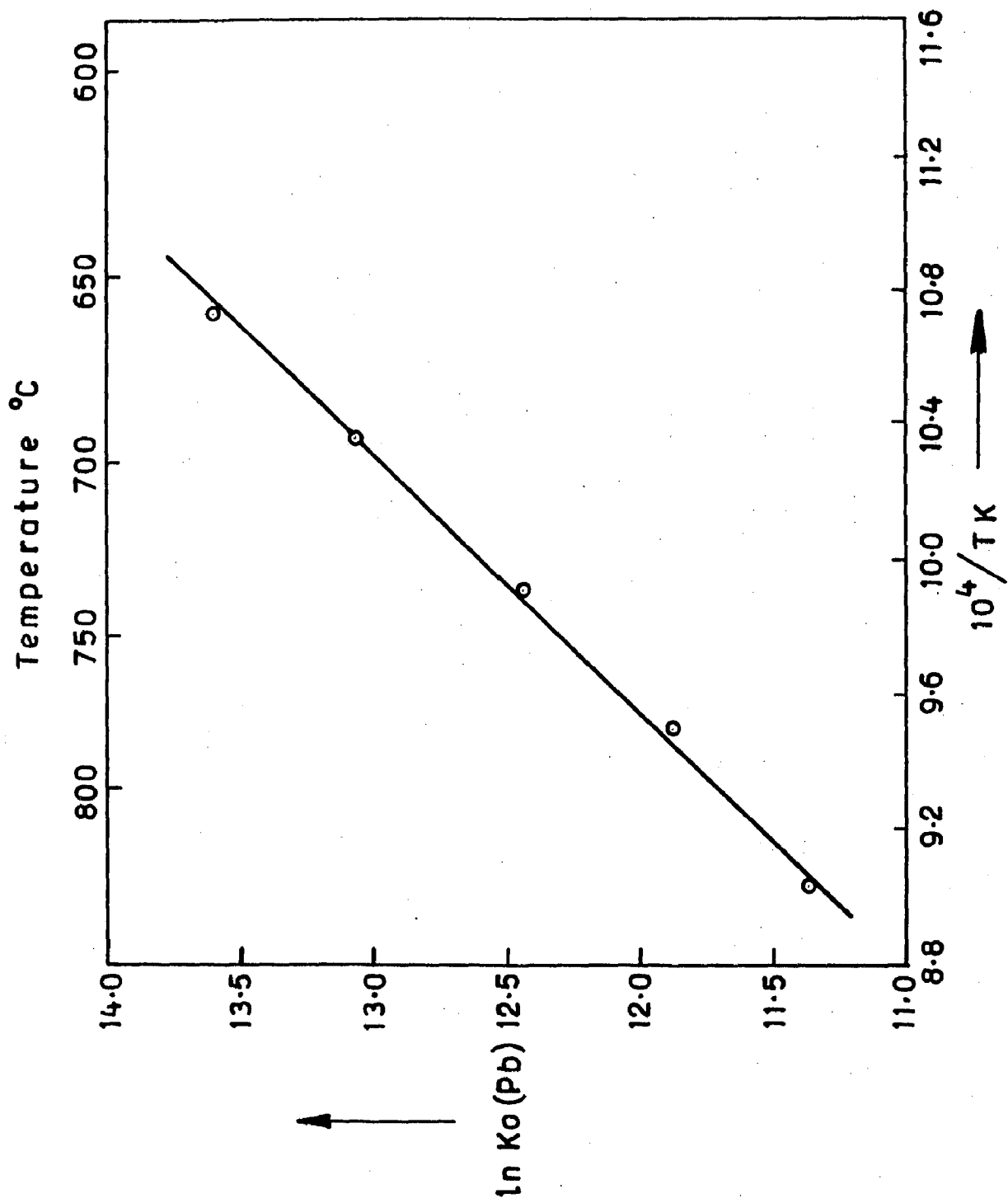


FIG. 3-2: PLOT OF FUNCTION $\ln K_o(\text{Pb})$ VS $1/T$ FOR EQUILIBRIA OF OXYGEN IN PURE LEAD

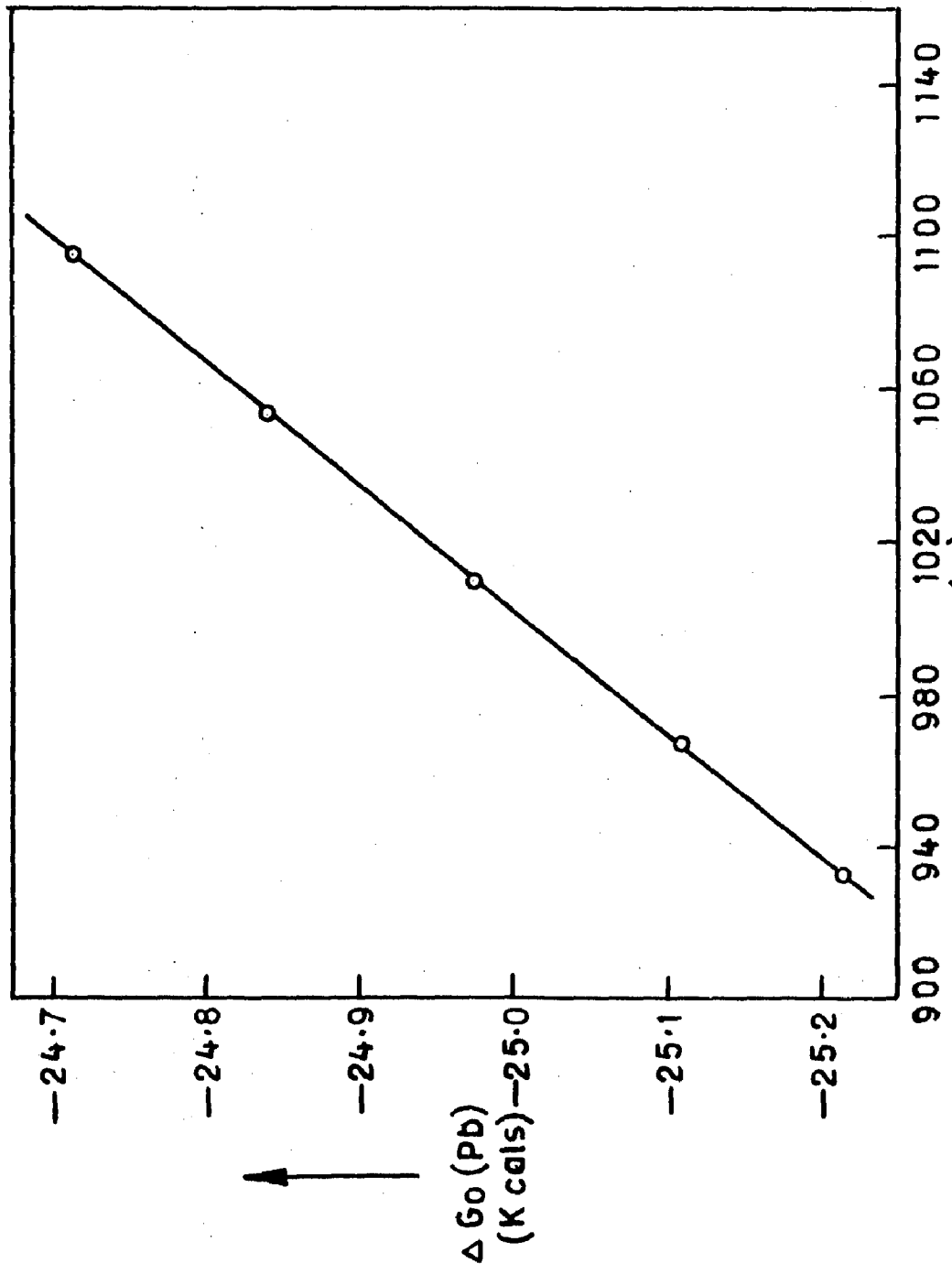


FIG. 3-3: PLOT OF $\Delta G_0(\text{Pb})$ VS TEMPERATURE FOR EQUILIBRIA OF OXYGEN IN PURE LEAD.

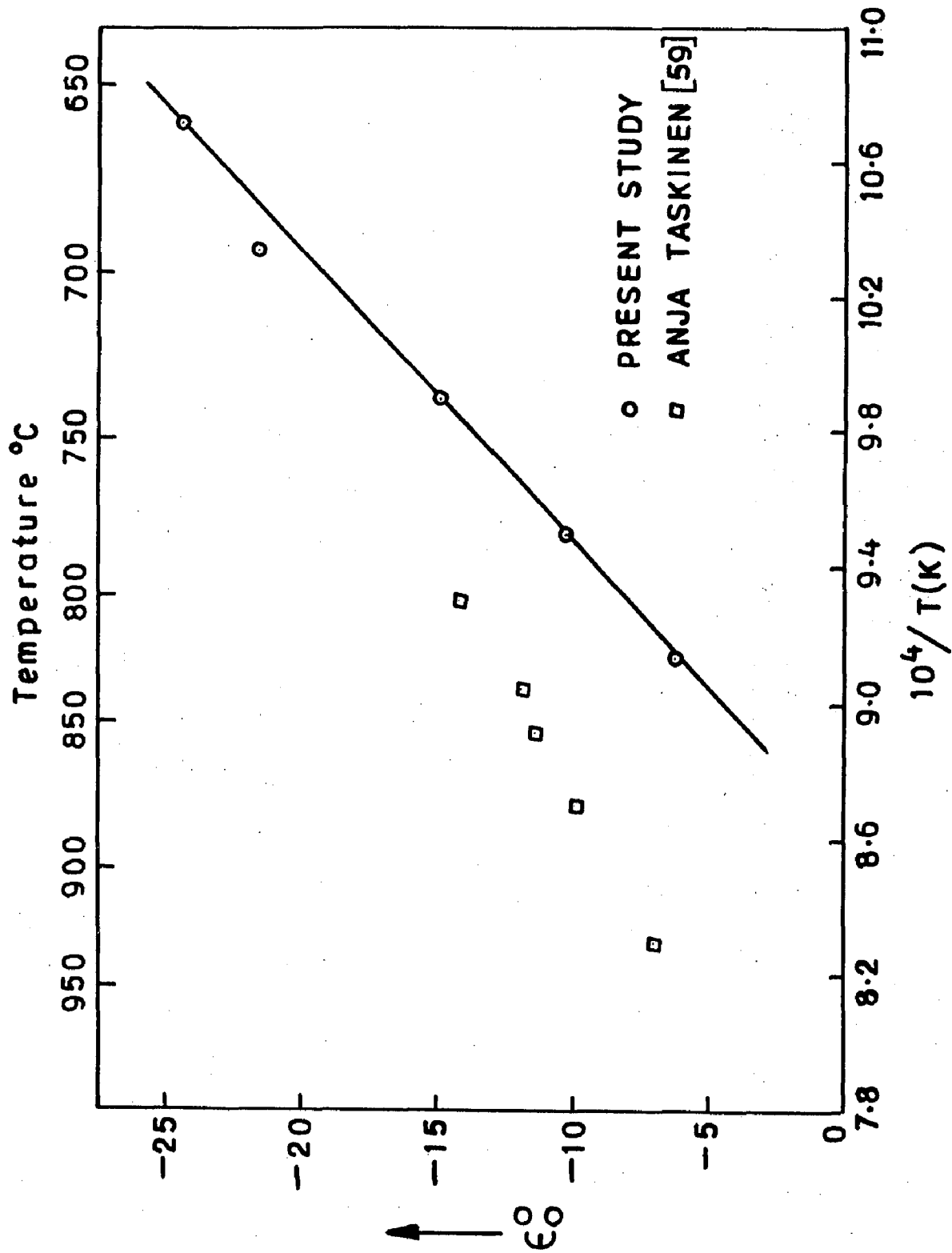


FIG. 3-4: PLOT OF TEMPERATURE DEPENDENCE OF ϵ_0^O IN LIQUID LEAD

employed a new method called 'open bubble technique' and conducted measurement of oxygen potential in a large mass of lead (30 kg), wherein the oxygen was injected in pulses, making use of a rotameter and peristaltic changeover valve. The large deviation in the reported value (in Table 3.4) in this study, is probably on account of non attainment of uniform concentration of oxygen in such a large mass of lead. The emf results therefore may not be corresponding to true equilibria.

The self interaction parameter, ϵ_0^O , obtained in the present investigation is in good agreement with that of Taskinen [59]. Fig. 3.4 shows variation of ϵ_0^O with reciprocal of temperature and includes for comparison the Taskinen's data on ϵ_0^O , calculated using his expression,

$$\epsilon_{O(Pb)}^O = 51.99 - 70.9 \times 10^3/T(K).$$

However, the self interaction coefficient of oxygen arrived at by Charle [93] and Isecke [94] are more negative than obtained in the present investigation. As discussed by Taskinen [59], both of them in their investigations used an Ir contact and did not equilibrate the atmosphere with the melt at different oxygen activities, which resulted in the measurements. The poor reproducibility with an Ir contact caused by an incomplete mixing of

Table 3.4 Free energy change, $\Delta G_{\text{O}}(\text{Pb})$, for dissolution of gaseous oxygen into molten lead
(1 atom pct. standard state)

Temperature Range (K)	$\Delta G_{\text{O}}(\text{Pb})$ (J gm atom ⁻¹)	$\Delta G_{\text{O}}(\text{Pb})$ (J gm atom ⁻¹) (at 1000K)	Author	Reference
1373	-118,336.1 + 12.142T	-106,194.1	Jacob & Jeffes	22
783-973	-119,414.4 + 14.226T	-105,185.4	Alcock & Bedford	25
1003-1353	-105,855.2 + 18.644T	- 87,211.2	Szwarc, Oberg & Rapp	30
1073-1323	-118,600.0 + 14.100T	-104,500.0	Otsuka & Kozuka	32
1073-1203	-116,713.3 + 12.703T	-104,010.3	A.Taskinen	59
723-883	- 60,693 - 26.97T	-87,663.0	Conochie	75
903-1253	-106,394.9 + 10.255T	-96.139.9	Fischer & Ackerman	91
-	-119,829 + 15.786T	-104,043.8	Charles	93
-	-120,370.2 + 16.255T	-104,115.2	Isecke	94
933-1095	-117,616.0 + 12.983T	-104,633.0	This study	-

3.7 has been investigated by several workers; all employing solid electrolyte emf technique. Table 3.4 sums up the reported data on $\Delta G_{O(Pb)}$. For sake of comparison, the values of $\Delta G_{O(Pb)}$ has been calculated at 1000K and also listed in Table 3.4. It is seen that the value of $\Delta C_{O(Pb)}$ arrived at, in this investigation are in excellent agreement with the reported data of most other workers except that of Szwarc et al. [30] Fischer and Ackerman [91] and Conochie [75]. The results of these workers being more positive. In the experiments conducted by Szwarc et al., truly potentiostatic conditions could not be established at somewhat higher oxygen concentrations corresponding to $E > 500$ mV, wherein sustained transient ionic current caused the experiments to deviate from a truly potentiostatic conditions and resulted in a voltage drop, $I_{ion} \cdot \Omega_{ion}$, relative to the value of applied voltage. Otsuka et al. modified the apparatus by employing two pairs of lead wires connected to each electrode. The truly potentiostatic experiments became possible by the application of a voltage between one pair of leads, so that emf developed between the other pair (connected to the same electrode) had a preselected value. This eliminated the IR drop in the lead wires, that had lead to the deviation in the results obtained by Szwarc et al. [30] and Fischer and Ackerman [91].

Conochie [75] on the other hand in his investigation

especially when larger amounts of PbO were added respectively by Charle and Isecke in their studies. Thus their emf readings did not correspond to true equilibrium conditions.

CHAPTER - IV

LEAD-COPPER-OXYGEN SYSTEM

As already pointed out, a knowledge of thermodynamic behaviour of dilute solution of oxygen in liquid lead-copper alloys is of importance in understanding the mechanism and thermodynamics of extraction and refining processes and design of alloys. Accordingly, some experimental studies [22, 61] have been conducted to arrive at thermodynamic data on solution of oxygen in copper-lead alloys. However, the reported data by different researchers shows considerable variation. Hence it was decided to reinvestigate this system to arrive at reliable data.

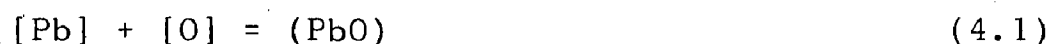
Further a number of theoretical models have been already reviewed in chapter I to predict the behaviour of oxygen in binary metallic solvents. In this chapter these models shall be applied to the present system under study to arrive at the one which is most suitable for theoretical calculation and prediction of thermodynamic properties of oxygen in binary copper-lead solvents.

4.1 RESULTS AND CALCULATIONSS

The experimental set-up used and procedure adopted for study have already been discribed in detail in chapter II. In the present case, E.M.F. measurements

were made on lead-copper-oxygen alloys of varying compositions, copper 0 - 3.0 weight percent and covered with $\text{PbO-B}_2\text{O}_3$ ($N_{\text{PbO}} = 0.5$) and PbO-SiO_2 ($N_{\text{PbO}} = 0.4$) slags. The results of these experiments are presented in Table 4.1.

The dissolved oxygen content of the metal is determined by the following equilibrium reaction,



where, the components in square brackets indicated on the left hand side of the expression for above dissolution reaction, represent those present in the metal phase and those in the parenthesis on the right hand side express components present in the slag phase.

Oxygen partial pressure in the system, which can be calculated from emf data of the cell, is determined by the following reaction,



where, as usual, curvilinear brackets represents the gaseous phase. Eqs. 4.1 and 4.2 lead to the following equation for the dissolution of oxygen in molten alloys,



The value of oxygen partial pressure is calculated using the expression,

$$E = -(RT/4F) \ln(p_{\text{O}_2}(\text{Ni, NiO})/p_{\text{O}_2}(\text{Pb, PbO})) \quad (4.4)$$

Table 4.1 EMF data on Pb-Cu-O at different temperatures and values of copper concentration

Slag cover	Copper concentration (atomic pct.)	Temperature (K)	EMF (mv)	Oxygen concentration (atomic pct.)
PbO.B ₂ O ₃ (N _{PbO} =0.5)	0.0000	967	13.65	0.004045
	0.6492	967	13.69	0.004240
	1.0680	967	13.61	0.004360
	1.6440	967	13.59	0.004540
	2.4210	967	13.61	0.004800
	3.3750	967	13.64	0.004514
PbO.SiO ₂ (N _{PbO} =0.4)	0.0000	967	12.50	0.004000
	0.8159	967	12.55	0.004244
	1.6345	967	12.55	0.004498
	2.3985	967	12.56	0.004750
	3.3755	967	12.57	0.005091
PbO.B ₂ O ₃ (N _{PbO} =0.5)	0.0000	1010	11.90	0.007100
	0.6492	1010	12.20	0.007450
	1.0680	1010	11.93	0.007600
	1.6440	1010	11.92	0.007880
	2.4210	1010	11.94	0.008280
	3.3750	1010	11.94	0.008793

Contd..

Table 4.1 Contd..

1	2	3	4	5
PbO.SiO ₂ (N _{PbO} =0.4)	0.0000	1010	18.40	0.008400
	0.8159	1010	18.37	0.008837
	1.6345	1010	18.38	0.009310
	2.3985	1010	18.37	0.009765
	3.3755	1010	18.30	0.001037
PbO.B ₂ O ₃ (N _{PbO} =0.5)	0.0000	1053	10.01	0.01180
	0.6492	1053	10.06	0.01218
	1.0680	1053	10.05	0.01240
	1.6440	1053	10.06	0.01276
	2.4210	1053	10.06	0.01324
3.3750	1053	10.06	0.01385	
PbO.SiO ₂ (N _{PbO} =0.4)	0.0000	1053	23.50	0.01610
	0.8160	1053	23.90	0.01688
	1.6345	1053	23.92	0.01755
	2.3985	1053	23.89	0.01818
	3.3755	1053	23.92	0.01905

Contd..

Table 4.1 Contd..

1	2	3	4	5
PbO.B ₂ O ₃ (N _{PbO} =0.5)	0.0000	1095	08.20	0.01880
	0.6492	1095	08.21	0.01920
	1.0680	1095	07.69	0.01945
	1.6440	1095	08.25	0.01981
	2.4210	1095	08.25	0.02029
	3.3750	1095	08.25	0.02090
PbO.SiO ₂ (N _{PbO} =0.4)	0.0000	1095	28.80	0.0295
	0.8159	1095	28.65	0.0302
	1.6345	1095	28.64	0.0309
	2.3985	1095	28.65	0.0317
	3.3755	1095	28.64	0.0326

In Table 4.2, calculated values of oxygen partial pressure from the emf data alongwith oxygen content of the alloys studied at different temperatures are presented. Equilibrium constant, $K_{\text{Pb-Cu}}$ for dissolution of oxygen in Pb- Cu alloys, can be expressed as,

$$K_{\text{Pb-Cu}} = h_{\text{O}} / (p_{\text{O}_2})^{\frac{1}{2}} \quad (4.5)$$

or,

$$\ln \{ [\text{at \% O}] / (p_{\text{O}_2})^{\frac{1}{2}} \} = \ln K_{\text{Pb-Cu}} - \ln f_{\text{O}} \quad (4.6)$$

where h_{O} represents the Henrian activity of oxygen in metallic solution and f_{O} , the activity coefficient of oxygen. Calculated values of parameter, $\ln \{ [\text{at \% O}] / (p_{\text{O}_2})^{\frac{1}{2}} \}$, are also given in Table 4.2

4.2 DISCUSSION ON RESULTS

For interpretation of experimental results and for their quantitative expression in terms of standard parameters, following two formulations are used:

4.2.1 Wagner's Interaction Parameter Formulation

In this formulation, the effect of additive, (which in this case is copper) on a component in solution (here oxygen) is considered to be incorporated in the activity coefficient term, f_{O} , and the value of equilibrium constant, $K_{\text{Pb-Cu}}$ is considered to be equal to that

Table 4.2 Calculated values on oxygen dissolution in Pb-Cu-O system from emf data

Temperature (K)	Copper concentration (atm pct)	Oxygen partial pressure P_{O_2} (atm)	Oxygen concentration (atm pct O)	$\ln\left\{\frac{[\text{atm pct O}]}{(P_{O_2})^{\frac{1}{2}}}\right\}$
1	2	3	4	5
967	0.0000	7.6305×10^{-17}	0.004523	13.0714
	0.6492	7.6452×10^{-17}	0.004319	13.1174
	1.0680	7.6166×10^{-17}	0.004192	13.1471
	1.6440	7.6086×10^{-17}	0.004024	13.1879
	2.4210	7.6159×10^{-17}	0.003808	13.2430
	3.3750	7.6269×10^{-17}	0.003558	13.3107
	0.0000	7.2207×10^{-17}	0.004005	13.0713
	0.8159	7.2381×10^{-17}	0.003780	13.1291
	1.6345	7.2381×10^{-17}	0.003566	13.1873
	2.3985	7.2416×10^{-17}	0.003378	13.2415
	3.3755	7.2451×10^{-17}	0.003151	13.3107
1010	0.0000	8.1732×10^{-16}	0.009043	12.4349
	0.6492	8.2866×10^{-16}	0.008679	12.4757
	1.0680	8.1844×10^{-16}	0.008453	12.5022
	1.6440	8.1807×10^{-16}	0.008152	12.5383
	2.4210	8.1882×10^{-16}	0.007762	12.5871
	3.3750	8.1882×10^{-16}	0.007309	12.6480

Contd..

Table 4.2 Contd..

1	2	3	4	5
	0.0000	1.1018×10^{-15}	0.008393	12.4348
	0.8159	1.1003×10^{-15}	0.007926	12.4805
	1.6345	1.1008×10^{-15}	0.007571	12.5375
	2.3985	1.1003×10^{-15}	0.007215	12.5857
1053	0.0000	6.9909×10^{-15}	0.01880	11.8574
	0.6492	7.0063×10^{-15}	0.01841	11.8873
	1.0680	7.0032×10^{-15}	0.01815	11.9078
	1.6440	7.0069×10^{-15}	0.01780	11.9348
	2.4210	7.0063×10^{-15}	0.01733	11.9711
	3.3750	7.0063×10^{-15}	0.01678	12.0159
	0.0000	1.2674×10^{-14}	0.02950	11.8707
	0.8159	1.2899×10^{-14}	0.02869	11.9090
	1.6345	1.2911×10^{-14}	0.02790	11.9475
	2.3985	1.2893×10^{-14}	0.02719	11.9833
	3.3755		0.02630	12.0291

Contd..

Table 4.2 Contd..

1	2	3	4	5
1095	0.0000	4.9623×10^{-14}	0.01880	11.3418
	0.6492	4.9708×10^{-14}	0.01841	11.3639
	1.0680	4.8579×10^{-14}	0.01815	11.3793
	1.6440	4.9737×10^{-14}	0.01780	11.3976
	2.4210	4.9737×10^{-14}	0.01733	11.4283
	3.3750	4.9722×10^{-14}	0.01680	11.4565
	0.0000	1.1888×10^{-13}	0.02950	11.3570
	0.8159	1.1818×10^{-13}	0.02869	11.3847
	1.6345	1.1807×10^{-13}	0.02790	11.4125
	2.3985	1.1812×10^{-13}	0.02720	11.4383
	3.3755	1.1807×10^{-13}	0.02630	11.4716

of oxygen in the major solvent component (viz. lead in this case) i.e. $K_{\text{Pb-Cu}} \approx K_{\text{Pb}}$. Further the function, $\ln f_{\text{O}}$, because of continuity conditions, can be assumed to be expressed in terms of Taylor series as follows,

$$\ln f_{\text{O}} = [\partial \ln f_{\text{O}} / \partial (\text{at.}\% \text{O})] \cdot [\text{at.}\% \text{O}] + [\partial \ln f_{\text{O}} / \partial (\text{at.}\% \text{Cu})] \cdot [\text{at.}\% \text{Cu}] + \dots \quad (4.7)$$

As the concentrations of oxygen and copper in the metallic solution are small, one can neglect higher order terms of the series and write,

$$\ln f_{\text{O}} \approx \epsilon_{\text{O}}^{\text{O}} [\text{at.}\% \text{O}] + \epsilon_{\text{O}}^{\text{Cu}} [\text{at.}\% \text{Cu}] \quad (4.8)$$

where, $\epsilon_{\text{O}}^{\text{O}}$, is the self-interaction parameter of oxygen in solution, and, $\epsilon_{\text{O}}^{\text{Cu}}$, the interaction parameter of copper on oxygen in solution. Thus Eq.4.6 can be rewritten as:

$$\ln \left\{ \frac{[\text{at.}\% \text{O}]}{(p_{\text{O}_2})^{1/2}} \right\} = \ln K_{\text{Pb}} - \epsilon_{\text{O}}^{\text{O}} [\text{at.}\% \text{O}] + \epsilon_{\text{O}}^{\text{Cu}} [\text{at.}\% \text{Cu}] \quad (4.9)$$

For the calculation of interaction parameter, $\epsilon_{\text{O}}^{\text{Cu}}$, one can make use of values of K_{Pb} and $\epsilon_{\text{O}}^{\text{O}}$ obtained from Pb-O system. But this method will suffer from the drawback that any error in these two parameters will be carried over to calculated value of $\epsilon_{\text{O}}^{\text{Cu}}$. Therefore, to avoid this error, instead of this method, multivariant linear regression technique is used to evaluate $\epsilon_{\text{O}}^{\text{Cu}}$. The computer programme for the analysis is given in Appendix V. Values of $\epsilon_{\text{O}}^{\text{Cu}}$ thus obtained for various temperatures are given

in Table 4.3. Further, it has been found that values of K_{Pb} and ϵ_{O}^{Cu} thus obtained, vary within error limits from

Table 4.3 Calculated Values of Ternary Interaction Parameters at different temperatures

Temperature (K)	Ternary interaction parameter	
	$\epsilon_{O(Pb)}^{Cu}$ (mole basis)	$\epsilon_{O(Pb)}^{Cu}$ (atom.pct.basis)
967	-7.095	-0.0709
1010	-6.464	-0.0646
1053	-4.566	-0.0457
1095	-3.526	-0.0353

those obtained from corresponding binary systems. In Fig. 4.1, ϵ_{O}^{Cu} is plotted against $1/T$. It has been found to follow the relation ship,

i. Molar basis

$$\epsilon_{O(Pb)}^{Cu} = 23.9 - 30.3 \times 10^3 / T \quad (4.10a)$$

ii. Atom pct. basis

$$\epsilon_{O(Pb)}^{Cu} = 0.247 - 310 / T \quad (4.10b)$$

Also plotted in Fig. 4.1 are the values obtained by Jacob and Jeffes [22] and Taskinen and Holopainen [62]. These authors have arrived at following relationships:
Jacob and Jeffes (molar basis)

$$\epsilon_{O(Pb)}^{Cu} = 3.42 - 7767 / T \quad (4.11)$$

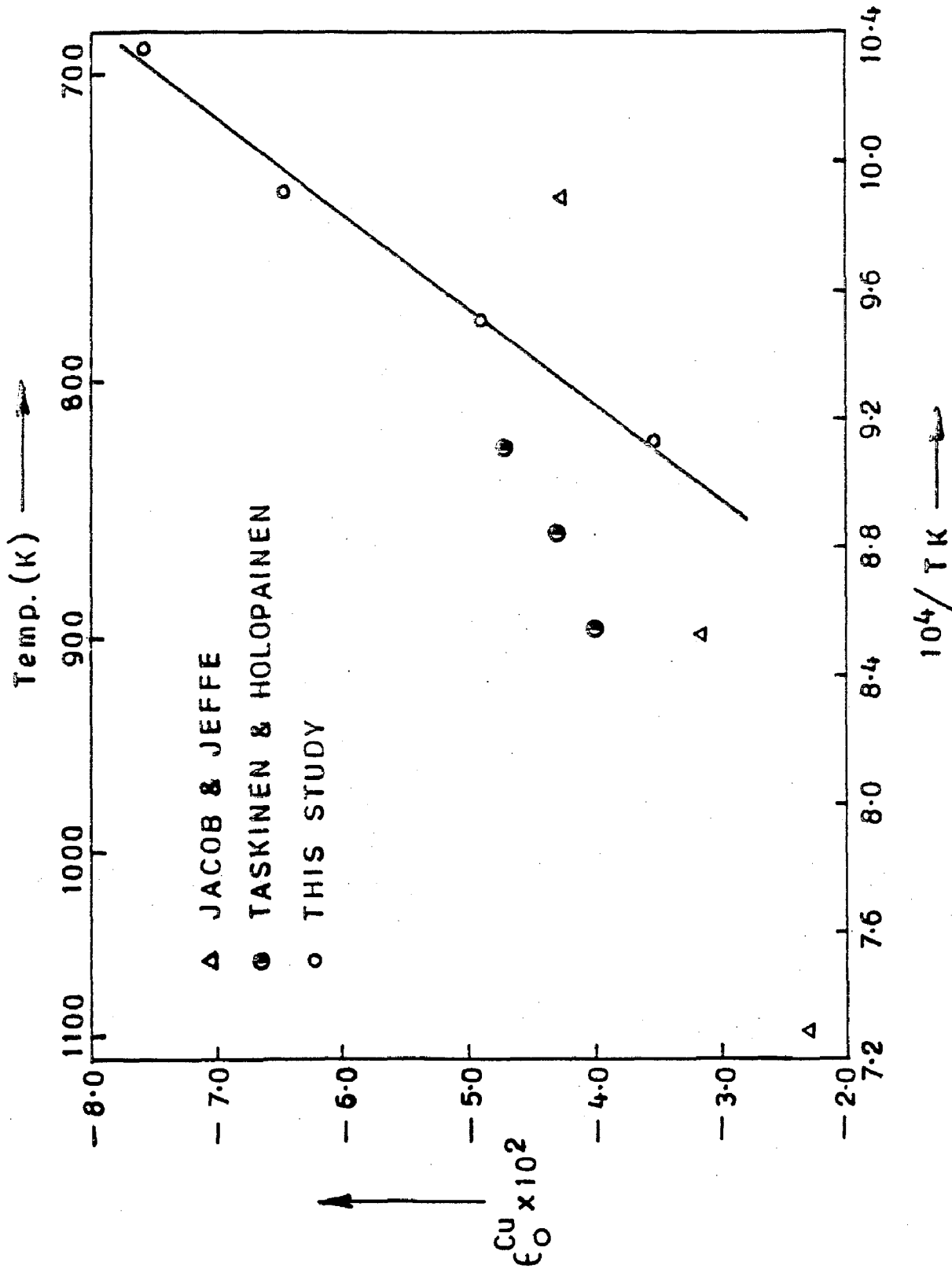


FIG. 4-1: PLOT OF TEMPERATURE DEPENDENCE OF FIRST ORDER INTERACTION PARAMETER, ϵ_0^{Cu} IN Pb-Cu-O SYSTEM

Taskinen and Holopainen (molar basis),

$$\epsilon_{O(Pb)}^{Cu} = 5.93 - 11.6 \times 10^3 / T \quad (4.12)$$

Calculated values for all the three above mentioned relationships are given in Table 4.4 for the different temperatures of study in the range 967-1095K.

It is seen that all the values show a good agreement at temperatures above 1050°C but differ considerably at low temperatures. The present work approaches more closely the values reported by Taskinen than those reported by Jacob and Jeffes.

Table 4.4 Experimental values of Ternary Interaction parameter, $\epsilon_{O(Pb)}^{Cu}$, at different temperatures*

Temperature (K)	$\epsilon_{O(Pb)}^{Cu}$		
	Present study	Jacob and Jeffes	Taskinen and Holopainen
967	-7.10 (-0.071)	-4.61 (-0.0461)	-6.07 (-0.061)
1010	-6.46 (-0.646)	-4.27 (-0.0427)	-5.56 (-0.556)
1053	-4.89 (-0.0489)	-3.96 (-0.0396)	-5.09 (-0.051)
1095	-3.53 (-0.035)	-3.67 (-0.037)	-3.74 (-0.037)

*Values within parentheses refer to calculated values on atom pct. basis, whereas others refer to those on molar basis.

This linear formulation as is evident from Eq. 4.6 is applicable only in very dilute solution ranges and also for solute components which do not show a vast difference in their reactivity towards the solvent components. In all other cases the quasi-chemical formulation is better suited.

4.2.2 Quasi-chemical Formulation

In this formulation all effects due to the solute, itself i.e. oxygen are summed up in the Henrian activity coefficient, f_O^0 , for oxygen, whereas the effect of solvent components are summed up in the value of equilibrium constant K . Thus Eq. 4.6 can be rewritten as,

$$\ln \left\{ \frac{[\text{at.}\%O]}{(p_{O_2})^{\frac{1}{2}}} \right\} = \ln K_{(\text{Pb}+\text{Cu})} - \ln f_{O(\text{Pb}+\text{Cu})}^0 \quad (4.13)$$

where $K_{(\text{Pb}+\text{Cu})}$ and $f_{O(\text{Pb}+\text{Cu})}^0$ represent, respectively the equilibrium constant for dissolution of oxygen in Pb-Cu alloys and activity coefficient of oxygen.

Further, for the special case of $[\text{at.}\%O] \rightarrow 0$, $f_{O(\text{Pb}+\text{Cu})}^0 \rightarrow 1$, hence one can write

$$\ln \left\{ \frac{[\text{at.}\%O]}{(p_{O_2})^{\frac{1}{2}}} \right\} [\text{at.}\%O] \rightarrow 0 = \ln K_{(\text{Pb}+\text{Cu})} \quad (4.14)$$

The effect due to presence of a minor component (i.e. copper in this case) as solute is represented as, f_O^{Cu} , which is defined as,

$$\ln f_{\text{O}}^{\text{Cu}} \equiv \ln K_{\text{O}}(\text{Pb}) - \ln K_{\text{O}}(\text{Pb+Cu}) \quad (4.15)$$

where $K_{\text{O}}(\text{Pb})$ and $K_{\text{O}}(\text{Pb+Cu})$ are respectively the equilibrium constants for dissolution of oxygen in pure lead and (Pb+Cu) binary metallic solvent

It may be pointed out that both the parameters, $K_{\text{O}}(\text{Pb+Cu})$ and $f_{\text{O}}(\text{Pb+Cu})$ are functions of composition. As oxygen content of the solution is very small so one can rewrite Eq. 4.15 as follows,

$$\ln \left\{ \frac{[\text{at.}\% \text{O}]}{(p_{\text{O}_2})^{\frac{1}{2}}} \right\} = \ln K_{\text{O}}(\text{Pb+Cu}) - \epsilon_{\text{O}}^{\text{O}}(\text{Pb+Cu}) \cdot [\text{at.}\% \text{O}] \quad (4.16)$$

where, $\epsilon_{\text{O}}^{\text{O}}(\text{Pb+Cu})$ is the self-interaction parameter of oxygen in the solvent. The above equation suggests that values of $K_{\text{O}}(\text{Pb+Cu})$ and $\epsilon_{\text{O}}^{\text{O}}(\text{Pb+Cu})$ can be determined experimentally by considering a series of experiments each on a solvent of fixed-composition and by varying oxygen content. Coulometric technique makes use of this method, but a precise control of oxygen content of the alloys becomes difficult. In the present set of experiments it has not been possible to make use of this procedure. Therefore, to calculate $K_{\text{O}}(\text{Pb+Cu})$ some approximation had to be made. According to Anik et al. [187], $\epsilon_{\text{O}}^{\text{O}}(\text{Pb+Cu})$ in a binary solvent (Pb+Cu) can be expressed as,

$$\epsilon_{\text{O}}^{\text{O}}(\text{Pb+Cu}) = N_{\text{Pb}} \epsilon_{\text{O}}^{\text{O}} + N_{\text{Cu}} \epsilon_{\text{O}}^{\text{O}}(\text{Cu}) + \delta_{\text{q}} \cdot N_{\text{Cu}} \cdot N_{\text{Pb}} \quad (4.17)$$

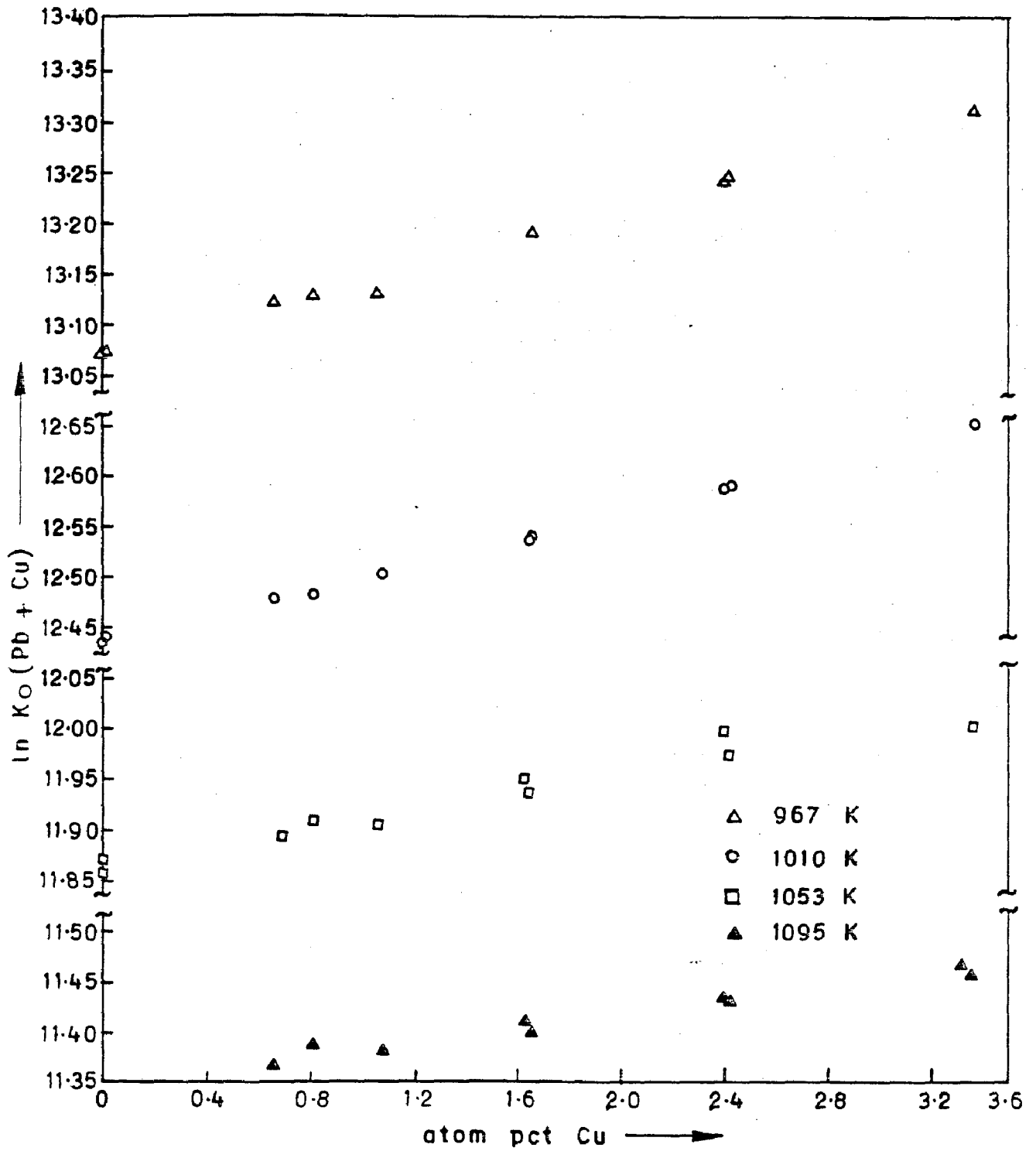


FIG. 4-2: VARIATION OF $\ln K_O$ (Pb + Cu) WITH CONCENTRATION OF COPPER IN LEAD - COPPER ALLOYS

As the copper content present in this study is very small, maximum being 3.375 atomic percent, one can neglect the last two terms in the above expression and hence write.

$$\epsilon_{O(Pb+Cu)}^O \approx \epsilon_{O(Pb)}^O \quad (4.18)$$

with this approximation, Eq. 4.17 assumes the form,

$$\ln K_{O(Pb+Cu)} = \ln\{ [\text{at.\%O}] / (p_{O_2})^{\frac{1}{2}} \} + \epsilon_{O(Pb)}^O [\text{at.\%O}] \quad (4.19)$$

One can therefore calculate the value of parameter $\ln K_{O(Pb+Cu)}$ from a knowledge of ϵ_{O}^O and experimental data on [at.%O] and $p_{O_2}^{\frac{1}{2}}$ in different alloy compositions. The values of $\ln K_{O(Pb+Cu)}$ thus calculated are presented in Table 4.5.

In Fig. 4.2 the function $\ln K_{O(Pb+Cu)}$ is plotted against copper concentration of the alloy for various temperatures. It is seen that the addition of copper to alloy or solvent increases, the value of $\ln K_{O(Pb+Cu)}$.

In Fig. 4.3 function $\ln f_O^{Cu}$ is plotted against copper concentration along with the data of other authors. The results obtained at different temperatures and under different slag covers are shown by a characteristic symbol. The plot also shows data calculated from the study on Pb-Cu-O system by Jacob and Jeffs [22] as well

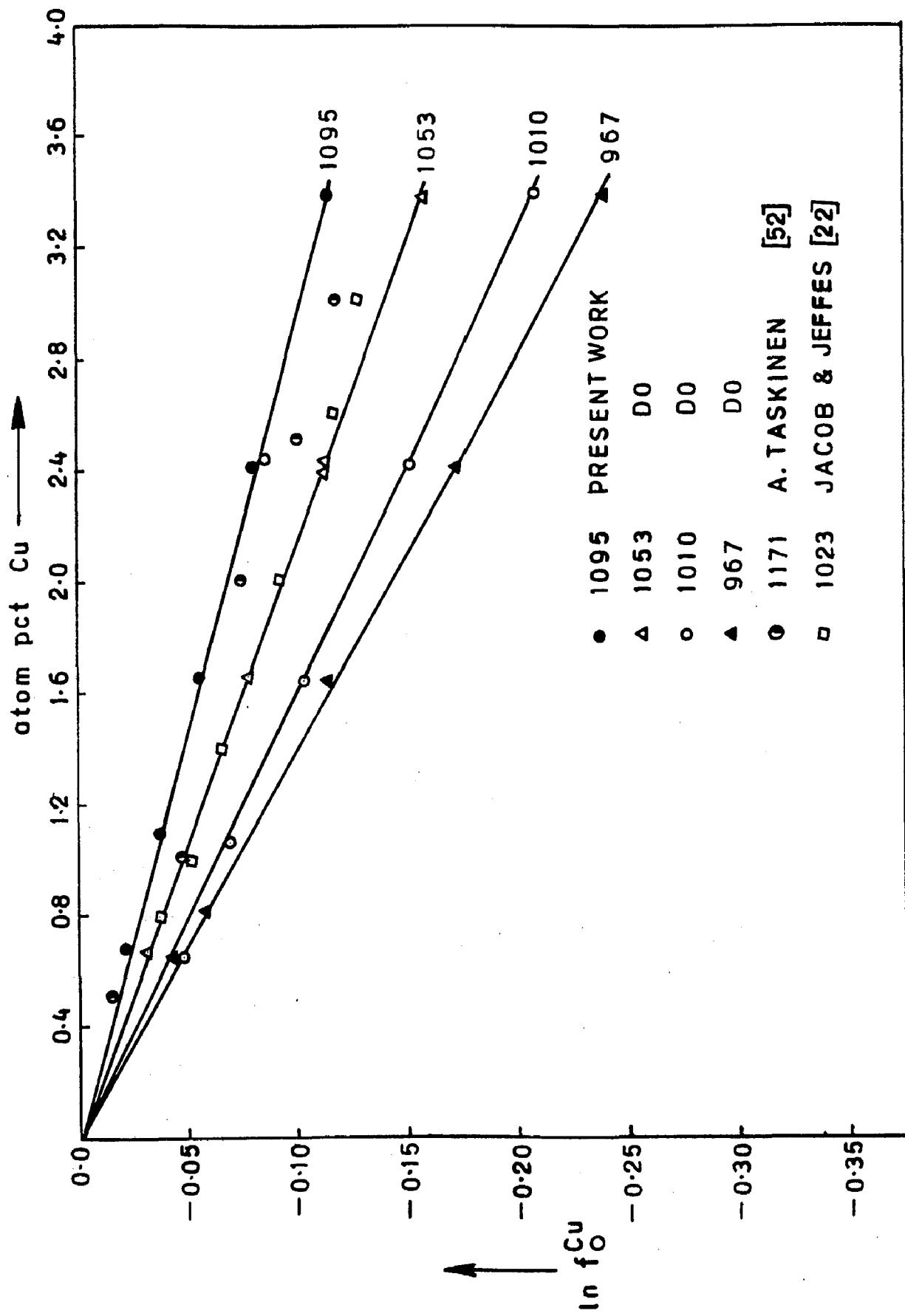


FIG. 4 — 3: EFFECT OF CU ON ACTIVITY COEFFICIENT OF OXYGEN IN LIQUID LEAD AT 967, 1010, 1053 AND 1095 K

Table 4.5 Activity coefficient, $\ln f_{\text{O}}^{\text{Cu}}$ in Pb-Cu-O system at different temperatures and copper concentrations.

Temperature	Copper concentration	$\ln K_{\text{O}}(\text{Pb}+\text{Cu})$	$\ln f_{\text{O}}^{\text{Cu}}$
967*	0.0000	13.0723	-0.000
	0.6492	13.1188	-0.0459
	1.0680	13.1275	-0.1552
	1.6440	13.1877	-0.1164
	2.4210	12.2437	-0.1715
	3.3750	13.3114	-0.2391
967**	0.0000	13.0721	-0.0000
	0.8159	13.1298	-0.0578
	1.6340	13.1880	-0.1159
	2.3980	13.2421	-0.1701
	3.3750	13.3113	-0.2392
1010*	0.0000	12.4362	-0.0000
	0.6492	12.4770	-0.0475
	1.0680	12.5035	-0.0672
	1.6440	12.5395	-0.1033
	2.4210	12.5882	-0.1520
	3.3750	12.6491	-0.2128
1010**	0.0000	12.4360	-0.0000
	0.8159	12.4817	-0.0456
	1.6345	12.5386	-0.1026
	2.3985	12.5868	-0.1507

* with $\text{PbO} \cdot \text{B}_2\text{O}_3$ slag cover

** with $\text{PbO} \cdot \text{SiO}_2$ slag cover

Table 4.5 Activity Coefficient, f_{O}^{Cu} in Pb-Cu-O system at different temperatures and copper concentrations.

Temperature (K)	Copper concentration (atom pct)	$\ln K_{\text{O}}(\text{Pb}+\text{Cu})$	$\ln f_{\text{O}}^{\text{Cu}}$
1053*	0.0000	11.8586	0.0000
	0.6492	11.8885	-0.0298
	1.0680	11.9089	-0.0503
	1.6440	11.9359	-0.0773
	2.4210	11.9722	-0.1136
	3.3750	12.0169	-0.1583
1053**	0.0000	11.8723	0.0000
	0.8159	11.9106	-0.0382
	1.6345	11.9490	-0.0767
	2.3985	11.9848	-0.1124
	3.3755	12.0305	-0.1582
1095*	0.0000	11.3429	0.0000
	0.6492	11.3650	-0.0221
	1.0680	11.3804	-0.0375
	1.6440	11.3987	-0.0557
	2.4210	11.4293	-0.0864
	3.3750	11.4575	-0.1146
1095**	0.0000	11.3568	0.0000
	0.8159	11.3865	-0.0276
	1.6345	11.4142	-0.0554
	2.3985	11.4340	-0.0812
	3.3755	11.4732	-0.1144

* with $\text{PbO} \cdot \text{B}_2\text{O}_3$ slag cover

** with $\text{PbO} \cdot \text{SiO}_2$ slag cover

by Taskinen et al.[62] under dilute concentration range of copper selected for this study. The plots follow nearly a linear variation with temperature and thus the representation of interaction parameter,

$$\epsilon_{O(Pb)}^{Cu} = \left(\frac{\partial \ln f_O}{\partial N_{Cu}} \right)_{N_{Pb} \rightarrow 1} \quad (4.20)$$

As a temperature function is justified. The interaction coefficients have been found by regressional analysis of the data and reported earlier in Table 4.4.

The variation of the logarithm of the activity coefficient of oxygen at constant atomic % of copper with reciprocal of temperature has been represented as straight lines in Fig. 4.4. The relative partial molar enthalpy and entropy of oxygen at 1 atom percent in Pb-Cu alloys with respect to gaseous oxygen as the standard state may be calculated from the slope of these lines and in comparison with equation,

$$\ln f_O = \Delta \bar{H}_O / RT - \Delta \bar{S}_O / R \quad (4.21)$$

The values of $\Delta \bar{H}_O$ and $\Delta \bar{S}_O$ so obtained are given in Table 4.6

Table 4.6 Relative Partial Molar Enthalpy and Entropy of oxygen relative to gaseous oxygen in Pb-Cu alloys

Temperature	Copper conc.	Partial Molar Enthalpy*	Partial Molar Entropy**
1095	1 atom %	-2309	-1.782
	2 atom %	-5184	-4.129
	3 atom %	-7581	-6.025

* $\Delta \bar{H}_O$, joule ; ** $\Delta \bar{S}_O$ joule deg⁻¹ mole⁻¹

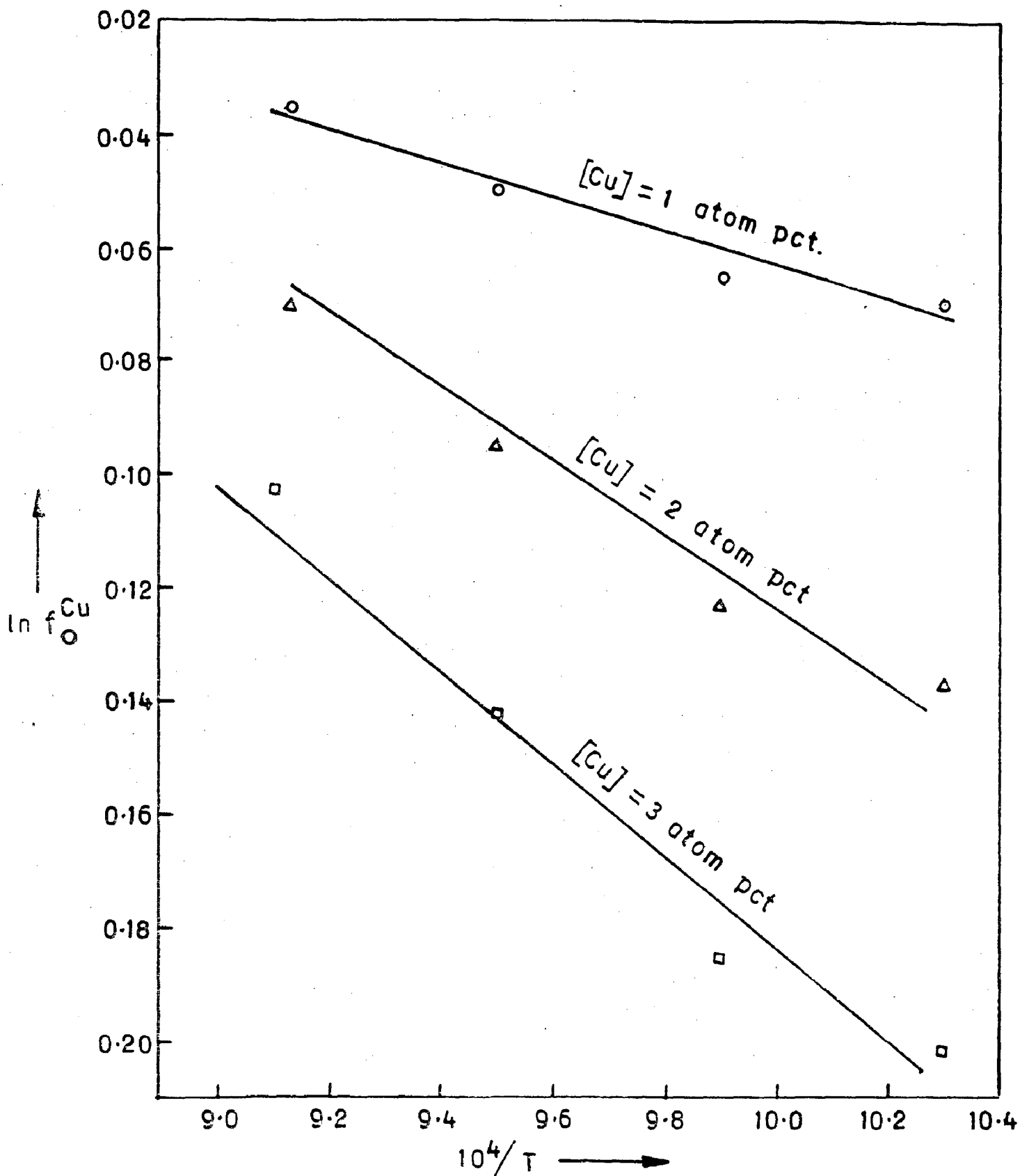


FIG. 4 - 4: VARIATION OF f_{O}^{Cu} IN Pd - Cu ALLOYS WITH RECIPROCAL OF TEMPERATURE

4.3 APPLICABILITY OF SOLUTION MODELS

The measured values of activity coefficient of oxygen, $f_{O(A+B)}$ at 1095 K in liquid lead-copper alloys for present study are compared in Fig. 4.5. with those those predicted by several classical models. For this purpose the binary data required for necessary calculations are adopted from compilations of Hultgren et al.[1]. These theoretical models have been reviewed in Chapter I. But for the sake of completeness the equations used for calculation are being rewritten here.

Alcock and Richardson [152] obtained the equation,

$$\ln f_{O(A+B)} = N_A \ln f_{O(A)} + N_B \ln f_{O(B)} - N_A \ln f_{A(A+B)} - N_B \ln f_{B(A+B)} \quad (4.22)$$

where, A+B above stand for the solvent Pb and solute Cu respectively.

This equation was derived on the assumption that the distribution of atoms in the solution is random; the coordination number of all three types of atoms is equal and that the energy of interaction between atom pairs is independent of concentration. The predicted values of $\ln f_{O}$ are reported in Table 4.7 and plotted in Fig. 4.5 and as will be observed do not match with the measured values. The basic assumption of the regular solution model that the energies of interaction between different atom-pairs are independent of composition of the solution seems to be responsible for the mismatch.

Table 4.7 Predicted values of Inf_O^{Cu} in Pb-Cu-O system obtained using theoretical models at 1095K

Theoretical Models	Ternary interaction parameter, Inf_O^{Cu} at $N_{\text{Cu}} =$				
	0.01	0.02	0.03	0.04	0.05
Alcock & Richardson (Regular solution model)	+0.006	+0.0146	+0.0236	+0.0330	+0.0435
Alcock & Richardson (QCT)					
Z = 2	+0.005	+0.012	+0.019	+0.026	+0.0334
Z = 8	-0.0736	-0.0141	-0.0226	-0.031	-0.041
Jacob & Jeffes (3 bond No.)	-0.021	-0.0318	-0.0591	-0.1266	-0.1705
Carl Wagner's					
h = 0	-0.0023	-0.048	-0.0723	-0.077	-0.122
h = 3026 J gatom ⁻¹	-0.022	-0.041	-0.0596	-0.077	-0.092
This study	-0.0375	-0.0625	-0.102	-	-

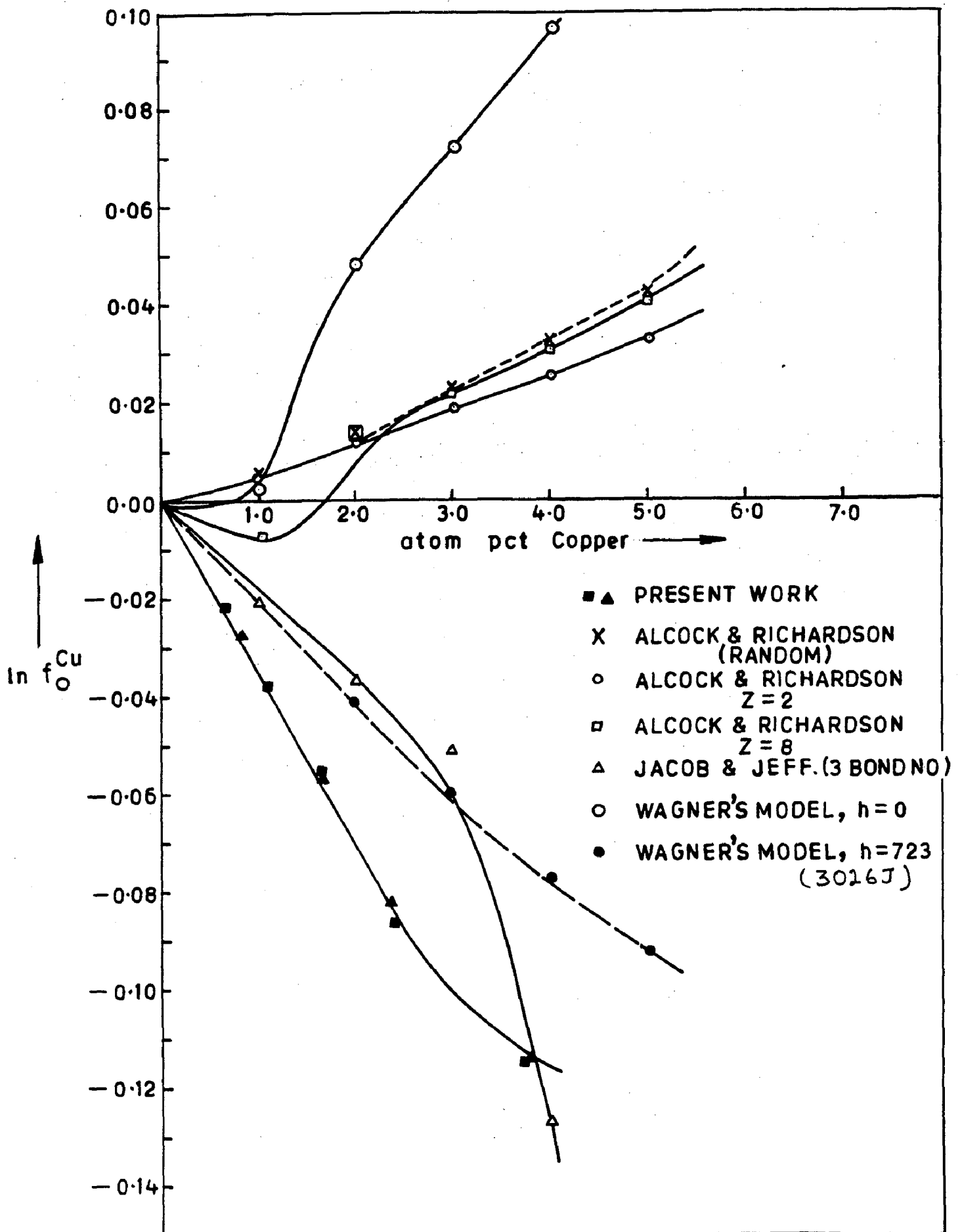


FIG. 4-5: ACTIVITY COEFFICIENT OF OXYGEN IN Pb-Cu ALLOYS AT 1095 K

The neglect of clustering may not be the main source of error for the Pb-Cu-O system.

To predict the effect of a metallic component on the activity coefficient of an electronegative solute viz. oxygen, Alcock and Richardson [154] modified the regular solution model by using quasi-chemical approximation. According to this model, the activity coefficient, $f_{O(A+B)}$ of oxygen in the (A+B) alloy solvent can be expressed as,

$$f_{O(A+B)} = [N_A (f_{A(A+B)} / f_{O(A)})^{1/Z} + N_B [(f_{B(A+B)} / f_{O(B)})^{1/Z}]^{-Z} \quad (4.23)$$

where, Z is the co-ordination number assumed to be same for all the three types of atoms viz. A, B and oxygen constituting the solution. Using Eq. 4.23, $f_{O(Pb+Cu)}$ has been calculated for Z=2 and Z=8 and is also plotted in Fig. 4.5. The predicted values again do not match with the measured ones. The calculated values being no better than those obtained using Eq. 4.23. This is attributed to the fact that the error in the regular solution model probably also remains in the quasichemical treatment. The ratio of the number of Pb-O bonds to Cu-O bonds would be greater than the ratio of the mole fractions of lead and copper in the solution as indicated obviously by the ratio $f_{O(Cu)} / f_{O(Pb)} \approx 22$ at 1095 K. However, for the development of the model, all the atoms

are assumed to have the same co-ordination number (Z). Further, the ratio of the number of Pb-O bonds to Cu-O bonds has been assumed to follow the relation,

$$n(\text{Cu-O})/n(\text{Pb-O}) = (N_{\text{Cu}}/N_{\text{Pb}}) \cdot e^{W/ZKT} \quad (4.24)$$

where, W/Z is the energy exchange which occurs by exchange of a copper-atom in the co-ordination shell of the oxygen-atom with a lead atom in the body of the solution.

The measured values of $f_O(\text{Pb+Cu})$ in the Pb-Cu-O system are also compared with those predicted by Jacob and Alcock's [22] following quasichemical equation,

$$f_O(\text{A+B}) = N_A [f_A^\alpha(\text{A+B})/f_O^{1/n}(\text{A})] + N_B [f_B^\alpha(\text{A+B})/f_O^{1/n}(\text{B})]^{-1} \quad (4.25)$$

where, functions $f_O(\text{A})$, $f_O(\text{B})$, $f_A(\text{A+B})$ and $f_B(\text{A+B})$ have already been defined; n , is the number of bonds made by each oxygen atom, and, α represents the degree to which metal-metal bonds are weakened with oxygen dissolution in solution. The values of $n=4$ and $\alpha=1/2$ as proposed by authors are used in the calculation of $f_O(\text{A+B})$ in Pb-Cu-O system. A fair agreement between the predicted and the measured values is observed, with the predicted values being slightly on the higher side. This is attributed to the fact that in generalized chemical equation viz. Eq. 4.25, Jacob and Alcock assumed that the strong oxygen metal bonds distorted the electronic configuration

and thus reduced the strength of bonds formed by these metal atoms with neighbouring metal atoms. This was unlike the basic assumption of models developed by Alcock and Richardson as discussed above. These authors, however, further assumed that the average composition of the metal atoms forming bonds with metal atoms bonded to oxygen was equal to the bulk composition of alloys. This, in the present system, with $fO(Cu)/fO(Pb) \approx 22$ at $T=1095$ K, does not seem to be totally reasonable. This may account for the fact that the agreement between the predicted and measured values is not very close.

Wagner [157] proposed another theoretical model to predict $fO(A+B)$ with one adjustable energy parameter, h ,

$$fO(A+B) = \left\{ \sum_{i=0}^Z \binom{Z}{i} [N_A / fO^{1/Z}(A)]^{Z-i} \cdot [N_B / fO^{1/Z}(B)]^i \right. \\ \left. [\exp((Z-i)ih/2RT)] \right\}^{-1} \quad (4.26)$$

where, Z is the co-ordination number of dissolved oxygen and is normally taken as 6. The basic assumptions underlying this model being that the solvent atoms exhibit ideal solution behaviour, the dissolved oxygen atoms occupy quasi-interstitial sites and the solvation energy exhibits a parabolic dependence on the number of metal atoms A and B in the solvation shell around oxygen atoms. Chang et al. [162] reported following empirical relationship for calculation of h in Eq. 4.26, from a knowledge

of the corresponding binaries,

$$h = 2\varepsilon/Z^2 + u[\varepsilon(Vb/Va)^2] + V[\Delta G^\circ O(A) - \Delta G^\circ O(B)] \quad (4.27)$$

where, V_a and V_b represent metallic valances given by Pauling [192] of the alloying elements A and B; $\Delta G^\circ O(A)$ and $\Delta G^\circ O(B)$ are the respective free energies for dissolution of oxygen in metals A and B and ε is the regular solution parameter defined by expression $\varepsilon = \Delta H/N_A \cdot N_B$ where ΔH is the enthalpy of formation of $A_{1-x}B_x$. Values of the coefficients u & v in above expression were determined by Chang et al. [164] as $u = 0.04$ and $v = 0.09$ on the basis of the available data.

Values of $fO(A+B)$ calculated using Eqs. 4.26 and 4.27 are given in Table 4.7 and plotted in Fig. 4.5. The value of 'h' used for these calculations was taken as 3025J calculated at 1373 K by Chiang et al. [162] using the data available at this temperature in the compilation of Hultgren et al. [1]. When compared with the values of $\ln fO$ as predicted by other models, those by Wagner's model seem to have a closer match with the corresponding measured values of $\ln fO$.

It is however, to be noted that the values of h used in these calculations at 1373 K, in view of the binary data available at this temperature in the compilation of Hultgren et al. [1] for this system. The value of 'h' at 1095 K, however, should be somewhat

higher than 3026 J. It is proposed that a value of $h=3620$ J gives a satisfactory representation of the data. This higher value of h at 1095 K seems obvious, because a preferential attachment of oxygen for a particular component in solution can be observed. This is also found true when value of $fO(Pb)$ is compared with that of $fO(Cu)$. A close match at this value between the measured and predicted values of $fO(A+B)$ is given in Fig.4.6.

For a limiting case with $h=0$, one may obtain a following simpler expression from Eq. 4.25,

$$fO(A+B) = [N_A/fO^{1/Z}(A) + N_B/fO^{1/Z}(B)]^{-Z} \quad (4.2)$$

This refers to a configuration, wherein $fO(A+B)$ will be independent of composition. As obvious, plot of $fO(A+B)$ in Fig. 4.5 does not match the measured values.

Chiang and Chang [162] further modified Wagner's equation by introducing two energy parameters h_1 and h_2 . However in view of the very dilute concentrations of Copper (1-4 atomic %) taken for this study, it is felt that the predicted values on the basis of this model would not be significantly different from those predicted by Wagner's equation. Calculations based on Chiang and Chang's model have therefore been not attempted for the interpretation of results on the present system.

CHAPTER V

LEAD-BISMUTH-OXYGEN SYSTEM

Copper, bismuth, arsenic, antimony, tin etc. form common impurities in lead obtained from blast furnace. During the refining of crude lead the impurities viz. copper is removed during drossing; arsenic, antimony and tin on account of their greater affinity for oxygen are eliminated during the oxidation stage. Bismuth, however, has to be removed as Bi_3Ca , Bi_2Ca_2 and Bi_2Mg_3 by the addition of calcium and/or magnesium. A knowledge of thermodynamic behaviour of oxygen in liquid Lead-bismuth alloys in the dilute concentration range is of importance in understanding the mechanism and thermodynamics of refining process. The only study reported in literature on the effect of bismuth on activity coefficient of oxygen in liquid lead is by A. Taskinen [65]. Accordingly some experimental studies have been conducted to arrive at thermodynamic data on solution of oxygen in lead-bismuth alloys.

Further, theoretical models already reviewed in Chapter I for binary metallic solvents shall be applied to this system to arrive at the one, most suitable for theoretical calculation and prediction of thermodynamic properties of oxygen in lead-bismuth solvents.

6.1 RESULTS AND CALCULATIONS

The experimental set-up used and procedure adopted for study have already been described in detail in Chapter II. In the present case, E.M.F. measurements were made on lead-bismuth-oxygen alloys of varying compositions with bismuth upto 3.0 atomic percent and covered with PbO-SiO₂ ($N_{\text{PbO}}=0.4$) and PbO-B₂O₃ ($N_{\text{PbO}}=0.5$) slags. The results of these experiments are presented in Table 5.1.

The dissolved oxygen content in the metal is determined by the reaction,



Square brackets indicate the components present in the metal phase and parenthesis represent that in the slag phase. Oxygen partial pressure in the system can be calculated from emf data of the cell and is determined by the following reaction,



O₂ in the curvilinear indicates the gaseous oxygen. Eqs. 5.1 and 5.2 lead to the following equation for dissolution of oxygen in the molten alloy,



The value of oxygen partial pressure is calculated using the expression,

Table 5.1 EMF data on Pb-Bi-O at different temperatures and values of bismuth concentration

Slag cover	Bismuth concentration (atom pct.)	Temperature (K)	EMF (mv)	Oxygen concentration (atom pct x 10 ²)
1	2	3	4	5
PbO.B ₂ O ₃ (N _{PbO} =0.5)	0.0000	913	11.33	0.1712
	0.5010		12.75	0.1743
	1.061		14.33	0.1778
	1.467		15.48	0.1805
	2.082		17.22	0.1845
	2.489		18.38	0.1872
	3.054		19.98	0.1911
PbO.SiO ₂ (N _{PbO} =0.4)	0.000	913	02.65	0.1373
	0.7406		04.75	0.1410
	1.434		06.71	0.1445
	2.231		08.97	0.1488
	2.974		11.07	0.1528
PbO.B ₂ O ₃ (N _{PbO} =0.5)	0.000	953	15.72	0.3562
	0.501		16.91	0.3614
	1.061		18.25	0.3673
	1.467		19.21	0.3716

Contd..

Tab 5.1 Contd..

1	2	3	4	5
	2.082	953	20.67	0.3783
	2.489		21.64	0.3828
	3.054		22.99	0.3892
PbO.SiO ₂	0.000		09.90	0.3091
(N _{PbO} =0.4)	0.7406		11.69	0.3160
	1.434		13.31	0.3222
	2.231		15.21	0.3296
	2.974		16.98	0.3369
PbO.B ₂ O ₃	0.000	993	20.00	0.6871
(N _{PbO} =0.5)	0.5010		20.79	0.6935
	1.061		21.67	0.7005
	1.467		22.32	0.7060
	2.082		23.30	0.7140
	2.489		23.94	0.7195
	3.054		24.83	0.7270

Contd..

Table 5.1 Contd..

1	2	3	4	5
PbO.SiO ₂ (N _{PbO} =0.4)	0.000	993	16.10	0.6274
	0.7406		17.27	0.6358
	1.434		18.37	0.6440
	2.231		19.63	0.6536
	2.971		20.81	0.6626
PbO.B ₂ O ₃ (N _{PbO} =0.5)	0.000	1034	24.44	1.289
	0.501		24.93	1.296
	1.061		25.48	1.304
	1.467		25.87	1.310
	2.082		26.48	1.319
PbO.SiO ₂ (N _{PbO} =0.4)	2.489		26.88	1.325
	3.054		27.93	1.338
	0.000	1034	21.95	1.218
	0.7406		22.67	1.228
	1.434		23.36	1.238
2.231		24.14	1.249	
2.974		24.86	1.250	

$$E = -RT/2F \ln(p_{O_2}^{\frac{1}{2}}, Ni-NiO) / (p_{O_2}^{\frac{1}{2}}, Pb-PbO) \quad (5.4)$$

Table 5.2 represent the calculated values of oxygen partial pressure from the emf data along with oxygen content of the alloys studied at different temperatures.

5.2 CALCULATION OF THERMODYNAMIC FUNCTIONS

The interpretation of experimental results and their quantitative expression is based on the following two formulations, already discussed in Chapter four, but is being presented here for the sake of continuity.

6.2.1 Wagner's Interaction Parameter Formualtion

In this formulation, the effect of bismuth on oxygen in solution is considered to be incorporated in the activity coefficient term, f_O , and the value of equilibrium constant, K_{Pb-Bi} is considered to be equal to that of oxygen in the major solvent component viz. lead i.e.

$$K_{Pb-Bi} \approx K_{Pb} \quad (5.5)$$

Further the function, $\ln f_O$, because of continuity conditions, can be assumed to be expressed in terms of Taylor series as follows,

$$\begin{aligned} \ln f_O = & \left\{ \frac{\partial \ln f_O}{\partial [\text{at.}\% \text{ O}]} \right\} \cdot [\text{at.}\% \text{ O}] \\ & + \left\{ \frac{\partial \ln f_O}{\partial [\text{at.}\% \text{ Bi}]} \right\} \cdot [\text{at.}\% \text{ Bi}] + \dots \end{aligned}$$

(5.6)

As the concentration of oxygen and bismuth in the metallic solution are small, one can neglect higher order terms of the series and write,

$$\ln f_O \approx \epsilon_O^O \cdot [\text{at.}\% \text{ O}] + \epsilon_O^{\text{Bi}} \cdot [\text{at.}\% \text{ Bi}] \quad (5.7)$$

where, ϵ_O^O , is the self interaction parameter of oxygen in solution and ϵ_O^{Bi} , interaction parameter of bismuth on oxygen in solution. thus Eq. 5.6 can be rewritten as,

$$\ln\{[\text{at.}\% \text{ O}]/(p_{\text{O}_2})^{\frac{1}{2}}\} = \ln K_{\text{Pb}} - \epsilon_O^O \cdot [\text{at.}\% \text{ O}] + \epsilon_O^{\text{Bi}} \cdot [\text{at.}\% \text{ Bi}] \quad (5.8)$$

For the calculation of interaction parameter, ϵ_O^{Bi} , one can make use of values of K_{Bi} and ϵ_O^O obtained from Lead-oxygen system. But this method will suffer from the draw back that any error in these two parameters will be carried over to calculated value of ϵ_O^{Bi} . Therefore to avoid this error, instead of this method, multivariant linear regression technique is used to evaluate ϵ_O^{Bi} . The computer programme for the analysis is given in Appendix II. Values of ϵ_O^{Bi} thus obtained at various temperatures are given in Table 5.3. Further, it has been found that values of K_{Pb} and ϵ_O^O thus obtained, vary within error limits from those obtained from corresponding binary systems. In Fig.5.1, ϵ_O^{Bi} is plotted vs $1/T$ and has been found to follow the relationship,

i) molar basis

$$\epsilon_{\text{O(Pb)}}^{\text{Bi}} = -17.454 + 19.2 \times 10^3/T \quad (\pm 0.3) \quad (5.9)$$

Table 5.2 Calculated values on oxygen dissolution in Pb-Bi-O system from emf data.

Temperature (K)	Bismuth concentration (atom.pct.)	Oxygen partial pressure p_{O_2} (atom)	Oxygen concentration (atom pct $\times 10^2$)	$\ln \left[\frac{\text{atom pct. O}}{(p_{O_2})^{\frac{1}{2}}} \right]$
1	2	3	4	5
913	0.000	2.176×10^{-18}	0.1712	13.964
	0.501	2.339×10^{-18}	0.1743	13.946
	1.061	2.535×10^{-18}	0.1778	13.930
	1.467	2.687×10^{-18}	0.1805	13.911
	2.082	2.936×10^{-18}	0.1845	13.899
913	2.489	3.114×10^{-18}	0.1872	13.874
	3.054	3.378×10^{-18}	0.1911	13.854
	0.000	1.3993×10^{-18}	0.1373	13.964
	0.7406	1.5571×10^{-18}	0.1410	13.938
	1.434	1.7203×10^{-18}	0.1445	13.912
953	2.231	1.9299×10^{-18}	0.1488	13.884
	2.974	2.1474×10^{-18}	0.1528	13.857
	0.000	3.6234×10^{-17}	0.3562	13.291
	0.501	3.8398×10^{-7}	0.3614	13.276
	1.061	4.0988×10^{-17}	0.3673	13.260
1.467	4.2951×10^{-17}	0.3716	13.248	

Contd..

Table 5.2 Contd..

1	2	3	4	5
953	2.082	4.6118×10^{-17}	0.3783	13.231
	2.489	4.8351×10^{-17}	0.3828	13.219
	3.054	5.1638×10^{-17}	0.3892	13.203
	0.000	2.7287×10^{-17}	0.3091	13.291
	0.7406	2.9774×10^{-17}	0.3160	13.269
	1.434	3.2219×10^{-17}	0.3222	13.249
	2.231	3.5362×10^{-17}	0.3296	13.225
	2.974	3.8529×10^{-17}	0.3369	13.205
993	0.000	4.5090×10^{-16}	0.6871	12.687
	0.501	4.6787×10^{-16}	0.6935	12.678
	1.061	4.8752×10^{-16}	0.7005	12.667
	1.467	5.0257×10^{-16}	0.7060	12.660
	2.082	5.2614×10^{-16}	0.7140	12.648
	2.489	5.4312×10^{-16}	0.7195	12.641
	3.054	5.6516×10^{-16}	0.7270	12.631
	0.000	3.7572×10^{-16}	0.6274	12.687
	0.7406	3.9685×10^{-16}	0.6358	12.673
	1.434	4.1780×10^{-16}	0.6440	12.660
	2.231	4.4316×10^{-16}	0.6536	12.646
	2.974	4.6831×10^{-16}	0.6626	12.632

Contd..

Table 5.2 Contd....

1	2	3	4	5
1034	0.000	5.0374×10^{-15}	1.289	12.110
	0.501	5.1495×10^{-15}	1.296	12.104
	1.061	5.2783×10^{-15}	1.304	12.098
	1.467	5.3715×10^{-15}	1.310	12.094
	2.082	5.5207×10^{-15}	1.319	12.087
	2.489	5.6208×10^{-15}	1.325	12.082
	3.054	5.8922×10^{-15}	1.338	12.068
	0.000	4.5045×10^{-15}	1.218	12.109
	0.7406	4.6525×10^{-15}	1.228	12.101
	1.434	4.2989×10^{-15}	1.238	12.093
	2.231	4.970×10^{-15}	1.249	12.085
	2.974	5.1333×10^{-15}	1.250	12.077

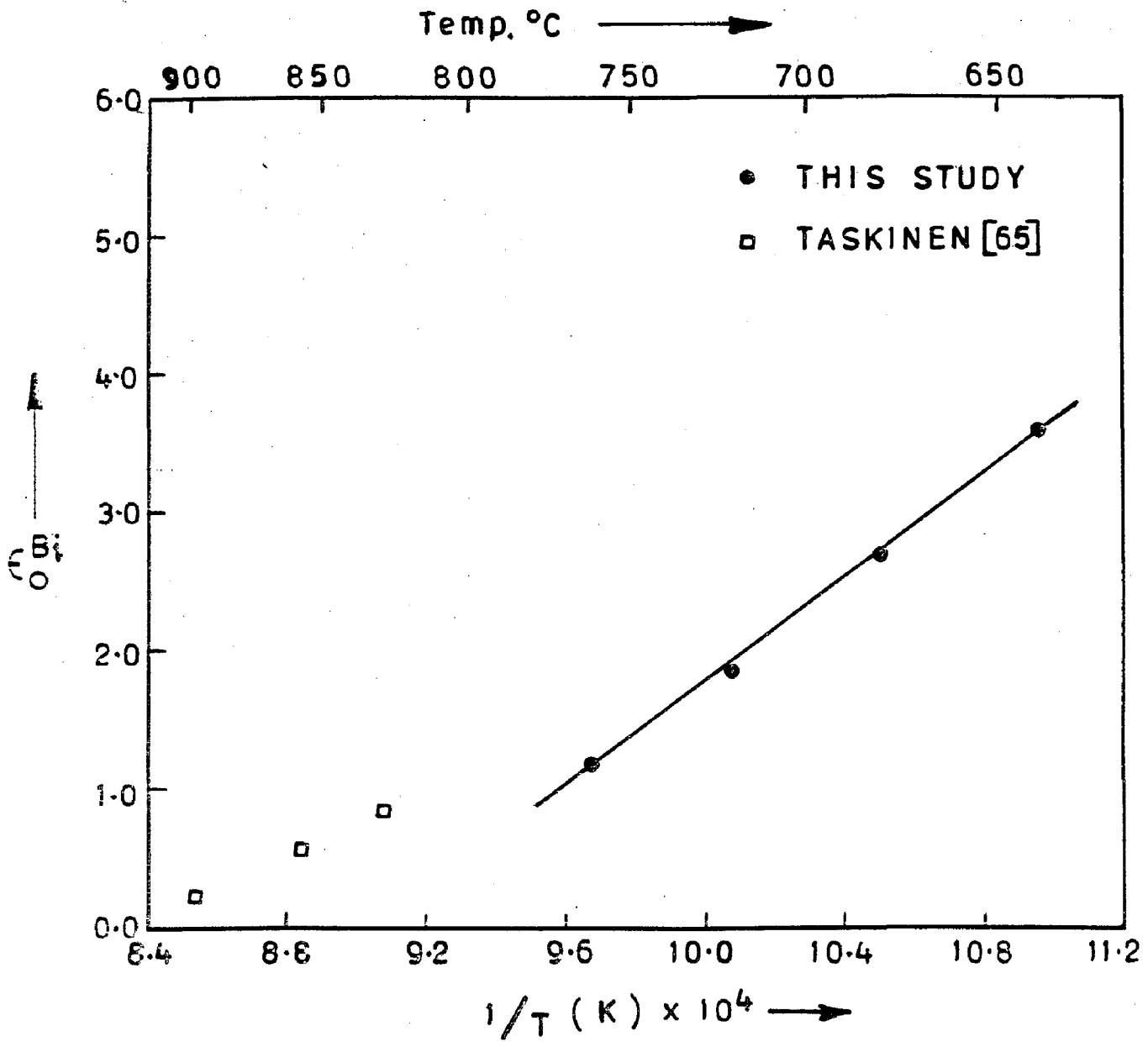


FIG. 5 - 1: PLOT OF TEMPERATURE DEPENDENCE OF FIRST ORDER INTERACTION COEFFICIENT, ϵ_{O}^{Bi}

Table 5.3 Experimental values of ternary interaction parameter, $\epsilon_{\text{O}}^{\text{Bi}}$ at different temperatures.

Temperature (K)	Ternary interaction parameter, $\epsilon_{\text{O}}^{\text{Bi}}$	
	(molar basis)	(atom pct.basis)
913	3.6026	0.0369
953	2.7178	0.0277
993	1.855	0.0193
1034	1.199	0.113

ii) Atom pct.basis

$$\epsilon_{\text{O}(\text{Pb})}^{\text{Bi}} = -0.18214 + 200.025/T \quad (\pm 0.003) \quad (5.10)$$

Also plotted in Fig.5.1, are the values obtained by Taskinen [65] at temperatures 1102, 1132 and 1173K. He arrived at the following temperature dependence of $\epsilon_{\text{O}}^{\text{Bi}}$ in lead,

$$\epsilon_{\text{O}(\text{Pb})}^{\text{Bi}} = -9.84 + 11.78 \times 10^3/T \quad (5.11)$$

Table 5.4 compares the calculated values of $\epsilon_{\text{O}}^{\text{Bi}}$ obtained from these two studies using Eqs. 5.9 and 5.10 at the temperatures of this study. It is seen that all the values show a fair agreement particularly those at 953 and 993 K.

The linear formulation, Eq. 5.9 and 5.10 are applicable only in very dilute solution range and also

Table 5.4 Calculated values of Ternary interaction parameter, $\epsilon_{O(Pb)}^{Bi}$ at different temperatures

Temperature (K)	Ternary interaction parameter, $\epsilon_{O(Pb)}^{Bi}$	
	This study	Taskinen's work
913	3.57	3.06
953	2.69	2.52
993	1.88	2.02
1034	1.11	1.55

for solute components which do not show a vast difference in their reactivity towards the solvent components. In all other cases, the quasi-chemical formulation is better suited.

5.2.2 Quasi-Chemical Formulation

In this formulation all the effects due to the solute i.e. oxygen are summed up in the henrian activity coefficient, f_O for oxygen, whereas the effect of solvent components are summed up in the value of equilibrium constant K . Thus Eq. 5.8 can be rewritten as,

$$\ln\left\{\frac{\text{at.\% O}}{(p_{O_2})^{\frac{1}{2}}}\right\} = \ln K_{Pb+Bi} - \ln f_{O(Pb+Bi)} \quad (5.12)$$

where $K_{(Pb+Bi)}$ and $f_O (Pb+Bi)$ represent respectively the equilibrium constant and activity coeff. of oxygen in Pb-Bi

alloys. for the special case of [at.pct.O] \rightarrow 0, $f_{O(Pb+Bi)} \rightarrow 1$ and hence one can write,

$$\ln \left\{ \frac{[\text{at.\% O}]}{(p_{O_2})^{\frac{1}{2}}} \right\} [\text{at.\% O}] \rightarrow 0 = \ln K_{O(Pb+Bi)} \quad (5.13)$$

The effect due to the presence of a minor component viz. bismuth, expressed as $f_{O(Pb)}^{Bi}$ which is defined as,

$$\ln f_{O}^{Bi} = \ln K_{O(Pb)} - \ln K_{O(Pb+Bi)} \quad (5.14)$$

where, $K_{O(Pb)}$ and $K_{O(Pb+Bi)}$ are respectively the equilibrium constants for dissolution of oxygen in pure lead and lead-bismuth binary alloys.

It may be pointed out that both parameters $K_{O(Pb+Bi)}$ and $f_{O(Pb+Bi)}$ in Eq. 5.12 are functions of composition. As oxygen content of the solution is very small, one can rewrite Eq. 5.12 as

$$\ln \left\{ \frac{[\text{at.\% O}]}{(p_{O_2})^{\frac{1}{2}}} \right\} = \ln K_{O(Pb+Bi)} - \epsilon_{O(Pb+Bi)}^O \cdot [\text{at.\% O}] \quad (5.15)$$

where, $\epsilon_{O(Pb+Bi)}^O$ is the self interaction parameter of oxygen in the solvent lead. The above equation suggests that the values of $K_{O(Pb+Bi)}$ and $\epsilon_{O(Pb+Bi)}^O$ can be determined experimentally by conducting a series of experiments each on a solvent of fixed composition and by varying oxygen content. Coulometric technique makes use of this method, but a precise control of oxygen

content of the alloy becomes difficult. In the present set of experiments it has not been possible to make use of this procedure. Therefore to calculate, $K_{O(Pb+Bi)}$ some approximation had to be made. According to Anik, Kapoor and Froberg [187], $\epsilon_{O(Pb+Bi)}^O$ in a binary solvent can be expressed as ,

$$\epsilon_{O(Pb+Bi)}^O = N_{Pb} \epsilon_{O(Pb)}^O + N_{Bi} \epsilon_{O(Bi)}^O + \delta q N_{Pb} \cdot N_{Bi} \quad (5.16)$$

The bismuth content being very small, maximum being 3.05 atomic percent, one can neglect the last two terms in the above expression and write,

$$\epsilon_{O(Pb+Bi)}^O \approx \epsilon_{O(Pb)}^O \quad (5.17)$$

with this approximation Eq. 6.15 assumes the form,

$$\ln K_{O(Pb+Bi)} = \ln \left\{ [\text{at.}\% \text{ O}] / (p_{O_2})^{\frac{1}{2}} \right\} + \epsilon_{O(Pb)}^O \cdot [\text{at.}\% \text{ O}] \quad (5.18)$$

One can therefore calculate the value of parameter $\ln K_{O(Pb+Bi)}$ from a knowledge of ϵ_{O}^O and experimental data on $[\text{at.}\% \text{ O}]$ and $p_{O_2}^{\frac{1}{2}}$ in different alloy compositions. The values of $\ln K_{O(Pb+Bi)}$ thus calculated are presented in Table 5.5.

In Fig. 5.2 the function, $\ln K_{O(Pb+Bi)}$ is plotted against Bismuth concentration of the alloy at experimental temperatures. It is seen that addition of Bismuth to the alloy increases the value of $\ln K_{O(Pb+Bi)}$; while an increase in temperature lowers $\ln K_{O(Pb+Bi)}$.

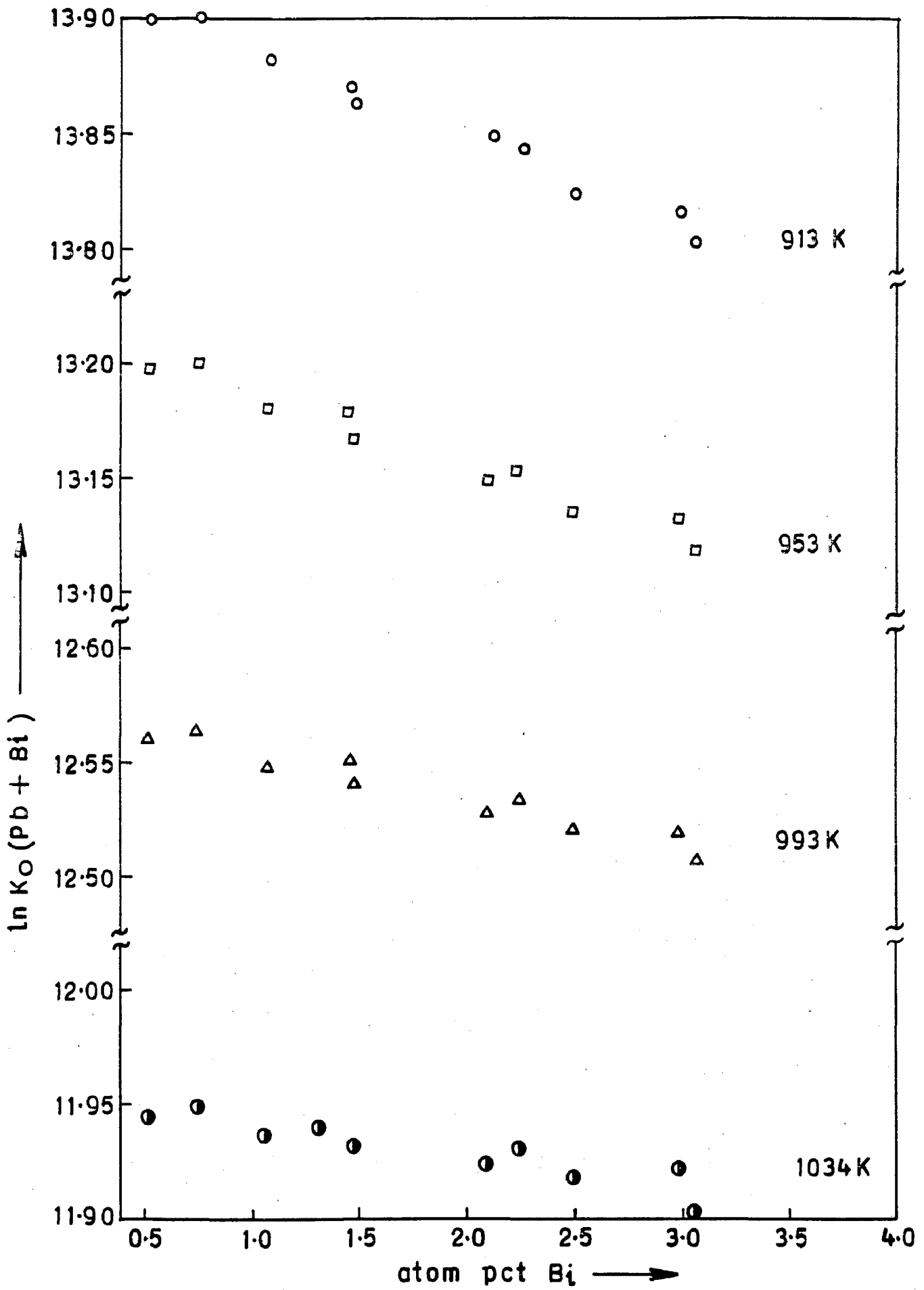


FIG. 5 - 2: VARIATION OF $\ln K_O (Pb + Bi)$ WITH CONCENTRATION OF BISMUTH IN LEAD-BISMUTH ALLOYS

Table 5.5 Activity coefficient, $\ln f_{\text{O}}^{\text{Bi}}$ in Pb-Bi-O system at different temperatures and values of bismuth concentration

Temperature (K)	Bismuth conc. atom pct	$\ln K_{\text{O}}(\text{Pb+Bi})$	$\ln f_{\text{O}}^{\text{Bi}}(\text{Pb})$
1	2	3	4
913	0.000	13.91827	-
	0.501	13.8944	0.01883
	1.061	13.8825	0.03576
	1.467	13.8628	0.05584
	2.082	13.8497	0.06855
	2.489	13.8240	0.09427
	3.054	13.8029	0.1153
913	00.000	13.9273	-
	0.7406	13.9003	0.02699
	1.434	13.8734	0.05392
	2.231	13.8442	0.08307
	2.974	13.8162	0.1111
953	0.000	13.2146	-
	0.501	13.1985	0.01611
	1.061	13.1812	0.03338
	1.467	13.1683	0.04630
	2.082	13.1499	0.06474
	2.489	13.1369	0.07770
	3.054	13.1195	0.09507

Contd..

Table 5.5 Contd..

1	2	3	4
953	0.000	13.2247	-
	0.7406	13.2012	0.02350
	1.434	13.1799	0.04483
	2.231	13.1543	0.0704
	2.974	13.1328	0.09198
993	0.000	12.5722	-
	0.501	12.5621	0.01007
	1.061	12.5499	0.02224
	1.467	12.5420	0.03016
	2.082	12.5287	0.04349
	2.489	12.5208	0.05141
	3.054	12.5095	0.06267
993	0.000	12.58216	-
	0.7406	12.5667	0.01540
	1.4340	12.5524	0.02977
	2.2310	12.5368	0.04533
	2.9740	12.5213	0.06088
1034	0.000	11.9529	0.0000
	0.501	11.9460	0.00685
	1.061	11.9390	0.01383
	1.467	11.9343	0.01856
	2.082	11.9262	0.02666
	2.489	11.9205	0.03237
	3.054	11.9049	0.0480
1034	0.000	11.9605	-
	0.7406	11.9513	+0.0092
	1.4340	11.9421	+0.0184
	2.2310	11.9327	+0.0278
	2.9740	11.9246	+0.0359

5.3 DISCUSSION OF RESULTS

Two studies have been reported on Pb-Bi-O system. Taskinen carried out his emf studies in the temperature range of 1103-1173K using the electrochemical cell; O in liq. Bi-Pb alloys $|ZrO_2+CaO|PO_2 = 1 \text{ atm.}$, Pt and in the alloy range up to $N_{Bi} = 0.55$. The $\ln f_O$ was observed to be linear with increasing concentration of bismuth in the Pb-Bi alloy up to 4 atom pct bismuth. The present study was carried out in the lower temp. range of 913-1034K and in the lower concentration range of alloy up to 3 atom pct. bismuth and follows similar linear variation of $\ln f_O$ with concentration of bismuth. The calculation of ternary interaction parameter ϵ_O^{Bi} defined as,

$$\epsilon_{O(Pb)}^{Bi} = (\partial \ln f_O / \partial N_{Bi})_{N_{Bi} \rightarrow 1}$$

is justified. As is obvious from table 5.4, the results appear to be consistent with Taskinen's findings. This is particularly so at temperatures 953 and 993K. The data from table 5.5 is plotted in Fig. 5.3, which shows that the ternary parameter decreases with increase in temperature. Otsuka et al. [48b] employed modified coulometric technique and studied Bi-Pb-O system. The value of ϵ_O^{Bi} obtained in this study was lower than that of Taskinen as well as this work. They obtained a value of 0.1 for $N_{Bi} = 0.1$ at 1073K.

5.3.1 Comparison with Solution Models

The experimental results on activity coefficient of oxygen in liquid Pb-Bi-O systems at 1034K are compared in Table 5.6 and 5.7 with those calculated on the basis of theoretical models based on classical concepts and applicable to strong electronegative solute, sulphur or oxygen. The data on the Pb-Bi was obtained from compilations of Hultgren et al. [1] while on activity coefficient of oxygen at its infinite dilution in liquid lead was employed from the work of Taskinen [59] viz.

$$\ln f_{O(Pb)} = 6.133 - 14040/T \quad (5.19)$$

and the activity coefficient of oxygen in pure bismuth $f_{O(Bi)}$ from Isecke [94] viz.

$$\ln f_{O(Bi)} = 6.488 - 12160/T \quad (5.20)$$

The effect of third element B, in the system A-B-O (here Bi in Pb-Bi-O) and represented as f_{O}^{Bi} in lead has been calculated using,

$$\ln f_{O}^B = \ln f_{O(A+B)} - \ln f_{O(A)} \quad (5.21)$$

The results on $\ln f_{O}^{Bi}$ so obtained are summed up in Table 5.7 and plotted in Fig. 5.4 for comparison with those obtained experimentally.

Alcock and Richardson [152] assuming the distribution of atoms in the solution to be random and the

energy of interaction between atom pairs as independent of concentration, arrived at an expression, Eq. 4.21, Chapter IV. -

This model was applicable to systems following regular solution behaviour. Same co-ordination number, Z was assumed for all the atoms constituting the system. The value of $\ln f_{O(Pb+Bi)}$ were calculated using Eq. 4.21 for the Pb-Bi-O system under consideration and are presented in Table 5.7, while on $\ln f_{O}^{Bi}$ in lead in Table 5.6. A comparison with the measured values suggests a fair agreement between the two, with the predicted values being on the positive side of the measured ones. This implies approximately similar behaviour of lead and bismuth towards oxygen in solution. This seems reasonable in view of the values of $f_{O(Pb)}$ and $f_{O(Bi)}$ given by Eqs. 5.20 and 5.21 as well as by the fact that the difference in $\ln[f_{O(Pb)}/f_{Pb(Pb+Bi)}]$ and $\ln[f_{O(Bi)}/f_{Bi(Pb+Bi)}]$ is less than unity.

Alcock and Richardson modified the regular solution treatment using quasichemical approximation and derived Eq. 4.22 in Chapter IV. The calculated values on $\ln f_{O(Pb+Bi)}$ and $\ln f_{O}^{Bi}$ are presented in Tables 5.6 and 5.7 respectively for the co-ordination number, $Z = 2$ and 4 and plotted in Fig. 5.4. The predicted values show a good match with the measured ones. This is apparent

Table 5.6 Predicted values of ternary interaction parameter, $\ln f_{O(Pb)}^{Bi}$ at 1034K

Theoretical Models	Ternary interaction parameter, $\ln f_{O(Pb)}^{Bi}$				
	.01	.02	.03	.04	.05
Alcock & Richardson (Regular Solution Model)	0.0264	0.0544	0.0812	0.1084	0.1347
Alcock & Richardson (QCT) at Z=2	0.0154	0.0304	0.0454	0.0604	0.0764
Z=4	0.0204	0.0404	0.0604	0.0804	0.100
Jacob & Alcock (3 bond No.)	0.0227	0.0456	0.0684	0.0904	0.1134
Belton & Tankins	-0.1267	-0.1327	-0.1377	-0.1427	-0.1467
Carl Wagner h=0	0.0204	0.0364	0.0554	0.0730	0.0920
h=544	0.0113	0.0233	0.0433	0.0463	0.092
This Study	0.0128	0.0255	0.0380	-	-

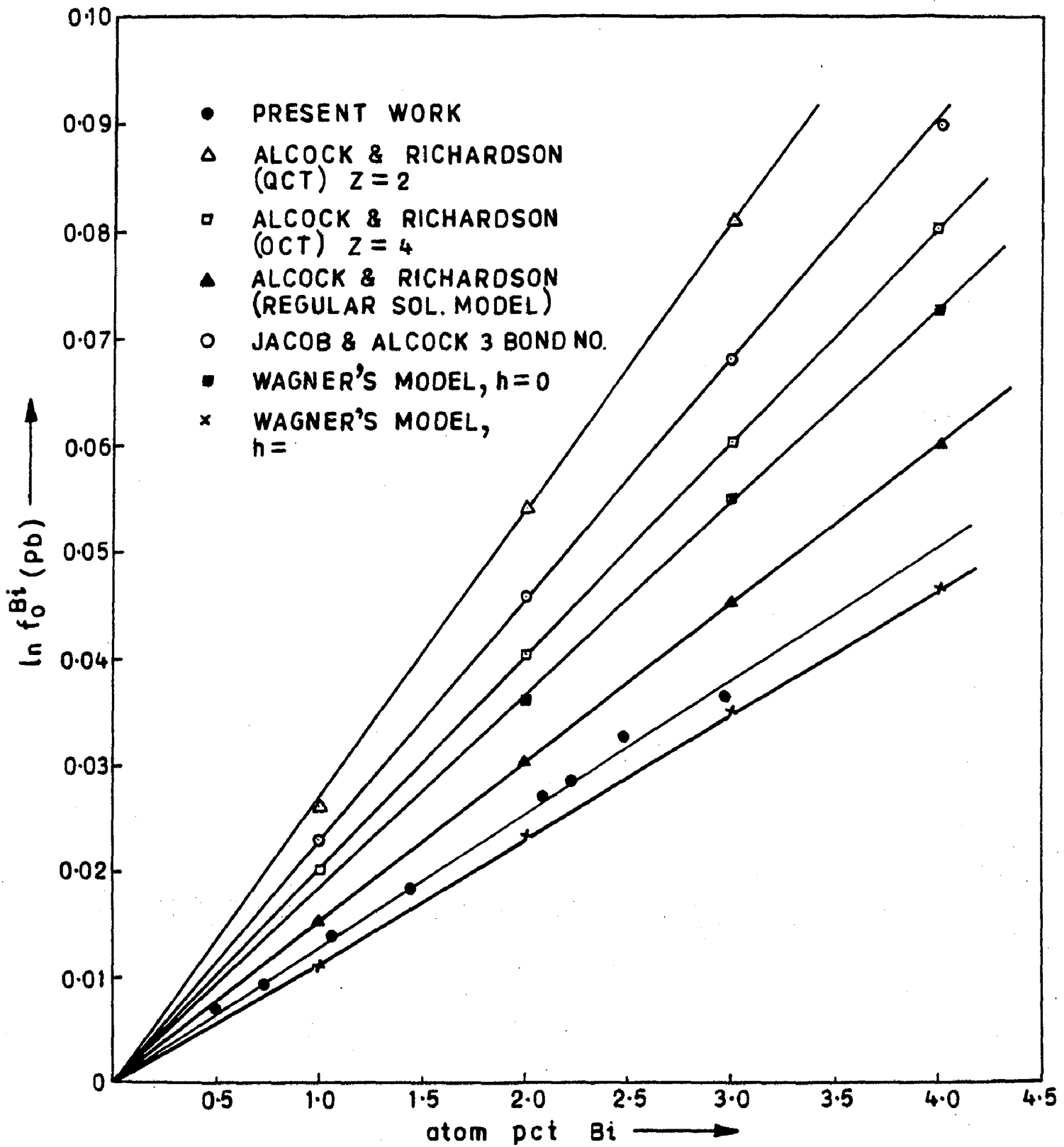


FIG. 5 - 4: EFFECT OF BISMUTH ON OXYGEN IN LEAD BISMUTH ALLOYS AT 1034 K

Table 5.7 Predicted values of activity coefficient, $\ln f_{O(Pb+Bi)}$ at 1034K.

Theoretical Models	Activity coefficient of oxygen, $\ln f_{O(Pb+Bi)}$ at N_{Bi} ,				
	0.01	0.02	0.03	0.04	0.05
Alcock & Richardson (Regular Solution Model)	-7.419	-7.391	-7.364	-7.337	-7.311
Alcock & Richardson (QCT) at Z=2	-7.430	-7.415	-7.400	-7.385	-7.369
Z=4	-7.427	-7.407	-7.386	-7.366	-7.346
Jacob & Alcock (3 bond No.)	-7.423	-7.400	-7.377	-7.355	-7.332
Jacob & Effes	-7.489	-7.465	-7.435	-7.405	-7.379
Belton & Tankins	-7.572	-7.578	-7.583	-7.588	-7.592
Carl Wagner					
h=0	-7.425	-7.409	-7.390	-7.372	-7.353
h=544	-7.439	-7.422	-7.402	-7.399	-
This Study	-7.431	-4.420	-7.412	-	-

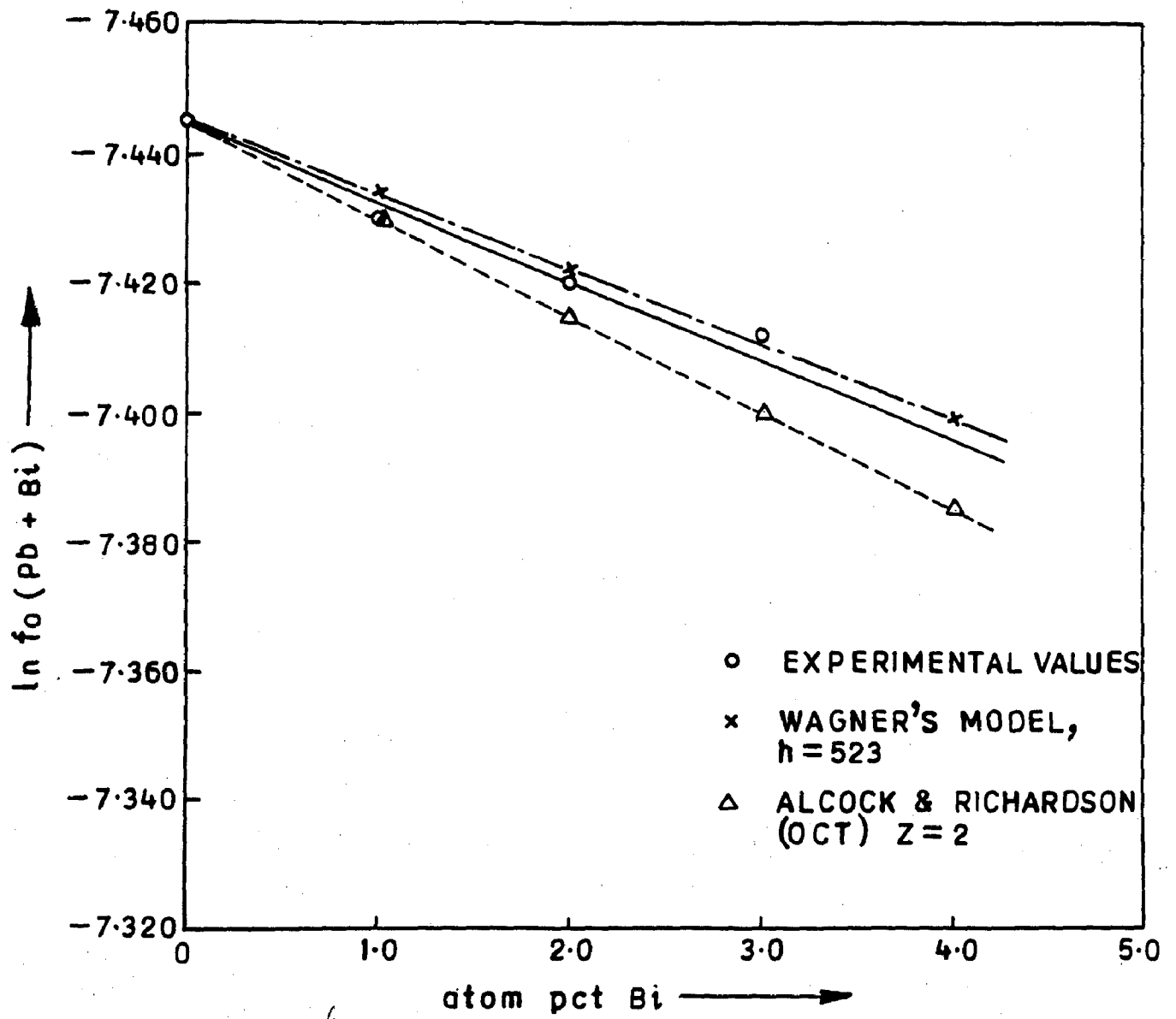


FIG. 5 - 5: ACTIVITY COEFFICIENT OF OXYGEN IN Pb + Bi ALLOYS, $f_o(\text{Pb} + \text{Bi})$ AT $T = 1034 \text{ K}$

in view of the stronger lead-oxygen interaction in the Pb-Bi-O system, as seen by the more negative departure of lead-oxygen than bismuth-oxygen from Raoult's law in view of the fact that $f_{O(Pb)} < f_{O(Bi)}$ such that at $T = 1034K$, $f_{O(Pb)}/f_{O(Bi)} \sim 0.1$. This is also true when the heats of dissolution of oxygen from gaseous state into the respective pure metals are compared, $\Delta H_{O(Pb)}$ being more negative. Besides, there is no strong pairwise interaction in Pb-Bi-O, the greater interaction of lead-oxygen in comparison to bismuth oxygen makes the model better applicable. The model, however, leads to a better description of the quantitative behaviour of oxygen at $Z=2$.

Jacob and Effes [193] obtained an expression for the quantitative prediction of oxygen and sulphur in binary metallic solvents, A+B,

$$\Delta \bar{G}_{O(A+B)} = N_A \Delta G_{O(A)} + N_B \Delta G_{O(B)} - 2 H_{(A+B)}^M \quad (5.22)$$

Where, $\Delta G_{O(A)}$ and $\Delta G_{O(B)}$ are the free energies of solution of oxygen in pure metals A and B respectively and $H_{(A+B)}^M$ the molar heat of mixing of metals A and B at a given alloy composition. These authors assumed the presence of molecular species A_2O and B_2O in solution.

Belton and Tankins [155] on the other hand assumed the presence of molecular species viz. AO and BO in solution. They assumed that oxygen and sulphur in metallic solution exist as negatively charged ions. The energy

of the system will therefore be lowered by the formation of solute-solvent screened dipoles: in a very dilute solution of oxygen in liquid mixture of metals A and B, the molecular species will be formed. The average interaction energy of these species with the surrounding metal atoms was assumed to be small and the partial molar properties of these species were considered ideal. This model can be expressed by,

$$\begin{aligned} \Delta \bar{G}_{O(A+B)} = & X_{AO}/X_O [\Delta G_{O(A)} - H_A^M + RT \ln(X_{AO}/X_O)] \\ & + X_{BO}/X_O [\Delta G_{O(B)} - H_B^M + RT \ln(X_{BO}/X_O)] \end{aligned} \quad (6.23)$$

On the distribution of the species, two approximations were made.

(i) a random distribution, when

$$X_{AO}/X_O = N_A \quad \text{and} \quad X_{BO}/X_O = N_B$$

(ii) a quasichemical distribution, when

$$X_{AO}/X_O = N_A \cdot \beta / (N_B + N_A \cdot \beta) \quad \text{and} \quad X_{BO}/X_O = N_B / (N_B + N_A \cdot \beta)$$

where, $\beta = \exp[-(H_{O(A)}^M - H_{O(B)}^M - H_A^M + H_B^M)/RT]$

where, $H_{O(A)}^M$ and $H_{O(B)}^M$ are the heats of solution of oxygen in pure metals and H_A^M and H_B^M are the partial molar heats of mixing of the metals in the binary metal mixture at a given composition. According to Belton and Tankins, the model is applicable to those systems wherein the solvent

metals do not deviate widely from ideal behaviour and for which heat of solution of oxygen in solvent metals A and B differ only slightly. Using the data in case of Pb-Bi-O system under consideration, the values on $\ln f_{O(Pb+Bi)}$ are calculated and presented in Table 5.7.

The calculated values are more negative when compared with the measured ones. This may be attributed to the assumption of zero heats of solution for the molecular species. This may not be correct if the activity coefficient of oxygen in A is much smaller or bigger than in B.

Jacob and Alock [156] derived a generalised model with three bond numbers. The expression arrived at is given as Eq. 4.24 (Chapter IV). With α , the degree to which metal-metal bonds are weakened with oxygen dissolution as $\frac{1}{2}$ and n , the number of bonds made by each oxygen atom as 4 as suggested by the authors, $f_{O(Pb+Bi)}$ has been calculated. It is seen that from Fig. 6.5, the calculated values exhibit a small positive deviation from the measured values. This is to be expected because the binary alloys show a negative deviation from Raoult's law and the difference between $\ln f_{O(Pb)}$ and $\ln f_{O(Bi)}$ is not significantly large. Similar observations have been seen in case of In-Sb-O [37] system.

The activity coefficient of oxygen in the system, Pb-Bi-O under study has also been calculated on the basis of Wagner's model [157] with one adjustable energy parameter, h . Knowing this parameter and the thermodynamic properties of the non-metallic solute viz oxygen in the separate metal-oxygen binary systems constituting the ternary system, A-B-O at any temperature; the variation of activity coefficient of the solute with alloy composition can be easily computed. Using Eq. 4.25 (Chapter IV) and the value of h as 544 J gatom^{-1} at $T=1034$; $\ln f_{\text{O}}(\text{Pb+Bi})$ has been calculated and presented in Table 5.6. The effect of bismuth on the activity of oxygen in Pb+Bi alloys, $\ln f_{\text{O}}^{\text{Bi}}$ has been obtained employing relation 5.21 and separately presented in Table 5.7 and plotted in Fig. 5.5 for comparison with the experimentally determined values in the present study. It is seen that the predicted values on $\ln f_{\text{O}}(\text{Pb+Bi})$ or $\ln f_{\text{O}}^{\text{Bi}}$ very closely match with the measured data. Similar prediction of experimental data was observed by Ossuka et al. [48b] at 1073K in Bi-Pb-O system with the value of $h=600 \text{ J.gatom}^{-1}$.

In his treatment Wagner assumed the solvent atoms A & B in a system A-B-O exhibit ideal solution behaviour with oxygen atoms occupying quasi-interstitial sites and a binomial distribution of complexes consisted of oxygen surrounded by solvent metals in varying proportions.

To calculate the value of energy parameter, h , Chang and Coworkers [163,166] proposed an empirical relationship given as Eq. 4.26 in Chapter IV. This was based on a knowledge of thermodynamic properties of respective binaries and applicable to systems wherein, $G_{O(A)} > G_{O(B)}$ and $(V_b/V_a)^2 < 1$. V_b and V_a are the valences of the solvent metals A and B given by Pauling [192].

$\ln f_{O(Pb+Bi)}$ value have been calculated using Eqs. 4.26 and 4.27. In these calculations values of 2.56 and 1.56 were used as metallic valences of Pb and Bi respectively as given by Pauling. Values for regular solution parameter, ϵ , were estimated using the relation, $\epsilon = \Delta H/N_A \cdot N_B$, where H is the value of mixing enthalpy of A-B alloys. The value of ϵ was estimated as $-4.4 \text{ KJ gatom}^{-1}$. This gives a value of h from Eq.4.26 as $-1.076 \text{ KJ gatom}^{-1}$ against $0.66 \text{ KJ gatom}^{-1}$ calculated by Otsuka et al. [48b] at 1073K for Bi-Pb-O system. The value of activity coefficient calculated using this value leads to erroneous results and does not fit with the measured data. It is felt that better correlation needs to be proposed for systems such as Pb-Bi-O with $\Delta G_{O(A)} < \Delta G_{O(B)}$, not covered by Eq. 4.27 proposed by Chang and Co-workers' for the estimation of h .

Chang and Chang [162] further modified Wagner's equation by introducing two energy parameters h_1 and h_2 .

However, in view of very dilute concentration of bismuth (1-3 atom pct.) taken for this study, it is felt that the predicted values on the basis of this model would not be significantly different from those predicted by Wagner's Equation. Calculations based on Chiang and Chang's model have therefore been not attempted for the interpretation of results on Pb-Bi-O system under study. For similar reasons, the calculation of $\ln f_{O(Pb+Bi)}$ on the basis of statistical models [187,193] have not been attempted.

CHAPTER - VI

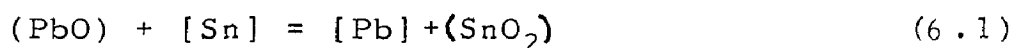
LEAD-TIN-OXYGEN SYSTEM

In the multistage refining of lead bullion, the removal of copper is followed by an oxidation stage during which tin, arsenic and antimony are eliminated. The influence of tin on the activity coefficient of oxygen in lead is therefore important. A knowledge of thermodynamic behaviour of dilute solution of oxygen in liquid lead-tin alloys is also important in the design of alloys. However, only one study [23] has been reported to evaluate the thermodynamic data on the solution of oxygen in lead-tin alloys. It was therefore decided to reinvestigate this system in the dilute solution range.

Further a number of theoretical models have been reviewed in Chapter I. These have been suggested to predict the behaviour of oxygen in binary metallic solvents. Most of the models, were developed after Jacob and Jeffes study on Pb-Sn-O system and hence these authors interpreted their results on the basis of regular solution model [152]. In this chapter these models shall be applied to arrive at the one, most suitable for theoretical prediction of thermodynamic properties of oxygen in lead-tin system.

6.1 RESULTS AND CALCULATIONS

The experimental set up used and procedure adopted for study has been discussed in detail in Chapter II. While (PbO) slag was employed for variation of oxygen concentration in Pb-Cu and Pb-Bi alloys; such an arrangement was risky in the study of Pb-Sn-O system. The free energies of formation of PbO [2], $\Delta G^\circ_{\text{PbO}(s)}$ when combined with the corresponding value of SnO_2 , $\Delta G^\circ_{\text{SnO}_2}$ [23] gives the standard free energy change for the reaction,



where, small brackets indicate the slag phase, square brackets the components in the metallic phase.

$$\Delta G^\circ = -361288.4 + 104.26T \text{ Jmol}^{-1} \quad (6.2)$$

The large negative value of ΔG° as per Eq.6.2 in the temperature range, 973-1095K selected for this investigation will favour the oxidation of solute tin in the Pb-Sn alloys, when equilibrated underneath a (PbO) slag. In view of this the Pb-Sn-O system in the dilute concentration range was not investigated with a slag cover, rather under an inert gas atmosphere as has been described in Chapter II. The oxygen concentration in the alloy was raised by adding a weighed amount of analytical grade lead oxide (melted in alumina crucible and preserved as solid specimen). The activity

of SnO in the experiment at 1095K calculated by the use of standard free energy of formation of SnO [23a] given by,

$$\Delta G_{\text{SnO}}^{\circ} = -266186.1 + 87.236T \text{ Jmol}^{-1} \quad (6.3)$$

using the activity of tin in the lead tin alloys [1] and the chemical potential of oxygen in the solution ~~and~~ obtained from the emf data, is very low*. Loss of oxygen as SnO vapour is therefore unlikely at 1095K or in the range 973-1095K, selected for this study. Further no discoloration or penetration of the solid electrolyte tube by SnO was observed indicating the negligible activity of SnO vapours. Loss or gain of oxygen by the melt during the course of experiment was checked with or without titanium as internal getter as was done by Jacob and Jeffes in their study on the system [23] and the possibility for such an exchange was ruled out.

The dissolution of oxygen in the molten alloys may be rewritten as,

$$\frac{1}{2} \{ \text{O}_2 \} = [\text{O}] \quad (6.4)$$

The concentration of oxygen as well as tin in the alloys samples has been determined analytically as described

$$*[\text{Sn}] + [\text{O}] = (\text{SnO})$$

$$a_{\text{SnO}} = a_{\text{Sn}} \cdot a_{\text{O}} \cdot \text{Exp}(-\Delta G/RT)$$

$$\text{at } T = 1095\text{K}; a_{\text{Sn}} = 0.173 (\text{at } N_{\text{Sn}} = 0.05)$$

$$a_{\text{SnO}} = 3.10 \times 10^{-4}$$

in Chapter II and given in Table 6.1 along with the emf data at different temperatures. The value of oxygen partial pressure may be calculated from the cell emf, using,

$$E = -RT/2F \{ \ln N_O / (P_{O_2})^{1/2} \} \quad (6.5)$$

where N_O is the atom fraction of oxygen in the alloy. Table 6.2 give the calculated values of oxygen partial pressure along with the oxygen content of the alloy. Equilibrium constant, K_{Pb-Sn} for dissolution of oxygen in the Pb-Sn alloys can be expressed as,

$$K_{Pb-Sn} = h_O / (P_{O_2})^{1/2} \quad (6.6)$$

or taking logarithm and rearranging,

$$\ln \{ [\text{at.}\% \text{ O}] / (P_{O_2})^{1/2} \} = \ln K_{Pb-Sn} - \ln f_O \quad (6.7)$$

where h_O represents the henrian activity coefficient and f_O , the activity coefficient of oxygen in the metallic solution. Calculated values of parameter,

$$\ln \{ [\text{at.}\% \text{ O}] / (P_{O_2})^{1/2} \}$$

are given in Table 6.2.

6.2 CALCULATION OF INTERACTION PARAMETERS

The interpretation of experimental results and their quantitative expression in terms of standard parameters is arrived at on the basis of following

Table 6.1 EMF data on Pb-Sn-O system at different temperatures and values of Tin concentration

Temperature (K)	Tin conc. (atom pct.)	EMF (mv)	Oxygen Conc. (atom pct. $\times 10^2$)
1	2	3	4
973	0.000	77.8	2.100
	0.892	22.4	1.080
	1.499	-87.3	0.123
	1.795	-33.8	0.552
	2.691	-89.6	0.284
	2.988	-172.8	0.0480
	3.597	-145.9	0.145
	4.456	-264.1	0.0163
	4.496	-201.8	0.0746
	5.368	-256.1	0.0389
1014	0.000	81.6	3.727
	0.892	32.7	2.124
	1.499	-63.1	0.346
	1.795	-16.8	1.203
	2.691	-66.0	0.685
	2.988	-144.7	0.136
	3.597	-115.7	0.387
	4.456	-225.2	0.054
	4.496	-165.0	0.220
	5.368	-212.8	0.127
5.917	-305.4	0.0216	
1054	0.000	85.4	6.318
	0.892	40.5	3.852
	1.499	-50.5	0.720
	1.795	-4.5	2.336
	2.691	-49.4	1.423
	2.988	125.1	0.316

Contd..

1	2	3	4
1054	3.597	-94.8	0.863
	4.496	-139.9	0.525
	4.455	-198.7	0.141
	5.368	-183.6	0.324
	5.917	-271.9	0.0628
1095	0.000	89.5	10.450
	0.892	46.8	6.627
	1.499	-41.9	1.372
	1.795	-3.5	4.183
	2.691	-39.4	2.651
	2.988	113.2	0.644
	3.597	-82.8	1.672
	4.496	-125.9	1.058
	4.455	-183.6	0.305
	5.368	-167.7	0.879
	5.917	-253.6	0.145

two formulations.

6.2.1 Wagners Interaction Parameter Formulation

In this formulation, the effect of additive, Sn on oxygen in solution is considered to be incorporated in the activity coefficient term, f_O , and the value of equilibrium constant, K_{Pb-Sn} is considered to be equal to that of oxygen in the major solvent component lead i.e. $K_{Pb-Sn} \approx K_{Pb}$. further, the function, $\ln f_O$ because of continuity conditions, can be assumed to be expressed in terms of Taylor series as follows,

$$\begin{aligned} \ln f_O = & \{ \ln f_O / [\text{at.}\% \text{ O}] \} \cdot [\text{at.}\% \text{ O}] \\ & + \ln f_O / [\text{at.}\% \text{ Sn}] \cdot [\text{at.}\% \text{ Sn}] + \dots \end{aligned} \quad (6.8)$$

As the concentration of oxygen and tin in the metallic solution are small, one can neglect higher order terms of the series and write,

$$\ln f_O = \epsilon_O^O \cdot [\text{at.}\% \text{ O}] + \epsilon_O^{Sn} \cdot [\text{at.}\% \text{ Sn}] \quad (6.9)$$

where, ϵ_O^O is the self interaction parameter of oxygen in solution, and, ϵ_O^{Sn} , the interaction parameter of tin on oxygen in solution. This Eq. 6.9 can be rewritten as,

$$\begin{aligned} \ln \{ [\text{at.}\% \text{ O}] / (p_{O_2})^{\frac{1}{2}} \} = & \ln K_{Pb} - \epsilon_O^O [\text{at.}\% \text{ O}] \\ & + \epsilon_O^{Sn} [\text{at.}\% \text{ Sn}] + \dots \end{aligned} \quad (6.10)$$

Table 6.2 Calculated values on oxygen dissolution in Pb-Sn-O system from emf data

Temperature (K)	Tin concentration		Oxygen concentration		Oxygen partial pressor, P_{O_2}		$\ln \left\{ \frac{[\text{at.pct.O}]}{(P_{O_2})^{\frac{1}{2}}} \right\}$
	[atom.pct]	[atom.pct]	[atom.pct.]x10 ²	[atom.]x10 ²	[atom.]	[atom.]	
1	2	3	4	5	6	7	8
973	0.000	2.100	2.3306x10 ⁻¹⁵	2.3306x10 ⁻¹⁵	12.982		
	0.892	1.080	1.6496x10 ⁻¹⁶	1.6496x10 ⁻¹⁶	13.643		
	1.499	0.1236	8.8096x10 ⁻¹⁹	8.8096x10 ⁻¹⁹	14.091		
	1.795	0.552	1.1309x10 ⁻¹⁷	1.1309x10 ⁻¹⁷	14.312		
	2.691	0.284	7.9169x10 ⁻¹⁹	7.9169x10 ⁻¹⁹	14.976		
	2.988	0.0486	1.4936x10 ⁻²⁰	1.4936x10 ⁻²⁰	15.195		
	3.597	0.145	5.3912x10 ⁻²⁰	5.3912x10 ⁻²⁰	15.647		
	4.456	0.0163	1.9167x10 ⁻²²	1.9167x10 ⁻²²	16.284		
	4.496	0.0746	3.7527x10 ⁻²¹	3.7527x10 ⁻²¹	16.315		
	5.368	0.0389	2.8086x10 ⁻²²	2.8086x10 ⁻²²	16.962		
1014	0.000	3.727	2.426x10 ⁻¹⁴	2.426x10 ⁻¹⁴	12.3854		
	0.892	2.124	2.5614x10 ⁻¹⁵	2.5614x10 ⁻¹⁵	12.94718		
	1.499	0.346	3.193 x10 ⁻¹⁷	3.193 x10 ⁻¹⁷	13.32594		
	1.795	1.203	2.6510x10 ⁻¹⁶	2.6510x10 ⁻¹⁶	13.51085		
	2.691	0.685	2.7922x10 ⁻¹⁷	2.7922x10 ⁻¹⁷	14.0749		
	2.988	0.136	7.5823x10 ⁻¹⁹	7.5823x10 ⁻¹⁹	14.26064		
	3.597	0.387	2.8677x10 ⁻¹⁸	2.8677x10 ⁻¹⁸	14.64340		
	4.456	0.054	1.9004x10 ⁻²⁰	1.9004x10 ⁻²⁰	15.18211		

Table 6.2 Contd..

1	2	3	4	5
1014	4.496	0.220	2.9997×10^{-19}	15.20736
	5.368	0.127	3.3547×10^{-20}	15.75506
	5.917	0.0216	4.8358×10^{-22}	16.09990
1054	0.000	6.318	2.040×10^{-13}	11.84860
	0.892	3.852	2.814×10^{-14}	12.34400
	1.499	0.720	5.117×10^{-16}	12.67033
	1.795	2.336	3.875×10^{-15}	12.83535
	2.691	1.423	5.360×10^{-16}	13.32890
	2.988	0.316	1.911×10^{-17}	13.49189
	3.597	0.863	7.250×10^{-17}	13.82860
	4.456	0.141	7.481×10^{-19}	14.30170
	4.496	0.525	9.960×10^{-18}	14.32443
	5.368	0.324	1.452×10^{-18}	14.80560
	5.917	0.0628	2.968×10^{-20}	15.10844
1095	0.000	10.450	1.562×10^{-12}	11.33403
	0.892	6.627	2.549×10^{-13}	11.78494
	1.499	1.372	5.934×10^{-15}	12.08997

Contd.....

Table 6.2 Contd..

1	2	3	4	5
1095	1.795	4.183	4.070×10^{-14}	12.24208
	2.691	2.651	6.59×10^{-15}	12.69635
	2.988	0.644	2.880×10^{-16}	12.84593
	3.597	1.672	1.045×10^{-15}	13.15596
	4.456	0.305	1.459×10^{-17}	13.59125
	4.496	1.058	1.683×10^{-16}	13.61226
	5.368	0.879	2.861×10^{-17}	14.05500
	5.917	0.145	7.492×10^{-19}	14.33348

For the calculation of interaction parameter, ϵ_{O}^{Sn} , one can make use of value of K_{Pb} and ϵ_{O}^0 obtained from Pb-O system. But this method will suffer from the drawback that any error in these two parameters will be carried over to calculated value of ϵ_{O}^{Sn} . Therefore, to avoid this error, instead of this method, multivariant linear regression technique is used to evaluate ϵ_{O}^{Sn} . The computer programme for the analysis is given in Appendix II. Values of ϵ_{O}^{Sn} thus obtained for various temperatures are given in Table 6.3. Further it has been found that values of K_{Pb} and ϵ_{O}^0 thus obtained, vary within error limits from those obtained from corresponding binary systems. In Fig. 5.1, ϵ_{O}^{Sn} is plotted against $1/T$. It has been found to follow the relationship,

i) Molar basis

$$\epsilon_{O(Pb)}^{Sn} = 139 - 20.6161 \times 10^3 / T \quad (\pm 4) \quad (6.11)$$

ii) Atom percent basis

$$\epsilon_{O(Pb)}^{Sn} = 1.39 - 0.2062 \times 10^3 / T \quad (\pm) \quad (6.12)$$

Also plotted in Fig. 6.1, are the values obtained by Jacob and Jeffes [23]. They also followed a similar experimental technique and worked in the temperature range of 1023-1173K and arrived at the following relationship:

$$\epsilon_{O(Pb)}^{Sn} = 115 - 18.3 \times 10^4 / T \quad (6.13)$$

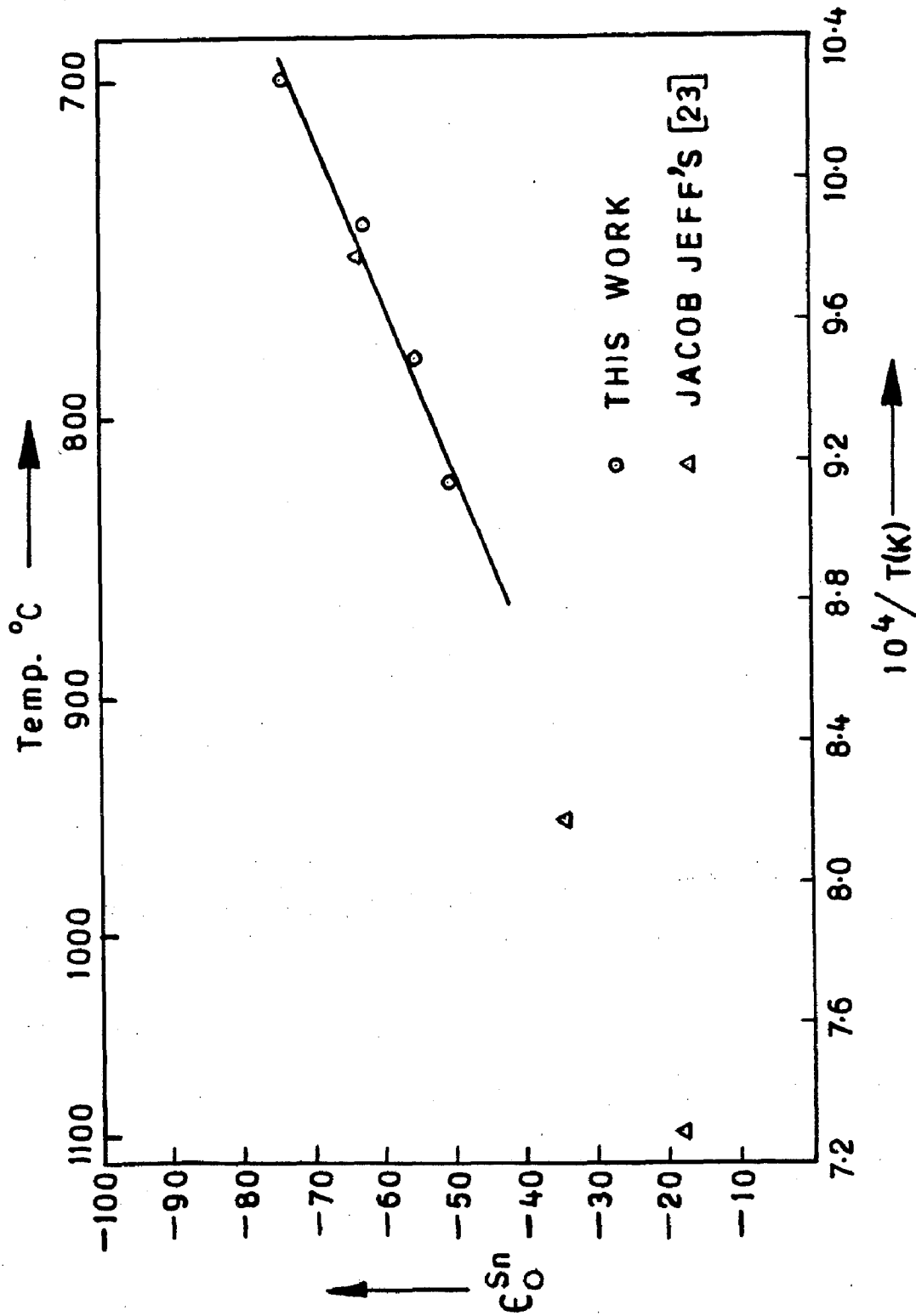


FIG. 6-1: PLOT OF TEMPERATURE DEPENDENCE OF FIRST ORDER INTERACTION COEFFICIENT, ϵ_{O}^{Sn} IN LEAD-TIN ALLOYS

Table 6.3 Calculated values of ternary interaction parameter, ϵ_{O}^{Sn} at different temperatures.

Temperature (K)	Ternary interaction parameter, ϵ_{O}^{Sn} (pb)	
	Molar basis	Atom pct.basis
973	-74.2	-.742
1014	-62.8	-.628
1054	-55.2	-.552
1095	-55.8	-.508

Calaculated values for this study as well as that of Jacob and Jeffes are given in Table 6.4 at different temperatures of study in the range 973-1095K. It is seen that all the values show a good agreement almost at all temperatures.

The linear formulation as is evident from Eq. 6.9 is applicable only in very dilute solution ranges and also for solute components which do not show a vast difference in their reactivity towards the solvent components. In all other cases the quasi-chemical formulation is better suited.

6.2.2 Quasichemical Formulation

In this formulation all effects due to the solute itself i.e. oxygen are summed up in the henrian activity coefficient, f_{O}^0 for oxygen, whreas the effect

Table 6.4 Comparison of ternary interaction parameter $\epsilon_{O(Pb)}^{Sn}$ at different temperature

Temperature (K)	Ternary interaction parameter, $\epsilon_{O(Pb)}^{Sn*}$	
	This Study	Jacob & Jeffes
973	-74.2 (-0.742)	-73.08 (-0.731)
1014	-62.8 (-0.628)	-75.47 (-0.654)
1054	-55.2 (-0.552)	-58.62 (-0.586)
1095	-50.8 (-0.508)	-52.12 (-0.521)

*Value in parenthesis refer to those on atom pct. basis; while others refer to those on molar basis.

of solvent components are summed up in the value of equilibrium constant K . This equation 6.9 can be re-written as,

$$\ln \left\{ \frac{[\text{at.}\% \text{ O}]}{(p_{O_2})^{\frac{1}{2}}} \right\} = \ln K_{(Pb+Sn)} - \ln f_{O(Pb+Sn)}^O \quad (6.14)$$

where, $K_{(Pb+Sn)}$ and $f_{O(Pb+Sn)}^O$ represent respectively the equilibrium constant for dissolution of oxygen in Pb-Sn alloys and activity coefficient of oxygen. For the special case of $[\text{at.}\% \text{ O}] \rightarrow 0$, $f_{O(Pb+Sn)}^O \rightarrow 1$, one can write,

$$\ln \left\{ \frac{[\text{at.}\% \text{ O}]}{(p_{O_2})^{\frac{1}{2}}} \right\}_{[\text{at.}\% \text{ O}] \rightarrow 0} = \ln K_{(Pb+Sn)} \quad (6.15)$$

The effect due to presence of a minor component viz.

Sn as solute and expressed as, $f_{O(Pb)}^{Sn}$, may be defined as,

$$\ln f_{O}^{Sn} = \ln K_{O(Pb)} - \ln K_{O(Pb+Sn)} \quad (6.16)$$

where, $K_{O(Pb)}$ and $K_{O(Pb+Sn)}$ are respectively the equilibrium constants for dissolution of oxygen in pure lead and Pb-Sn binary alloys.

It may be pointed out that both parameters, $K_{O(Pb+Sn)}$ and $f_{O(Pb+Sn)}$ in Eq. 6.14 are functions of composition. As oxygen content of the solution is very small, one can rewrite Eq. 6.14 as follows,

$$\ln \{ [\text{at.}\% \text{ O}] / (P_{O_2})^{\frac{1}{2}} \} = \ln K_{O(Pb+Sn)} - \epsilon_{O(Pb+Sn)}^O \cdot [\text{at.}\% \text{ O}] \quad (6.17)$$

where $\epsilon_{O(Pb+Sn)}^O$ is the self interaction parameter of oxygen in the binary Pb-Sn alloy. The above equation suggests values of $K_{O(Pb+Sn)}$ and $\epsilon_{O(Pb+Sn)}^O$ can be determined experimentally by conducting a series of experiments each on a solvent of fixed composition and by varying oxygen content as is done in coulometric technique. However, a precise control of oxygen content of the alloy becomes difficult. In the present set up of experiments it has not been possible to make use of this procedure. Therefore, to calculate $K_{O(Pb+Sn)}$ some approximation had to be made. According to Anik, Kapoor and Froberg [187], $\epsilon_{O(Pb+Sn)}^O$ in a binary solvent can be expressed as,

$$\epsilon_{O(Pb+Sn)}^O = N_{Pb} \epsilon_{O(Pb)}^O + N_{Sn} \epsilon_{O(Sn)}^O + \delta_q N_{Sn} \cdot N_{Pb} \quad (6.18)$$

The tin content in this study being very small, maximum being 5.45 at percent, the last two terms in the above Eq. 5.18 may be neglected and expression rewritten as,

$$\epsilon_{O(Pb+Sn)}^O \approx \epsilon_{O(Pb)}^O \quad (6.19)$$

with this approximation Eq. 6.17 assumes the form,

$$\ln K_{O(Pb+Sn)} = \ln \{ [\text{at.}\% \text{ O}] / (p_{O_2})^{\frac{1}{2}} \} + \epsilon_{O(Pb)}^O [\text{at.}\% \text{ O}] \quad (6.20)$$

One can therefore, calculate the value of parameter, $\ln K_{O(Pb+Sn)}$ from a knowledge of the self interaction parameter of oxygen in pure lead, $\epsilon_{O(Pb)}^O$ and experimental data on [at.% O] and p_{O_2} in different alloy compositions. The values of $\ln K_{O(Pb+Sn)}$ thus calculated are presented in Table 6.5.

In Fig. 6.2 the function, $\ln K_{O(Pb+Sn)}$ is plotted against tin concentration of the alloys for various temperatures. It is seen that addition of tin to lead increases the value of $\ln K_{O(Pb+Sn)}$. Further with increase in temperature $\ln K_{O(Pb+Sn)}$ decreases.

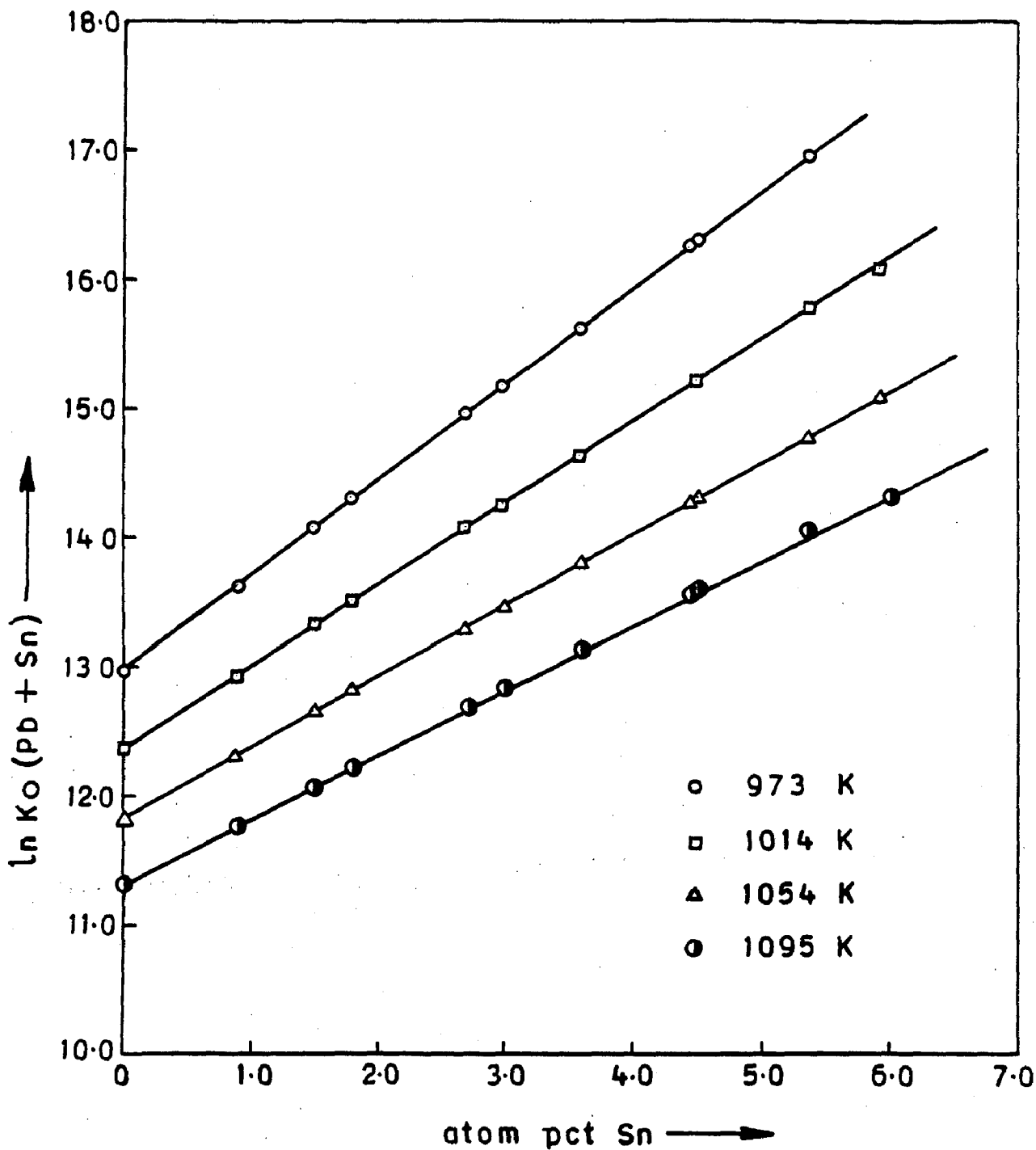


FIG. 6 -2: VARIATION OF $\ln K_O$ (Pb + Sn) WITH atom pct Sn IN LEAD-TIN ALLOYS AT DIFFERENT TEMPERATURES

Table 6.5 : Activity coefficient of oxygen, in Pb-Sn-O system at different temperatures and tin concentrations

Temperature (K)	Tin conc. (atom pct.)	$\ln K_O(\text{Pb+Sn})$	$\ln f_O^{\text{Sn}}$
1	2	3	4
973	0.000	12.9780	0.000
	0.892	13.6409	-0.663
	1.499	14.0907	-1.114
	1.795	14.3109	-1.332
	2.691	14.9754	-1.997
	2.988	15.1949	-2.218
	3.597	15.6467	-2.669
	4.456	16.2839	-3.307
	4.496	16.3008	-3.323
	5.368	16.9546	-3.977
1014	0.000	12.3801	0.000
	0.892	12.9441	-0.564
	1.499	13.3254	-0.945
	1.795	13.5111	-1.131
	2.691	14.0739	-1.694
	2.988	14.2604	-1.880
	3.597	14.6428	-2.263
	4.456	15.1820	-2.802
	4.496	15.2070	-2.827
	5.368	15.7549	-3.375
5.917	16.0999	-3.719	

Contd....

Table 6.5 contd...

1	2	3	4
1054	0.000	11.8422	0.0000
	0.892	12.3401	-0.4979
	1.499	12.6696	-0.8274
	1.795	12.8329	-0.9908
	2.691	13.3275	-1.4852
	2.988	13.4916	-1.6494
	3.597	13.8277	-1.9855
	4.456	14.3015	-2.4594
	4.496	14.3239	-2.4817
	5.368	14.8053	-2.9631
	5.917	15.1084	-3.2662
1095	0.000	11.3277	0.000
	0.892	11.7809	-0.4532
	1.499	12.0891	-0.7614
	1.795	12.2395	-0.9119
	2.691	12.6947	-1.3671
	2.988	12.8455	-1.5178
	3.597	13.1549	-1.8273
	4.456	13.5911	-2.2633
	4.496	13.6116	-2.2839
	5.368	14.0545	-2.7268
	5.917	14.3334	-3.0051

6.3 DISCUSSION OF RESULTS

In the study on Pb-Sn-O system, the oxygen level was of the order of 16-80 ppm in the lead melts. This is well below the levels of oxygen in lead for the precipitation of added tin as SnO_2 . The tin content obtained by chemical analysis of the metal samples drawn from the melt during the course of experiment was in accordance with the weight of Pb+Sn master alloys added to the bath. This confirms that no tin was lost by oxidation as SnO_2 from the alloys melt.

The variation of $\ln f_{\text{O}}^{\text{Sn}}$ at experimental temperatures with composition is shown in Fig. 6.3. The linear variation in the dilute concentration range of the metallic solute, tin up to 5 atom pct. enables the calculation of ternary interaction parameter, $\epsilon_{\text{O}}^{\text{Sn}}$ in the Pb-Sn-O system using the relation,

$$\epsilon_{\text{O}}^{\text{Sn}} = \left(\ln f_{\text{O}} / \ln N_{\text{sn}} \right)_{N_{\text{sn}} \rightarrow 1} \quad (6.21)$$

The data obtained is given in Table 6.3 and 6.4 are in good agreement with those of Jacob & Jeffes [23]. Using Fig. 6.3 values on $\ln f_{\text{O}}^{\text{Sn}}$ at several atomic percents of tin at different temperatures of study were obtained and presented in Table 6.6. These are plotted in Fig. 6.4 vs $1/T$. From these straight line plots, the relative partial molar enthalpy ΔH_{O} and entropy, ΔS_{O} of oxygen dissolution in binary Pb-Sn alloys wrt gaseous oxygen

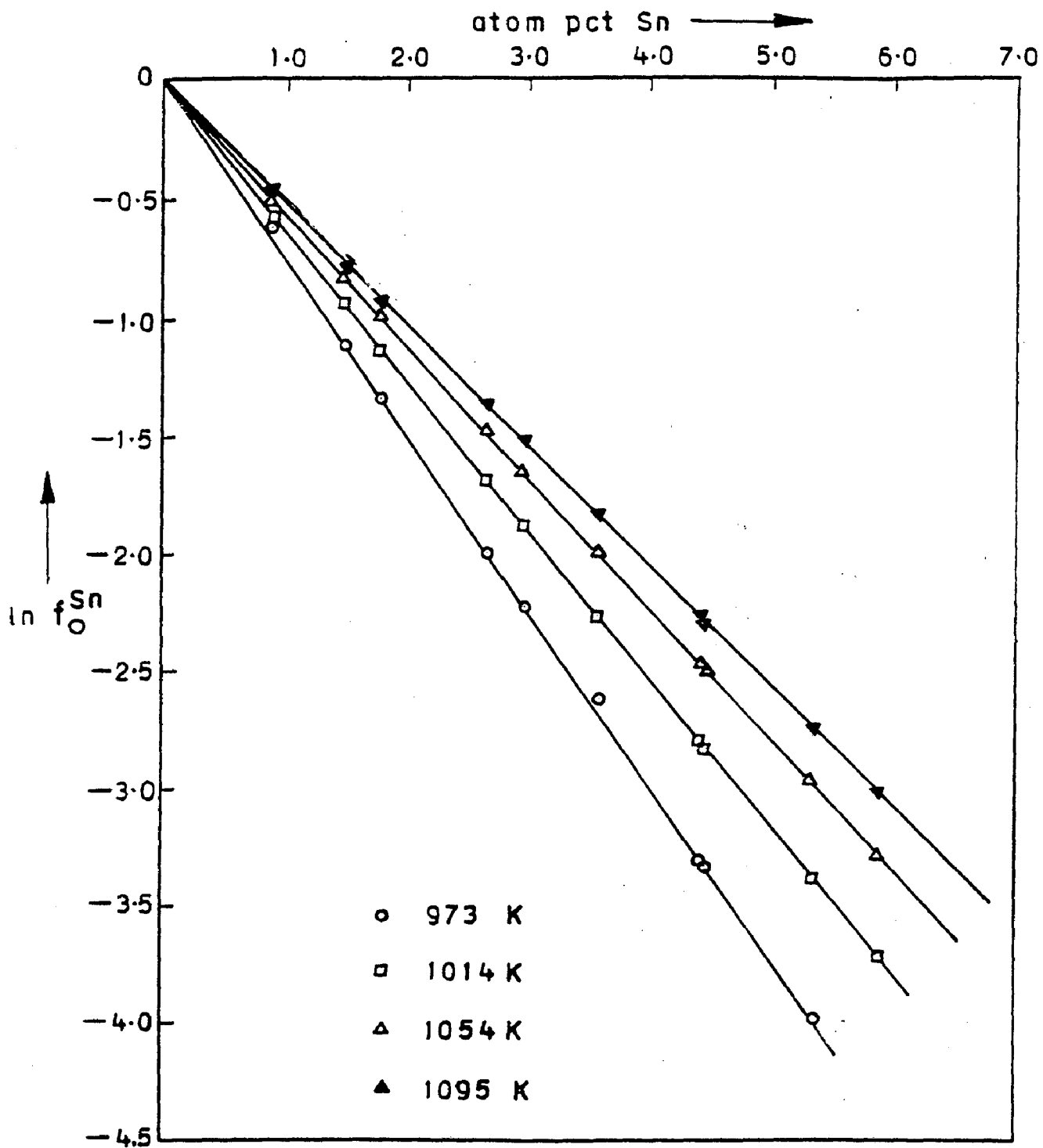


FIG. 6 -3: EFFECT OF TIN ON ACTIVITY COEFFICIENT OF OXYGEN IN LIQUID LEAD AT 973, 1014, 1054 & 1095K

Table 6.6 : $\ln f_{\text{O}}^{\text{Sn}}$ in lead at different atom pct Sn at different experimental temps.

Temperature (K)	$\ln f_{\text{O}}^{\text{Sn}}$, at conc. of tin			
	1 atom pct	2 atom pct	2 atom pct	4 pct atom
973	-0.775	-1.515	-2.27	-3.00
1014	-0.635	-1.265	-1.895	-2.525
1054	-0.555	-1.113	-1.670	-2.215
1095	-0.520	-1.013	-1.502	-2.025

as the standard state have been arrived at. This was done using linear regression technique (Appendix I) in comparison with the relation,

$$\ln f_{\text{O}} = \Delta \bar{H}_{\text{O}} / R.T - \Delta \bar{S}_{\text{O}} / R \quad (6.22)$$

The values on $\Delta \bar{H}_{\text{O}}$ & $\Delta \bar{S}_{\text{O}}$ at different concentration of tin are presented in Table 6.7.

Table 6.7 : $\Delta \bar{H}_{\text{O}}$ & $\Delta \bar{S}_{\text{O}}$ at different atom pct tin

Atom pct Sn	1.0	2.0	3.0	4.0
$-\Delta \bar{H}_{\text{O}}$, K.J.gatom ⁻¹	18.65	36.44	55.50	69.75
$-\Delta \bar{S}_{\text{O}}$, J gatom ⁻¹ K ⁻¹	12.90	25.10	38.60	48.50

As will be observed, addition of tin lowers both partial molar enthalpy and entropy of solution of oxygen in lead-tin alloys. This decrease in $\Delta \bar{H}_{\text{O}}$ in lead rich alloys is probably due to the increased number of Sn-O bonds

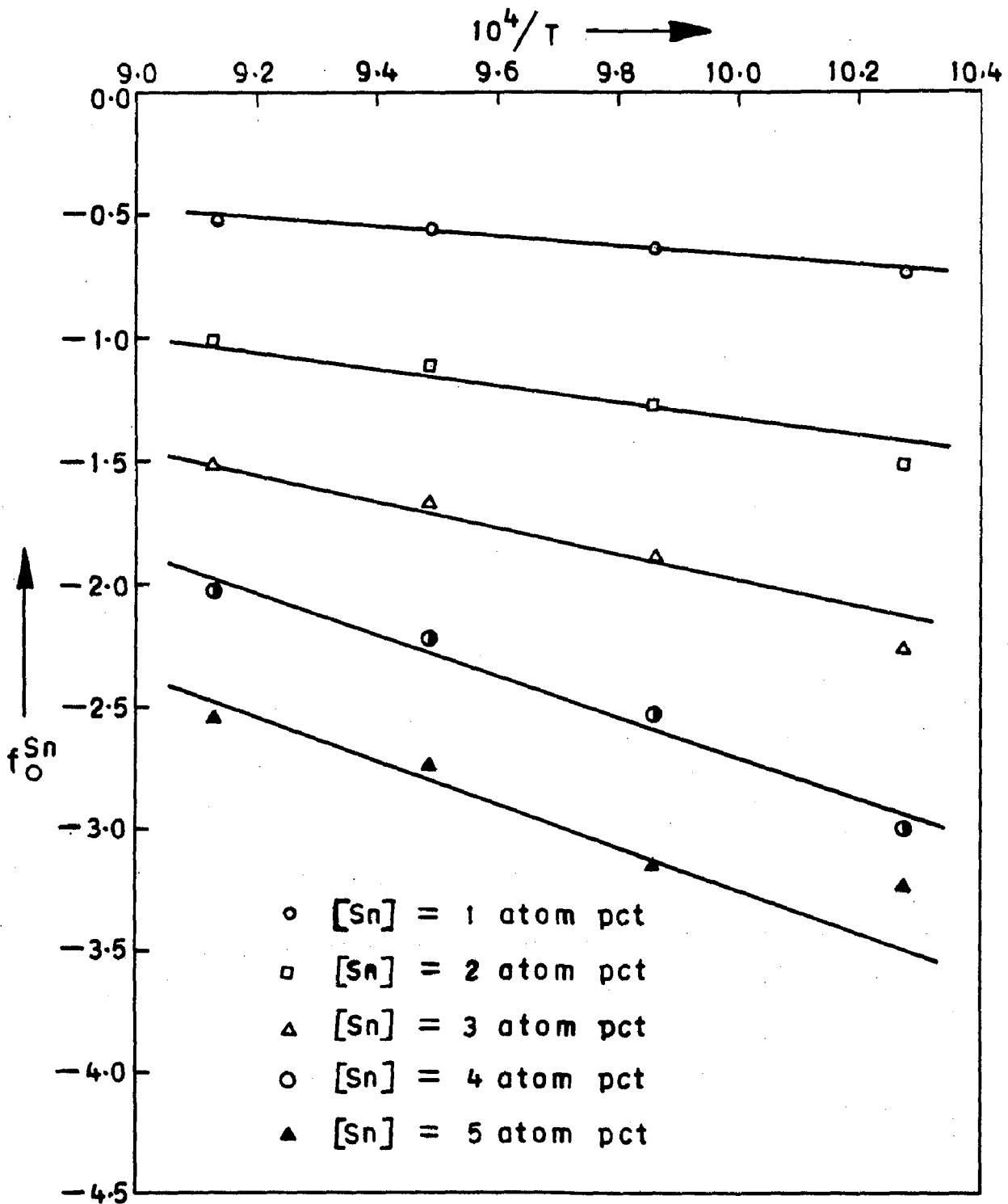


FIG. 6-4: VARIATION OF f_O^{Sn} IN Pd-Sn ALLOYS WITH RECIPROCAL OF TEMPERATURE (STANDARD STATE FOR OXYGEN IS 1 atom pct SOLUTION IN LEAD)

in preference to Pb-O bonds in solution. In other words the ratio Sn-O/Pb-O bonds would be greater than the ratio of mole fraction of tin and lead. The tin atoms are therefore likely to cluster around the oxygen atoms and lower the activity coefficient of oxygen in lead.

As pointed out by Jacob & Jeffes [23], addition of tin to lead-oxygen solution is likely to decrease both the configurational and vibrational entropy of oxygen. The configuration contribution arises from the clustering of tin atoms around oxygen atoms. The mole fraction of tin around oxygen is higher than in the bulk of solution. The vibration contribution is associated with the stronger bonds formed by oxygen and tin atoms. The latter is obvious from the higher enthalpy of formation of tin oxide as compared with lead oxide.

6.3.1 Applicability of Solution Models

The activity coefficient, $f_{\text{O}}(\text{Pb+Sn})$ in the Pb+Sn liquid alloys at $T=1014\text{K}$ has been calculated using different classical models. The binary data required for necessary calculations are adopted from compilations of Hultgren et al. [1]. The data on $f_{\text{O}}(\text{Pb})$ has been taken from Taskinen's [59] work viz., $\ln f_{\text{O}}(\text{Pb}) = 6.133 - 14040/T$ and that on $f_{\text{O}}(\text{Sn})$ has been calculated from the gibb's free energies of oxygen dissolution in pure metals viz. $\Delta G_{\text{O}}(\text{Pb})$ and $\Delta G_{\text{O}}(\text{Sn})$ using the relation,

$$\ln[fO(Pb)/fO(Sn)] = 1/RT[\Delta GO(Pb) - \Delta GO(Sn)] \quad (6.23)$$

The value of $\Delta GO(Sn)$ has been taken from the work of Bedford et al. [26] viz., $\Delta GO(Sn) = -182464.2 + 25.648T$ J gatom⁻¹.

The values of $\ln fO(Pb+Sn)$ thus calculated have been used to arrive at the effect of tin in Pb-O solution, f_O^{Sn} using the relation,

$$\ln f_O^{Sn} = \ln fO(Pb+Sn) - \ln fO(Pb) \quad (6.24)$$

The parameters, $\ln fO(Pb+Sn)$ and $\ln f_O^{Sn}$ so obtained are presented in Tables 6.8 and 6.9 and plotted respectively in Figs. 6.5 and 6.6 alongwith the experimental results at T=1014K for comparison.

Alcock and Richardson [152] assumed random distribution of atoms, A and B in a system A-B-O i.e. the ratio of the no. of A-O bonds to B-O bonds being given as,

$$n(B-O)/n(A-O) = N_B/N_A \quad (6.25)$$

with this, they arrived at the following expression to predict the activity coefficient of oxygen,

$$\begin{aligned} \ln fO(A+B) = N_A \ln[fO(A)/fA(A+B)] + \\ N_B \ln[fO(B)/fB(A+B)] \end{aligned} \quad (6.26)$$

For the Pb-Sn-O system, the values of $\ln f_O^{Sn}$ thus calculated, as is observed from Fig. 6.5 do not match

with the measured data, the predicted values being on the higher side. This mismatch may be attributed to the greater difference in the pairwise energies of interaction between Pb-O and Sn-O pairs. This is obvious from the greater interaction between Sn-O atoms as seen by, $f_O(\text{Pb})/f_O(\text{Sn}) \sim 454$ at $T=1014\text{K}$.

To account for systems with larger difference in energies of interaction of the metal atoms with oxygen, Alcock & Richardson [154] in their quasichemical treatment obtained the ratio of the two types of metal-oxygen bonds through the relationship,

$$n(\text{Sn-O})/n(\text{Pb-O}) = N_{\text{Sn}}/N_{\text{Pb}} \exp(-\Delta G^{\text{XS,exchange}}/RT) \quad (6.27)$$

where, $G^{\text{XS,exchange}}$ is the excess free energy change which occurs when an A-O contact is changed to a B-O contact by the exchange of an A atom in the co-ordination shell of the oxygen atom with a B atom in the body of the melt. The model lead to following expression to calculate the activity co-efficient of oxygen in the A-B alloy viz.,

$$\begin{aligned} [1/f_O(\text{A+B})]^{1/Z} &= N_A [f_A(\text{A+B})/f_O(\text{A})]^{1/Z} \\ &+ N_B [f_B(\text{A+B})/f_O(\text{B})]^{1/Z} \end{aligned} \quad (6.28)$$

Where, Z is the co-ordination number assumed to be the same for the atoms constituting the system. The values of activity coefficient so obtained at $T=1014\text{K}$ with $Z=2$ and 4 are shown in Fig.6.5. As is observed, the predicted

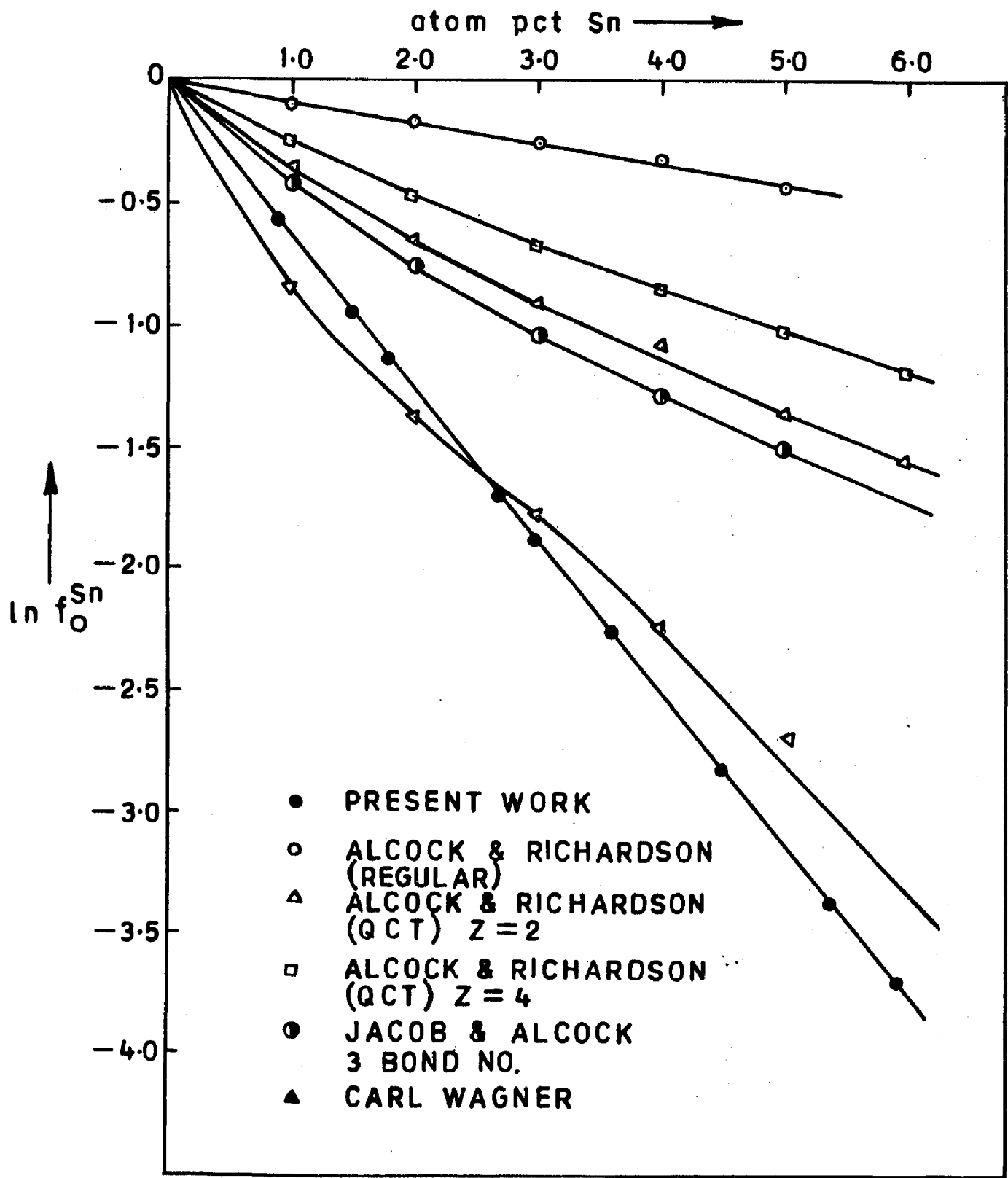


FIG. 6 - 5: ACTIVITY COEFFICIENT OF OXYGEN IN Pb-Sn ALLOYS AT 1014 K

Table 6.8 : Ternary interaction parameter, Inf_O^{Sn} in Pb-Sn-O system at 1014K

Theoretical Model	Ternary interaction parameter, Inf_O^{Sn} at $N_{\text{Sn}} =$				
	0.01	0.02	0.03	0.04	0.05
Alcock & Richardson's (Regular Solution Model)	-0.0825	-0.162	-0.242	-0.319	-0.396
Alcock & Richardson's (Q.C.T.) at					
Z = 2	-0.817	-1.395	-1.796	-2.210	-2.665
Z=4	-0.248	-0.469	-0.671	-1.0273	-1.320
Jacob & Alcock (3 bond No.)	-0.408	-0.745	-1.033	-1.282	-1.503
Carl Wagner					
h=3113 gatom ⁻¹	-0.324	-0.603	-0.851	-1.072	-1.273
h=4276 gatom ⁻¹	-0.464	-0.603	-1.149	-1.425	-1.666
This study	-0.6375	-1.245	-1.875	-2.505	-3.016

Table 6.9 : Activity coefficient, $\ln f_0(\text{Pb+Sn})$ in Pb-Sn-O system at 1014K

Theoretical Models	$\ln f_0(\text{Pb+Sn})$ at $N_{\text{Sn}} =$				
	0.01	0.02	0.03	0.04	0.05
ALCOCK & Richardson (Regular solution Model)	-7.796	-7.875	-7.955	-8.032	-8.109
Alcock & Richardson (A.C.T.) at					
Z = 2	-8.530	-9.108	-9.509	-9.922	-10.378
Z = 4	-7.961	-8.182	-8.384	-8.561	-8.741
Jacob & Alcock (3 bond No.)	-8.121	-8.458	-8.746	-8.995	-9.216
Carl Wagner					
$h = 3113 \text{ J gatom}^{-1}$	-8.037	-8.316	-8.564	-8.785	-8.986
$h = 4276 \text{ J gatom}^{-1}$	-8.177	-8.316	-8.862	-9.138	-9.379
This study	-8.351	-8.958	-9.588	-10.218	-10.729

values with $Z=2$ are in close agreement with the experimental results. The agreement at higher temperatures is still closer because the difference in activity coefficients of oxygen in pure metals, Pb & Sn decreases and the predicted values become more negative approaching the experimental results. Fig. 6.6 shows predicted values of $\ln f_{O(Pb+Sn)}$ with those computed from experimental results. The applicability of this model to the system Pb-Sn-O is apparent from the ratio, $f_{O(Pb)}/f_{O(Sn)} \gg 1$ as well as from the more negative heat of formation of tin oxide as compared to that of lead oxide. This leads to the conclusion that pair wise interaction energies of oxygen with each surrounding metal atom Pb and Sn varies considerably with alloy composition. The data on $\Delta \bar{H}_O$ in Table 6.7 also account for the same.

Alcock & Richardson's Eq. 6.28 has been found to fit the experimental data only when low coordination number, $Z=2$ is assigned to all the atoms in solution. It is therefore conceivable that strong electronegative solutes, oxygen or sulphur make smaller number of bonds than the metal atoms. Jacob and Alcock [156] therefore, developed a treatment using different co-ordination numbers for oxygen (n) and metal atoms (Z) and giving quasi-chemical treatment obtain an expression,

$$\frac{1}{f_{O^{1/n}}(A+B)} = N_A [f_A^\alpha(A+B) / f_{O^{1/n}}(A)] + N_B [f_B^\alpha(A+B) / f_{O^{1/n}}(B)] \quad (6.29)$$

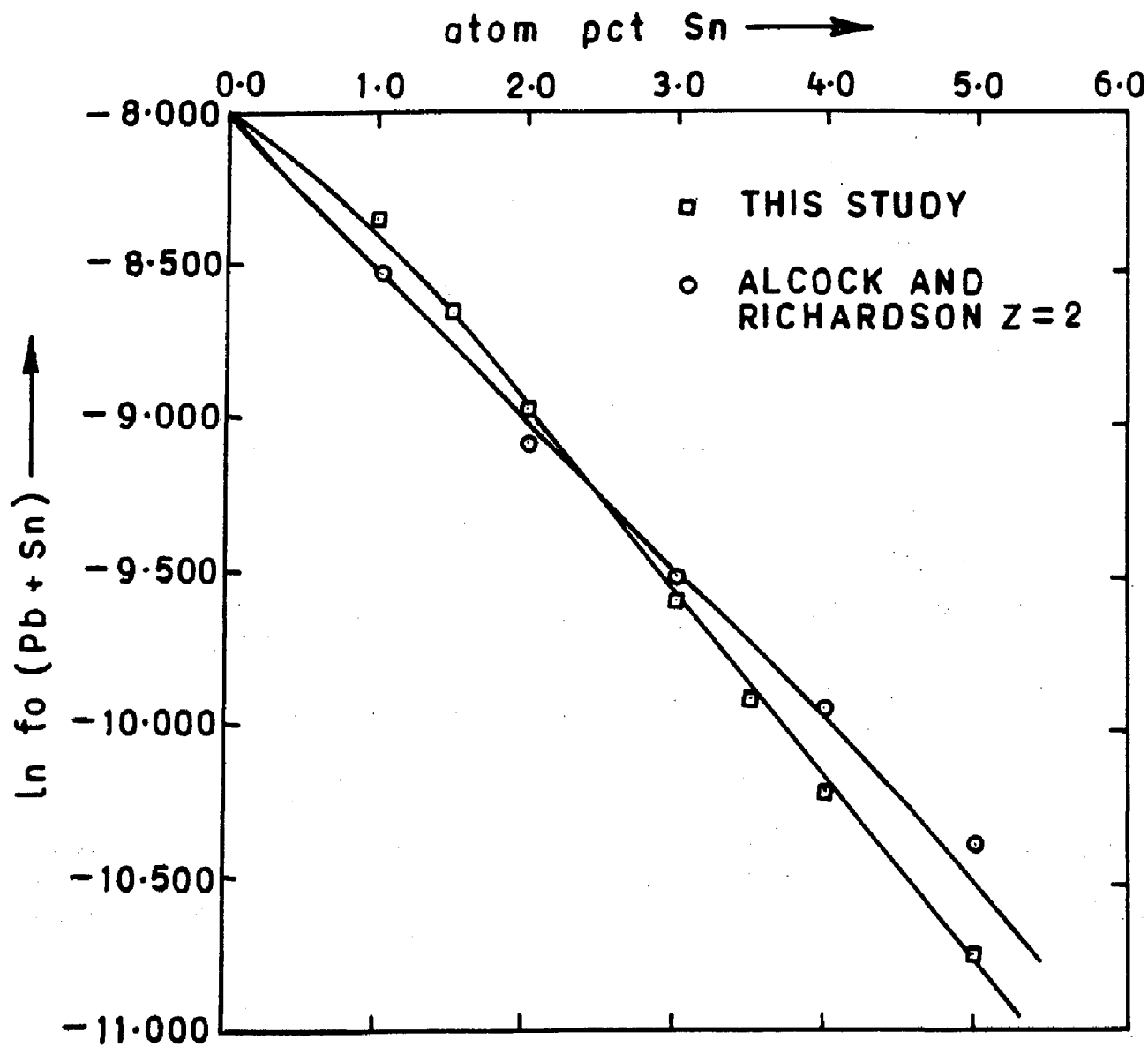


FIG. 6-6: VARIATION OF $\ln f_o(\text{Pb} + \text{Sn})$ WITH TIN CONC. IN Pb-Sn-O SYSTEM AT 1014 K

Eq. 6.29 represents the degree to which metal-metal bonds are weakened with oxygen dissolution in metallic solution. Using $n=4$ and $\alpha = 1/2$ as proposed by Jacob & Alcock, the predicted values are shown in Fig.6.6. The predicted values on $\ln f_O(\text{Pb+Sn})$ showing positive deviation wrt the experimental data. In their treatment Jacob & Alcock assumed that the stronger oxygen-metal bonds (Sn-O) distort the electronic configuration and thereby reduce the strength of bonds formed by these metal atoms with neighbouring metal (viz. Pb) atoms. By fitting their generalized equation in several alloy systems, the authors demonstrated that large number of systems viz. Cu-Sn-O and Ag-Sn-O [156]; Cu-In-O [46] etc. can be accounted on the assumption that oxygen makes four bonds only in the solution in metallic alloys and that half of the metal-metal bonds which are normally made by the metal atoms in the bulk of the alloy are broken when atoms of metals forming stronger bonds with oxygen viz. tin are added. such a reduction of the metal-metal bonds lead to a significant deviation of average composition of the metal atoms adjacent to those bonded to oxygen from the bulk of the alloy. This has not been considered in derivation of Eq. 6.29 and results in the lowering of the energy of the system. The measured values on $\ln f_O(\text{Pb-Sn})$ thus show a negative deviation wrt the calculated values.

Wagner proposed another theoretical model with one adjustable energy parameter, h . It was assumed that the dissolved oxygen atoms occupy interstitial positions on octa hedral sites with $Z=6$ and the solvation energy exhibits parabolic dependence on the number of metal atoms A and B in the solvation shell around oxygen atoms. With these basic assumptions, he arrived at an expression to calculate $f_O(A+B)$ viz.,

$$\frac{1}{f_O(A+B)} = \sum_{i=0}^Z \binom{Z}{i} [N_A / f_O^{1/Z}(A)]^{Z-i} [N_B / f_O^{1/Z}(B)]^i \cdot \exp[(Z-i)ih / ZRT] \quad (6.30)$$

To arrive at the value of h , Chang and HU [164,166] derived an empirical relationship from the experimental data for alloy systems satisfying the condition, $(V_b/V_a)^2 < \text{or } = 1$ and $\Delta G_O(A) > \Delta G_O(B)$; applicable to Pb-Sn-O system with V_{Pb} and V_{Sn} each being [2.56] viz.,

$$h = 2E/Z^2 + 0.09 \epsilon (V_b/V_a)^2 + 0.04[\Delta G_O(A) - \Delta G_O(B)] \quad (6.31)$$

in Eq. 6.31 is the regular solution parameter and can be calculated from the mixing enthalpy ΔH , of A-B alloy viz. $\epsilon = \Delta H / N_A N_B$. With these at $T=1014K$, h comes out as $3113 \text{ J/gatom}^{-1}$. The corresponding results on activity coefficient $\ln f_O(\text{Pb+Sn})$ or $\ln f_O^{\text{Sn}}$ are presented in Tables 6.8 & 6.9 and do not fit with the experimental data.

In the absence of experimental data on $f_O(\text{Sn})$, the upper limiting value of h_{max} may be calculated using an expression suggested by Wagner,

$$h_{\text{max}} = 2/5Z[\Delta H_O(A) - \Delta H_O(B)] \quad (6.32)$$

where $\Delta H_O(A)$ & $\Delta H_O(B)$ are the enthalpy changes for dissolution of oxygen in pure metals A and B respectively. For Pb-Sn-O system, the value of h_{max} comes out as 4276 J gatom⁻¹. This improves the calculated values but still these exhibit positive deviation when compared with the corresponding experimental results. In particular the predicted values fit to show the compositional dependence of activity coefficient with composition of solute Sn. This may be on account of the fact that the Pb-Sn-O system, Pb-Sn alloy in the dilute concentration range exhibit strong positive departure from ideality [1]. Thus significant deviations from random distribution of Pb and Sn atoms may occur in contradiction to the Wagner's assumption. Further, in the derivation of Eq. 6.30 Wagner did not consider the effect due to change in the ratio of the number of conduction electrons with alloy composition. This plays a significant role in Pb-Sn-O system, because at a given oxygen activity, the solubility of oxygen in tin is far greater than in liquid lead. This is obvious from the distinct parallelism between the solubility of oxygen in metal and the stability of respective solid

oxides, expressed in terms of the negative heats of formation per gatom oxygen [152]. This is an indication that the transfer of electrons from tin to oxygen atoms occur to a greater extent than from lead atoms. It may be surmised that upon gradual replacement of lead by tin atoms, in the solvation shell of an oxygen atom, the extent of electron transfer per tin atom is especially large for first tin atom and decreases gradually with the subsequent increase of tin atoms in solution.

Chiang & Chang [162] further modified Wagner's equation, by introducing two energy parameters h_1 and h_2 . However in view of very dilute concentration of tin (upto 6 atom pct) taken for this study, it is felt that the predicted values on the basis of this model would not be significantly different from those predicted by Wagner's equation. Calculations based on Chang and Chang's model have therefore been not attempted for the interpretation of results on the Pb-Sn-O system. For similar reasons the calculations of activity coefficient, $\ln f_{O}(Pb+Sn)$ on the basis of statistical models put forth by Anil, Kapoor and Froberg [187,188] and Blander et al. [193] have not been attempted.

CHAPTER - VII

SUMMARY AND CONCLUSIONS

Important results obtained in the present investigation and conclusions drawn from them are summarised below:

1. LEAD OXYGEN BINARY SYSTEM

- i) The standard free-energy of formation of solid lead oxide by the reaction, $\text{Pb(l)} + \frac{1}{2} \text{O}_2(\text{g}) = \text{PbO(s)}$ in the temperature range 933-1095K is expressed as:

$$\Delta G_{\text{PbO(s)}}^{\circ} = -224 + 0.1078T \quad (\pm 400) \text{ KJ.mole}^{-1}$$

- ii) The Gibb's energy change, $\Delta G_{\text{O(Pb)}}$ for the dissolution of molecular oxygen in pure lead and the self interaction parameter, $\epsilon_{\text{O(Pb)}}^{\text{O}}$ at different temperatures are given as,

T(K)	$\Delta G_{\text{O(Pb)}} \text{ J mol}^{-1}$	$\epsilon_{\text{O(Pb)}}^{\text{O}}$
933	-105,503	-24.4
967	-105,058	-19.17
1010	-104,499	-14.84
1053	-103,897	-10.25
1095	-103,403	- 6.06

The temperature dependence of these binary lead oxygen parameters may be expressed as,

$$\Delta G_{\text{O(Pb)}}^{\circ} = -117616.4 + 12.983T \quad (\pm 400) \text{ J gatom}^{-1}$$

$$\epsilon_{\text{O(Pb)}}^{\text{O}} = 97.35 - 113,270/T \quad (\pm 0.8)$$

II. LEAD-COPPER-OXYGEN TERNARY SYSTEM

i) Variation of $\ln f_{\text{O(Pb)}}^{\text{Cu}}$ with atomic percent copper is linear up to 3.5 atom percent copper, in the temperature range 967-1095K.

ii) The ternary interaction coefficient, $\epsilon_{\text{O(Pb)}}^{\text{Cu}}$ found at different temperatures are:

T(K)	967	1010	1053	1095
$\epsilon_{\text{O(Pb)}}^{\text{Cu}}$	-7.095	-6.464	-4.566	-3.53

The temperature dependence of $\epsilon_{\text{O(Pb)}}^{\text{Cu}}$ may be represented as,

$$\epsilon_{\text{O(Pb)}}^{\text{Cu}} = 23.9 - 30.3 \times 10^3 / T, \quad (\pm 0.5)$$

iii) The variation of $\ln f_{\text{O}}^{\text{Cu}}$ in lead with atom pct.copper at different temperatures are:

Temperature	$\ln f_{\text{O}}^{\text{Cu}}$		
	1 atom pct.Cu	2 atom pct.Cu	3 atom pct.Cu
967	-0.070	-0.137	-0.2015
1010	-0.065	-0.123	-0.185
1053	-0.045	-0.950	-0.142
1095	-0.035	-0.070	-0.102

$\ln f_{\text{O}}^{\text{Cu}}$ at 1095 is present in Fig.7.1

- iv) The relative partial molar enthalpy, $\Delta\bar{H}_O$ and entropy, $\Delta\bar{S}_O$, of oxygen dissolution relative to gaseous oxygen in lead copper-oxygen system is given as,

atom pct. Cu	1.0	3.0	3.0
$-\Delta\bar{H}_O$, KJ gatom ⁻¹	2.56	4.69	6.98
$-\Delta\bar{S}_O$, J gatom ⁻¹ K ⁻¹	2.06	3.67	5.47

- v) The measured value of $\ln f_O^{Cu}$ may be predicted using Wagner's theoretical model with one adjustable energy parameter, $h = 3620$ J gatom⁻¹. This accounts for a preferential attachment of oxygen for a particular component in solution. A fair agreement between predicted and measured values is observed with three bond model of Jacob & Alcock. The predicted values being on the higher side.

III LEAD-BISMUTH-OXYGEN TERNARY SYSTEM

- i) $\ln f_{O(Pb)}^{Bi}$ has a linear variation with atom percent bismuth up to 3 atom pct. i.e. up to the dilute solution range studied.
- ii) The measured values of ternary interaction parameter, $\epsilon_{O(Pb)}^{Bi}$ at the temperatures of study are,

T(K)	913	953	993	1034
$\epsilon_{O(Pb)}^{Bi}$	3.57	2.69	1.88	1.11

The interaction parameter decreases with increase in temperature. The temperature dependence of $\epsilon_{O(Pb)}^{Bi}$ may be expressed as,

$$\epsilon_{O(Pb)}^{Bi} = -17.454 + 19.2 \times 10^3 / T \quad (\pm 0.3)$$

- iii) $\ln f_O^{Bi}$ at different atom pct. Bi found at different experimental temperatures are;

T(K)	$\ln f_O^{Bi}$		
	1 atom pct. Bi	2 atom pct. Bi	3 atom pct. Bi
913	0.013	0.026	0.039
953	0.020	0.040	0.061
993	0.031	0.062	0.092
1034	0.038	0.075	0.113
(1095)	(0.047)	(0.097)	(0.147)

The values within the brackets are found by extrapolation and are plotted in Fig.7.1.

- iv) The relative partial molar enthalpy, $\Delta \bar{H}_O$ and entropy, $\Delta \bar{S}_O$ of oxygen dissolution relative to gaseous oxygen in Pb-Bi-O ternary system in the temperature range 913-1034K are,

Atom pct. Bi	1.0	2.0	3.0
$-\Delta \bar{H}_O, \text{KJ.gatom}^{-1}$	1.66	3.29	4.93
$-\Delta \bar{S}_O, \text{J gatom}^{-1} \text{K}^{-1}$	1.91	3.81	5.71

- v) The measured values of $\ln f_{O(Pb)}^{Bi}$ may be approximately predicted using Alcock and Richardson's quasichemical equation with $Z=2$. A close representation of the measured data is possible with

Wagner's theoretical model with one adjustable energy parameter, $h=544 \text{ J gatom}^{-1}$ at 1034K.

IV LEAD-TIN-OXYGEN TERNARY SYSTEM

- i) $\ln f_{\text{O(Pb)}}^{\text{Sn}}$ atom percent Sn follows a linear variation up to 6 atom percent tin under study in the temperature range 973-1095K.
- ii) Ternary interaction parameter, $\epsilon_{\text{O(Pb)}}^{\text{Sn}}$ measured at different temperatures are,

T(K)	973	1014	1054	1095
$\epsilon_{\text{O(Pb)}}^{\text{Sn}}$	-74.2	-62.8	-55.2	-50.8

The temperature dependence of $\epsilon_{\text{O(Pb)}}^{\text{Sn}}$ may be expressed as,

$$\epsilon_{\text{O(Pb)}}^{\text{Sn}} = 139 - 20.616 \times 10^3 / T, \quad (\pm 4)$$

- iii) $\ln f_{\text{O}}^{\text{Sn}}$ in lead at different atom pct.Sn found at different experimental temperatures are:

T(K)	$\ln f_{\text{O}}^{\text{Sn}}$				
	1 atom pct.Sn	2 atom pct.Sn	3 atom pct.Sn	4 atom pct.Sn	5 atom pct.Sn
973	-0.775	-1.515	-2.27	-3.00	-3.22
1014	-0.637	-1.265	-1.895	-2.525	-3.14
1054	-0.555	-1.113	-1.67	-2.215	-2.77
1095	-0.520	-1.013	-1.502	-2.025	-2.54

$\ln f_{\text{O}}^{\text{Sn}}$ at 1095K is presented in Fig. 7.1.

The relative partial molar enthalpy, $\Delta\bar{H}_O$ and entropy, $\Delta\bar{S}_O$ of oxygen dissolution relative to gaseous oxygen in lead-tin-oxygen system in the temperature range 973-1095K are,

atom pct. Sn	1.0	2.0	3.0	4.0
$-\Delta\bar{H}_O, \text{KJ.gatom}^{-1}$	18.65	36.44	55.50	69.76
$-\Delta\bar{S}_O, \text{J gatom}^{-1}\text{K}^{-1}$	12.9	25.1	38.6	48.5

Larger values of $\Delta\bar{H}_O$ in Pb-Sn-O as compared to Pb-Cu-O accounts for clustering of tin atoms around oxygen atoms.

v) The measured values of $\ln f_{O(\text{Pb})}^{\text{Sn}}$ may be predicted using Alcock and Richardson's quasichemical equation with $Z=2$. This equation is applicable as the energy of interaction of the solute, oxygen with two metal solvents, Pb and Sn differs widely viz. $f_{O(\text{Pb})}/f_{O(\text{Sn})} = 438$ at 1014K. This leads to the conclusion that pair wise interaction energies of oxygen with each of surrounding metal atom viz. Pb and Sn may vary considerably with alloy composition.

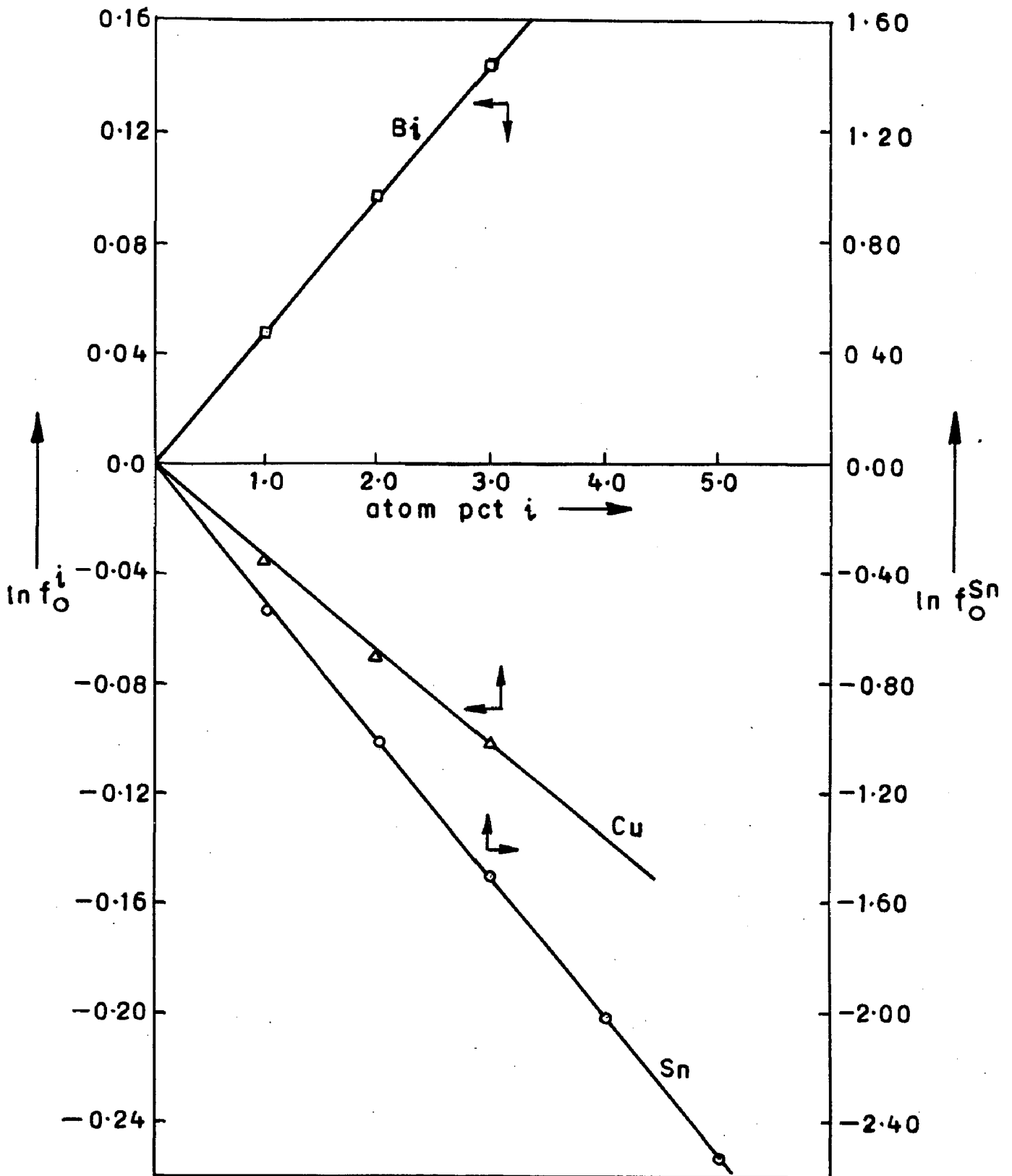


FIG. 7 - 1 VARIATION OF $\ln f_O^i$ & $\ln f_O^{Sn}$ LEAD IN THE TERNARY Pb-*i*-O AT 1095 K (*i*=Cu, Bi)

SUGGESTIONS FOR FUTURE WORK

1. Lot of work is required to be carried out on lead base alloys. Effect of solutes commonly present as impurities in lead bullion viz Zn, Fe, As, S and Ag has not been investigated on oxygen in lead. Besides, more work is required to be done on Pb-Cu-O, Pb-Sn-O and Pb-Bi-O in different temperature ranges and at higher concentration of the metallic solutes.
2. Leaving aside iron, copper etc. thermodynamic behaviour of oxygen in alloy systems viz. bismuth base alloys, chromium base alloys, manganese base alloys and zinc base alloys require investigation. There is hardly any work reported in literature on these systems.
3. Even all the important metal-oxygen systems have not been studied. More work is required to be done to generate the thermodynamic data on interaction parameters etc. in case of binaries such as Sn-O, Al-O, Co-O, Mn-O, Mo-O and Te-O etc. Further hardly any work has been reported on oxygen in metals viz. Al, B, Ti, Zn, Be etc.etc. These need investigation.
4. With the small data available in literature on some of the systems viz. copper base and iron base; their multicomponent systems can be easily taken up for study. Multicomponent systems in fact form an open field which require investigation.

APPENDIX - I

LEAST SQUARE METHOD (LINEAR CURVE FITTING)

```
00100      C      PROGRAM FOR STRAIGHT LINE FIT
00200          DIMENSION X(10),Y(10)
00300          OPEN(UNIT=1,DEVICE='DSK',FILE='LSQ.DAT')
00400          OPEN(UNIT=2,DEVICE='DSK',FILE='LSQ.RES',ACCESS=
          'APPEND')
00500      1      CONTINUE
00600          READ(1,*,END=60)N
00700          READ(1,*(X(I),I=1,N)
00800          READ(1,*)(Y(I),I=1,N)
00900          WRITE(2,10)
01000      10      FORMAT(5X,'INPUT VALUES OF X AND Y'//14X,'X',
          16X,'Y'//)
01100          WRITE(2,20)(X(I),Y(I),I=1,N)
01200      C      PRINT 20,(X(I),I=1,N)
01300      20      FORMAT(5X,2E18.11)
01400          SUMX=0.;SUMY=0.;SUMXY=0.;SUMX2=0.
01500          DO 40 I=1,N
01600          SUMX=SUMX+X(I)
01700          SUMY=SUMY+Y(I)
01800          SUMXY=SUMXY+X(I)*Y(I)
01900          SUMX2=SUMX2+X(I)*X(I)
```

```
02000    40    CONTINUE
02100          A=(FLOAT(N)*SUMXY-SUMX*SUMY)/(FLOAT(N)*SUMX2-
          SUMX*SUMX)
02200          B=(SUMY*SUMX2-SUMXY*SUMX)/(FLOAT(N)*SUMX2-
          SUMX*SUMX)
02300          WRITE(2,50)A,B
02400    C      PRINT 50,A,B
02500    50    FORMAT(5X,'THE VALUES OF A AND B IN EQUATION
          Y=A+B' /
02600          1 5X,'A=',E18.11,2X,'B=',E18.11)
02700          GO TO 1
02800    60    STOP
02900          END
```

APPENDIX - II

SOLUTION OF MATRICS

```

00100      DIMENSION A(50,500,B(50,XI(50),X2(50),Y(50)
00200      OPEN(UNIT=1,DEVICE='DSK',FILE=INPUT.DAT)
00312      READ(1,*)NOM
00325      DO 3211 IJ=1,NOM
00350      READ(1,*)NELEM
00400      READ(1,*)(X1(I),I=1,NELEM)
00450      C  READ(1,*,END=222)(X1(I),I=1,NELEM)
00500      READ(1,*)(X2(I),I=1,NELEM)
00600      READ(1,*)(Y(I),I=1,NELEM)
00700      PRINT 4
00800      PRINT 1,(X1(I),X2(I),Y(I),I=1,NELEM)
00900      1  FORMAT(5X,3E,3E15.6)
01000      4  FORMAT(/5X,'INPUT DATA'/)
01100      DO 2 I=1,3
01200      B(I)=0.0
01300      DO 2 J=1,3
01400      2  (A(I,J)=0.0
01500      A(1,1)=FLOAT(NELEM)
01600      DO 3 I=1,NELEM
01700      A(1,2)=A(1,2)+X1(I)
01800      A(1,3)=A(1,3)+X2(I)
01900      A(2,2)=A(2,2)+X1(I)*X1(I)
02000      A(2,3)=A(2,3)+X1(I)*X2(I)

```

```
02100      A(3,3)=A(3,3)+X2(I)*X2(I)
02200      B(1)=B(1)+Y(I)
02300      B(2)=B(2)+X1(I)*Y(I)
02400      B(3)=(B)+X2(I)*Y(I)
02500      3  CONTINUE
02600      A(2,1)=A(1,2)
02700      A(3,1)=A(1,3)
02800      A(3,2)=A(2,3)
02900      N=3
03000      N1=N-1
03100      DO 10 I=1,N1
03200      K=I+1
03300      AII=A(I,I)
03400      C  IF(ABS(AII).LT.0.1E08)GO TO 333
03500      AII=1./AII
03600      DO 10 J=K,N
03700      F=-A(J,I)*AII
03800      DO 20 L=K,N
03900      20  A(J,L)=A(J,L)+F*A(I,L)
04000      B(J)=B(J)+F*B(I)
04100      10  CONTINUE
04150      C  IF(ABS(A(N,N)).LT.0.1E-08)GO TO 333
04200      B(N)=B(N)/A(N,N)
04300      DO 30 K=1,N1
04400      I=N-K
04500      IP1=I+1
```

```
04600      SUM=0.0
04700      DO 40 J=IP1,N
04800      40  SUM=SUM+A(I,J)*B(J)
04900      B(I)=(B(I)-SUM)/A(I,I)
05000      30  CONTINUE
05100      PRINT 50
05200      50  FORMAT(/5X,'COEFFICIENTS A1  A2  A3 ARE'/)
05300      PRINT 60, (B(I),I=1,3)
05400      60  FORMAT(5X,3E15.6//5X,45('*'))
05500      C   GO TO 111
05550      3211 CONTINUE
05600      222  STOP
05700      333  PRINT 140
05900      140  FORMAT(/X,'** DIAGONAL COEFFICIENT ZERO **'/)
06000      END
```

REFERENCES

1. R.Hultgren, P.D. Desai, D.T. Hawkins, M. Gleiser K.K. Kelly, 'Selected values of Thermodynamic Properties of Binary Alloys', 1973, A.S.M., Ohio.
2. O.Kubaschewski and C.B. Alcock, 'Metallurgical Thermochemistry', 1979, Pergamon Press, Oxford.
3. John, H. Perry et al., Ed., 'Chemical Engineers Handbook', 4th Ed., 1963, McGraw Hill.
4. Colin, J. Smithells, Ed., 'Metals Reference Book', 5th Ed. Butterworths, London & Boston.
5. Wilhelm Hofman, 'Lead and Lead Alloys', 1970, Springer Verlag Berlin, Heilberg, New York.
6. M.L. Kapoor, 'Chemical and Metallurgical Thermodynamics', Vol.II, 1984, Nem Chand and Bros. Roorkee, India.
7. R.F. Bunshaw, Chief Ed., 'Techniques in Metal Research', Vol. IV, Part I and II, 'Physico-Chemical Measurements in Metal Research', R.A. Rapp, Ed. 1970, Interscience Publishers.
8. J.O.M. Bockris, J.L White and J.D. Mackenzie, Eds., 'Physico-Chemical Measurements at high temperatures, 1959, Butterworths, London.
9. P.R. Clopper, R.L. Altman & J.L. Margrane, 'The Characterisation of high temperature vapours', Chapter 3, 1967, Wiley, New York.
10. M.Knudsen, Ann. Physik, 29, 1909, pp.179.
11. I. Langmuir, Phys. Rev., 2, 1913, p. 329.
12. K.P. Abraham, Proceedings, II.Sc.Bangalore, 1981, pp.47-68.
13. K.Kiukola and C. Wagner, J. Electrochem. Soc. 104, 1957, pp.379.
14. H. Schmalzried, Metallurgical Chem. Symp. 1971, Ed.O.Kubaschewski, pp.39-64.

15. T.H.Etsell and S.N. Flengas, *Chemical Reviews*, 70(3), 1970, pp.339-376.
16. G.R. Fiterer, *Metall. Chem. Symp.*, 1971, Ed. O.Kubaschewski, pp. 589-604.
17. A.V. Rama Rao & V.B. Tare, *I.I.M. Silver Jubilee Symp.*, New Delhi, 1972, pp.79-129.
18. M.Iwase, S.Miki and T.Mori, *J. Chem. Thermo*, 11(4), Apr. 1979, pp.307-315.
19. Masanori Iwase & Toshisada Mori, *Met. Trans.B.*, 9B, Sept.1978, pp.365-370.
20. Masamori Iwase, Toshisada Mori, *Trans.ISIJ* 19, 1979, pp.126-132.
21. Henriët D, Datillier C, Olette, *Metall. Chem. Symp.*, 1971, Ed. O. Kubaschewski, pp.
22. K.T. Jacob and J.H.E. Jeffes, *Trans. Inst. Min. Metall. (Sec.C)*, 80, 1971, pp.32-41.
23. K.T. Jacob and J.H.E. Jeffes, *Trans. Inst. Min. Metall. (Sec.C)*, June 1971, pp. C79-C85.
- 23a. Carbo-Nover J., *Tin In Silicate melts*, Ph.D. Thesis, University of London, London, 1968.
24. C. Wagner, *J. Chem. Phys.* 21, 1953, p.1819.
25. T.N. Balford & C.B. ALcock, *Trans. F. Soc.* 60, 1964, pp.802-35.
26. C.B.ALcock and T.N. Bedford, *Trans. F. Soc.*, 61, 1965, pp.443-57.
27. Y.Kayahara, K.Ono, T. Oishi and J. Moriyama, *J. Jpn. Inst. Metals*, 42(15), May 1978, pp.527-533.
28. K.F. Tyre, *Z. Metallkunde.* 74(11), Nov.1983, pp.755-757.
29. R.L. Pastorek, R.A. Rapp, *Trans. Met.Soc. AIME*, 245, 1969, pp.1711.
30. R.Szware, K.E. Oberg, R.A. Rapp, *Met. Trans. B*, 10B, 1979, pp.565-74.
31. Shinya Otsuka, Masami Matsuyama & Z.Kojuka, *Met Trans.B*, 9B, Mar.1978, pp.21-24.

32. Shinya Otsuka, Z.Kojuka, Met Trans.B, 10B, 1979, pp.565-573.
33. Shinya Otsuka, Zensaku Kojuka, Met.Trans.B., 11B, Mar. 1980, pp.119-124.
34. Shinya Otsuka, Toyokaju & Zensaku Kojuka, Met. Trans. B., 11B, June 1980, pp. 313-319.
35. S. Otsuka & Z. Kojuka, Met. Trans.B., 12B, Sept. 1981, pp.616-620.
36. Shinya Otsuka, Toyokaju Sano & Zensaku Kojuka, Met. Trans.B., 12B, Sept.1981, pp.427-33.
37. Shinya Otsuka, Zensaku Kojuka, Met. Trans.B., 12B, Sept.1981, pp.455-459.
38. Shinya Otsuka, Zensaku Kozuka, 12B, Sept.1981, pp.501-507.
39. S.Otsuka, T. Saka, Z.Kojuka, Trans. JIM, 22(1), 1981, pp.35-42.
40. S.Otsuka & Z.Kojuka, Trans. JIM, 22(8), 1981, pp.558-566.
41. S.Otsuka, Hana Oka & Z. Kojuka, Trans. JIM, 23, 1982, p.563.
42. S.Otsuka, Hara Oko & Z. Kojuka, Trans. JIM, 23(2), Feb.1982, pp.70-76.
43. S.Otsuka, Y.Matsumura & Z.Kojuka, Met. Trans. B., 13B, 1982, p.71.
44. Shinya Otsuka, Hirotaka Haraoka, Zensaku Kojuka, Trns. JIM, 24(3), 1983, pp.132-138.
45. S. Otsuka, Y. Kurose & Z.Kojuka, Trans.JIM, 24(12), 1983, pp.817-828.
46. S.Otsuka, Yoshi hiro & Z.Kojuka, Trans. JIM, 24(12), pp.829-36.
47. S.Otsuka & Z. Kojuka, Trans. JIM, 25(2), 1984,
48. S.Otsuka, Z.Kojuka & Y.A. Chang, Met. Trans.B., 15B(2), June 1984, pp.329-336.

49. Shinya Otsuka, Yoichi Kaku, Zensaku Kojuka, Trans.JIM, 25(2), Feb.1984, pp. 497-503.
50. Shinya Otsuka, Yoshi Kaju Kurose & Zensaku Kojuka, Met. Trans.B, 15B, Mar.1984, pp. 141-147.
51. Szuwarc, R., Oberg, K.E. & Rapp, R.A., High Temp. Sci., 4, 1972, pp.347-352.
52. T.A. Ramanarayanan and R.A. Rapp, Met. Trans., 3, 1972, pp.3239-46.
53. Kemore Nobumasa, Iwao Katayama & Zensaku Kojuka, Trans.Jim, 21, 1980, pp.275-284.
54. Kemori Nobumasa, Iwao Katayara & Z. Kojuka, 21(5), 1980, pp.285-292.
55. M. Iwase, S.I. Takeshita & H. Mori, J. Chem. Thermo., 11(10), Oct.1979, pp.917-926.
56. M. Iwase, S.Miki & T. Mori, J. Chem. Thermo., 11(4), Apr. 1979, pp. 307-315.
57. S.Setharaman, L.I. Staffansson, Met. Trans.B., 10B, 1979, pp.539-543.
58. S.Setharaman, K.P. Abraham & L.I. Staffansson, Scand.J.Metall., 1978, 7(4), pp. 176-180.
59. Anja Taskinen, Scand J.Metall., 8, 1979, pp.185-190.
60. P. Taskinen & Hikka Hiltunen, Scand. J. Metall. 8, 1979, pp.39-42.
61. A. Taskinen & P. Taskinen, Z. Metallkde, Sept.1979, 70(9), pp. 594-596.
62. Anja Taskinen & Hannu Holopainen, Z. Metallkde, Bd. 71, H11, 1980, pp.729-734.
63. Anja Taskinen, Scand.J. Metall., 10, 1981, pp. 141-144.
64. Anja Taskinen, Scan.J. Met., 10, 1981, pp.185-188.
65. A. Taskinen, Z. Metallkde, 73, 1982, pp.163-168.

66. K.T.Jacob, 'Thermodynamic study of oxygen in liquid metallic solutions', Ph.D. Thesis, Univ. of London, 1970.
67. K.T. Jacob, S.K. Seshadri & F.D. Richardson, Trans.Inst.Min.Met., 1970, C79, pp.C274-C280.
68. K.T. Jacob & JHE Jeffes, J. Chem. Thermo. 6, 1971, pp.433-438.
69. K.T. Jacob & J.H.E. Jeffes, J.Chem. Thermo., 5, 1973, pp.365-69.
70. K.T. Jacob, K.Fitzner & C.B. Alcock, Met. Trans.B, 8B, Sept.1977, pp.451-56.
71. K.T.Jacob, C.B. Alcock, J. Less Common Metals, 53, 1977, pp.211-216.
72. K.T. Jacob, P.M. Mathew, Z. Metallkde, 70(6), June 1979, pp.366-371.
73. K.T. Jacob, Met. Trans.B, 12B, Dec. 1981, pp. 675-678.
74. Richard, F.D. & Webb, L.E., Trans. Inst. Min. Metal. 64, July 1955, pp.529-64.
75. D.C. Conochie, C. Ebiogwn, G.G.C., Robertson, Trans. Inst. Min. Met., 1984, pp. C45-C48.
76. K. Fitzner & Z. Moser, Met. Technol, 6(7), July 1979, pp. 273-275.
77. Shinya Otsuka, Zensaku Kojuka, Trans. JIM, 18, 1977, pp.690-696.
78. Yoshi Kayahara, Katsutosshi Ono, Toshio Oishi & Joichiro Moriyama, Trans. JIM, 22(7), 1981, pp.493-500.
79. P. Taskinen & H. Hiltunen, Scand. J. Metals, 8, 1979, pp.39-42.
80. N.Kemori, I. Katayama, Z. Kojuka, J.JIM, 44(2), Feb.1980, pp.197-202.
81. Z.Wyprtowicz, K. Fitzner, Arch. Hutn., 28(2), 1983, p.209-219.
82. Belton & Tankins, Trans AIME, 1965, 233, pp.1892-1897.

83. R.Kammel, J.Osterwalt, T.Oishi, Metall.,37(2), Feb.1983, pp.141-144.
84. V.I.Kotley Oron etal., Steel USSR, 14(1), Jan. 1984, pp.20-21.
85. T.Oishi, T. Goto, Y. Kayahara & J.Hushiyama, Met. Trans. B. 13B, 1982, pp.423-427.
86. F. Gustaffsson, 2nd Jpn.Sweeden joint Symp. on Ferrous Metallurgy (Proc.Conf.) Jpn. 11-12 Dec. 1978, pp.21-29.
87. F.Puchi and M.G. Frohberg, Metall, May 1979, 33(5), pp.449-450.
88. M.L. Kapoor, M.G. Frohberg, Can. Metall. Quart. 12(2), 1973, pp.137-146.
89. Shinya Otsuka, Y.Kurose & Zensaku Kozuka, Met Trans. B, 15B, Mar.1984 pp.141-146.
90. H.Suito, Y. Yamada & M.Ohtani, Trans. JIM, 17, 1976, pp.819-27.
91. W.A. Fischer, W.A. Ackerman, Arch. Eisen-Huttenwesen, 37, 1966, pp.697-703.
92. Charle H, Osterwald J., Electrochemische Z. Phys. Chem. Neue Folge, 1976, pp.199-208.
93. Charle, H. Dissertation, T.U. Berlin, 1973.
94. Isecke,B., Gleichgewichtsuntersuch ungen an den systemen wismut, Antimon & Blei-Sauer Stoff Dissertation, T.U. Berlin, 1977.
95. Darken L.S. & Gurry R.W., J.Am. Chem. Soc. 67, 1945, p.1398.
96. Dastur M.N & Chipman, J. Trans AIME, 185, 1949, p.441.
97. J. Osterwald, Z. Phys. Chem., N.F., 49, 1966, pp.138-143.
98. W.A. Fischer & W. Ackermann, Arch. Eisen-huttenwesen, 1966, 37, pp.43-47.
99. K. Sano and H. Sakao, Nippon Kinzoku Gakkaishi, 1955, 19, pp.655-59.
- 99a A.D. Kulkarni, Met. Trans. 4, pp.1713-1721.

100. A.D. Kulkarni, R.E. Johnson, *Met. Trans.* 4, 1973, pp.1723-1727.
101. T.A. Ramanarayanan & R.A. Rapp, *Met. Trans.*, 3, 1972, pp.39-46.
102. K.Fitzner, *Thermochin. Acta*, 35(3), 1980, pp.277-286.
103. Charle'H. & Osterwald J. *Z. Phys. Chem. Neue Folge*, 1976, pp.199-208.
- 103a Caley, W.F. & Masson, C.R., *Thermodynamics of lead phosphate slags by an electrochemical method.* In *Metal-slag-Gas Reactions & Processes*, Ed. z.a. foroulis & W.W. Smelzer.
- 103b Mehrotra G.M., Froberg M.G., Mathew, P.M. & Kapoor M.L., *Free energy of formation of intermediate compounds in the system PbO-TiO₂*, *Scripta Met.* 7, 1973, pp.1047-1051.
- 103c Mehrotra, G.M., *Beitrag Zur Thermodynamic*, Dissertation, T.U. Berlin 1975.
- 103d Charette, G.G. and Flengas, S.N. *Thermo. Props. of the oxides of Fe, Ni, Pb, Cu and Mn by EMF measurements*, *J. Electrochem. Soc.* 115, 1968, pp.796-804.
104. Charle'H, *Dissertation*, T.U. Berlin, 1973.
- 104a. C.Wagner, *Thermodynamics of Alloys*, Addison-Wesley, 1962.
- 105 C.B. Griffith & M.W. Mallet, *J. Am. Chem. Soc.*, 1953, 75, pp.1832-34.
106. C. Diaz, C.R. Masson & F.D. Richardson, *Trans. Inst. Min. Met.* 75, 1966, pp.183-187.
107. Masamori Iwase et al. *Metal-Gas-Slag Reactions and Processes*, 1975, pp.885-902.
108. K. Fitzner, K.J. Jacob & C.B. Alcock, *Met. Trans B*, 8B, Dec. 1977, pp.669-74.
109. C.B. Alcock, E. Ichise and J. Buttler, *Jl. JIM*, 44(11), Nov.1980, pp.1239-1243.
110. S.Otsuka & Z. Kojuka, *Met. Trans. B*, 10B, 1979, pp.565-74.

111. M.L. Narula, V.B. Tare & W.L. Worrell, *Met Trans. B*, 14B, Dec.1983, pp.673-77.
112. Toshiham Fuji Sawa et al., *Trans. I & S. Inst. Jpn.* 21, (9), 1981, pp.626-631.
113. S.C. Srivastava, L.L. Siegle, *Met. Trans.*, Jan. 1974, pp.49-54.
114. K.P. Abraham, *Trans. IIM*, 1969, 5, pp. 5-7.
115. W.A. Fischer, D.Janke, *Arch. Eisenhüttenwesen*, 39, 1968, pp.89-99.
116. N. Kemori, I.Katayama and Z. Kojuka, *J.JIM*, Feb. 1980, 44(2), pp.197-202.
117. U. Block and H.P.Stuwe, *Z. Metallkde*, 1969, 60, pp.709-12.
118. U.Block and H.P. Stuwe, *Z. Metallkde*, 60, 1969, p.766.
119. R.J. Fruchan, I.J. Martonik and E.T. Turkdogen, *Trans. Met. Soc. AIME*, 245, 1969, pp.1501-1505.
120. E.S. Tankins & N.A. Gocken, *High Temp. Sci.* 4, 1972, pp.393-404.
121. K.Fitzner, *Z. Metallkde*, Dec. 1978, 69(12), pp.751-754.
122. S.Otsuka and Y.A. Chang, 'Advances in Sulphide Smelting, Vol.I, Basic Principles (Proc. Conf.) San-francisco, Cal. USA, 6-9, Nov.1983, pp.33-39.
123. Shinya Otsuka & Y.A. Chang, *Met. Trans.B*, 15B(2), June 1984, pp.329-336.
124. Lars-Invar Staffansson et al., *Scand.J. Metall.*, 1974, 3(4), pp.153-157.
125. Shinya Otsuka, Hirotaka Haraoka, Zensaka Kojuka, *Trans. JIM*, 1983, 24(3), pp.132-138.
126. Kiyoshi Terayama, Masao Ibeda and Masao Tarriguchi, *Trans. JIM*, 27(3), 1986, pp.176-179.
127. Henriët, D., Datillier C. & Olette, *Metallurgical Chem. Symp.* 1971, Ed. O.Kubaschewski.

128. W.A. Fischer, O. Janke & W. Ackermann, Arch. Eisenhuttenwesen, 41, 1970, pp.361-367.
129. Franz.Oeters, Klaus Koch et al., Arch. Eisenhuttnwesen, Sept.1977, 48 (9), pp.475-480.
130. F.Gustafsson, 2nd Jpn. Sweeden Joint Symp. on Ferrous Metallurgy (Proc. Conf.), Dec. 1978, pp.21-29.
131. W.Dai, S. Seetharaman & L.I. Staffson, Met. Trans.B, 15B, June 1984.
132. G.K. Sigworth & J.F. Elliott, Metal Science 1974, 8, pp.298-310.
133. M.Nduaguba & J.F. Elliott, Met. Trans.B, 14B, Dec.1983, pp.679-682.
134. R. Kammel, J.Osterwalt & T. Oishi, Metall., 37(2), 1983, pp.141-144.
135. Young, D.R., The Thermodynamics of Oxygen in molten copper alloys. Ph.D. Thesis, University of London, 1965.
- 135a. T.A. Ramanarayanan & R.A. Rapp, Met. Trans., 3, Dec. 1972, pp.3239-3246.
136. F.Jacobsson & E. Rosen, Scand. J. Metal, 10(1), 1981, pp.39-43.
137. S.M. Averbukh et al., Steel USSR, 13(6), June 1983, pp.223-224.
138. D.C. Hu, A.Z. Vanzeeland, W.W. Liang & Y.A. Chang, Calphad, 5(2), 1981, pp.115-123.
139. Vasudeo Barburao Tare, Dieter Janke & W.A. Fischer, Met. Trans.B, 9B, Sept.1978, pp.399-401.
140. V.E. Shevtrov & V.L. Lekhtmets, IZV Akad Nank, SSSR Met., Nov-Dec.1977,6, pp.37-41.
141. Carl Wagner, Met. Trans. B, 7B, Sept. 1976, pp.339-346.
142. J.T. Sryvalin et al., Trudy Inst. Met. Suerdlovask, 18(3), 1969.

143. H.Scheneck & E.Steinmetz, Stahleisen-Sonderber, (7), 1966.
144. J.R. Wilson, Met. Rev., 1965, 10, p.381.
145. O.Kubaschewski, Third Internat. Conf. on Chemical Thermodynamics, Baden, Austria, 1973.
146. O.Kubaschewski, Proc. Ist Internat. Conf. on thermodynamical proerties of materials, 11, 1967, New York, Gorden and Beach.
147. I. Insara, 'Metallurgical Chemistry', 403, 1972, London, HMSO.
148. I. Insara and E. Bonnier, Rev. Chem. Minerals, 1972, 9, 245.
149. C.H.P.Lupis, 'Liquid Metals', 1, 1972, New York, Marcel Dekker.
150. M.L. Kapoor, International Metallurgical Reviews, 20, 1975, pp.150-165.
151. M.L. Kapoor, Proc. Conf., II Sc. Bangalore, 1983, pp.19-33.
152. C.B. Alcock and F.D. Richardson, Acta. Met., 6, 1958, p.365.
153. N. Gokcen & J. Chipman, Trans. Amer. Inst.Min. Metall. Engrs. 197, 1953, p.173.
154. C.B. Alcock and F.D. Richardson, Acta. Met. 8, Dec.1960, pp.882-887.
155. G.R. Belton and E.S. Tankins, Trans. Met. Soc. AIME, 233, October 1965, pp.1892-98.
156. K.T. Jacob and C.B. Alcock, Acta. Met., 20, 1972, pp.221-231.
157. Carl Wagner, Acta Met., 21, Sept. 1973, pp.1293-1303.
158. R.J. Fruehan and F.D. Richardson, Trans. Am. Inst. Min. Engrs. 245, 1969, pp. 1721-1726.
159. E.S. Tankins, Met. Trans. 1, 1970, pp.2637-42.
160. E.S. Tankins, J.F. Erthal & M.K. Thomas, J. EElectrochem. Soc. 112, 1964, pp.446-451.

161. G.R. Belton & E.S. Tankins, Trans. Am. Inst. Min. Engrs. 233, 1965, pp.1892-1897.
162. T. Chiang & Y.A. Chang, Met. Trans.B., 7B, Sept. 1976, pp.453-467.
163. Shin Hsin Kuo & Y.Astin Chang, Met. Trans.B., 9B, March 1978, pp.154-156.
164. T.A. Chang and D.C. Hu, Met. Trans. B., 10B, March 1979, pp.43-47.
165. M.L. Kapoor, Scripta Metallurgica, 10, 1976, pp.323-326.
166. D.C.Hu & Y.A. Chang, Met. Trans. B, 11B, March 1980, pp.171-175.
167. E.Ising, Z. Physik, 31, 1925, pp.253-257.
168. J.H. Hildebrandt, J.Am. Chem. Soc., 59, 1929, pp.56-60.
169. J.V. GLuck & R.D. Pehlke, Trans. AIME, 1969, 245; pp.711-716.
170. R.H. Fowler, Proc. Camb. Phil. Soc., 34, 1938, pp.382-86.
171. R.H. Fowler & E.A. Guggenheim, 'Statistical Thermodynamics', 1960, Cambridge Press.
172. H. Bethe, Proc. Roy. Soc., A150, 1935, pp.552-560.
173. G.S. Rushbrooke, *ibid*, A166, 1938, p.296.
174. E.A. Guggenheim, 'Mixtures', 1952, Oxford Univ. Press.
175. J.G. Kirkwood, J. Chem. Phys., 61, 1938, p.70.
176. G. Newall and E. Montroll, Rev. Mod. Physics, 25, 1953, p.253.
177. C.Domb, Advances in Physics, 9, 1960, p.149.
178. C.H.P. Lupis, Ph.D. Thesis, Massachusetts Institute of Technology, 1965.
179. C.H.P. Lupis and J.F. Elliot, Acta Met., 15, 1967, p.265.
- 179b. R.L. Sharkley et al., Met. Trans., 1971, 2, p.3039.

180. J.C. Mathieu et al., J.Chim. Phys., 62, 1965, p.1289.
181. J.C. Mathieu et al., *ibid*, p.1297.
182. J.C. Mathieu et al., Advances in Physics, 16, 1967, p.523.
183. B. Brion et al. J. Chim. Phys., 66, 1969, p.1238.
184. B. Brion et al., *ibid*, 67, 1970, p.1745.
185. J.C. Mathieu et al., Chemical Metallurgy of Iron & Steel, 344, 1973, London, The Iron & Steel Institute.
186. M.L. Kapoor, Trans. Jpn. Inst. Metals, 19(10), 1978, pp.109-119.
187. Sabri Anik, Madan Lal Kapoor & Martin G. Froberg, Z. Metallkde, Bd. 74, H1, 1983, pp.53-58.
188. Sabri Anik, Madan L. Kapoor and Martin G. Froberg, Z. Metallkde, Bd., 74, H6, 1983, pp.372-376.
189. Christman, J.R. and Huntington, H.B., Phys. Rev., 139, 1965, p.483.
190. Bolsaitis, P., Met. Trans. 4, 1973, pp.2395-2398.
191. Bansil A. et al., Phys. Cond. Matter, 19, 1975, p.391.
192. L. Pauling, 'The Nature of Chemical Bond', 3rd ed. Cornell, Ithaca, 1970.
193. Milton Blander, Marie-Lousie Saboungi and Pierre Cerisier, Met. Trans. B., 10B, December 1979, pp.613-622.
194. Jain & Aggarwal; A Text book of Metallurgical Analysis, 1978, Khanna Pub. Delhi.